DEVELOPMENT OF A UNIFIED APPROACH TO

THE DESIGN OF COLD-FORMED STEEL MEMBERS

by

Teoman Pekoz, PhD

Professor of Structural Engineering

Cornell University

Ithaca, New York

May 27, 1986

Report SG 86-4

PREFACE

This report, "Development of a Unified Approach to the Design of Cold-Formed Steel Members," is reference 50 of the draft Commentary on the May 1986 Edition of the Specification for the Design of Cold-Formed Steel Structural Members published by the American Iron and Steel Institute. It is being issued as a draft research report pending public review of the Specification, which is from June 1 to July 1, 1986.

The unified design approach developed in this report includes the treatments of compression elements, columns, beams and beam columns. The approach covers sections with compression elements that are locally stable as well as those in the post-local buckling range at overall failure. The overall failure modes include flexural, lateral, and torsional-flexural. The unified design approach developed was checked on the basis of analytical and parametric studies. The results of carefully conducted tests were also used in the verification of the proposed approach.

American Iron and Steel Institute
June 1986

TABLE OF CONTENTS

CORRELATION OF THE 1986 AISI
SPECIFICATION AND THIS REPORT

The 1986 AISI Specification Section:	Discussed in this report in Section:
B2.1	2.2.1
B2.2	2.2.2, 9.1 through .2
B2.3	2.3
B3.1	2.4.1
B3.2	2.4.2
B4	2.5
B5	2.5
C3.1	6.1 through .2, 6.5
C3.1.1	6.5
C3.1.2	6.2 through .5
C4	3.2, 4.1 through .3
	9.1 through .6
C4(c)	8.1 through .4
C4.1	3.2, 4.1 through .3
C4.2	3.2, 5.1 through .3
C5	3.3, 7.1 through .3
	8.1 through .4

PAGE INTENTIONALLY LEFT BLANK.

CHAPTER 1

INTRODUCTION

Studies to develop a unified approach to the design of cold-formed steel members will be discussed in this report. This approach has been the basis of many of the changes introduced in the 1986 Edition of the Specification for the Design of Cold-Formed Steel Structural Members published by American Iron and Steel Institute. This document will be referred to in this report as the 1986 AISI Specification.

The unified approach pertains to two general areas of design. These two areas are the design of compression elements and the design of members. For the design of compression elements, a generalized effective width approach is developed for stiffened and unstiffened compression elements, compression elements with intermediate or edge stiffeners and webs. For the design of members, the approach covers design of columns beams and beam-columns. The failure modes for members include flexural, lateral and torsional-flexural buckling. The approach treats members that are made up of elements that may or may not be in the post-buckling range. This approach encompassing both compression elements and members will be referred to in this report as the unified approach.

The 1980 AISI Specification has a mixed approach for compression elements and webs. Stiffened elements are treated by an effective width approach while unstiffened elements and webs are treated by an allowable stress approach. The accuracy and the consistency of this approach has been studied by the researchers at Cornell University and elsewhere. The unified approach developed in this report treats all compression elements by a generalized effective width approach in a consistent manner.

The unified approach is based on the data and conclusions reached in
several research projects carried out and reported by DeWolf, Peköz and
Winter (1973, 1974), Kalyanaraman, Peköz and Winter (1972, 1977),
Kalyanaraman and Peköz (1978), Desmond, Peköz and Winter (1978, 1981a),
Desmond, Peköz and Winter (1978, 1981b), Mulligan and Peköz (1983, 1984),
Loh and Peköz (1985), Cohen and Peköz (1987 - to be published), Weng and
Peköz (1986 - to be published) and the extensive parametric studies
carried out by the author as discussed in this report. In each phase of
the research, rigorous analytical models were developed and compared with
the results of several hundreds of experiments conducted within the
project as well as those conducted elsewhere, for example, those of
Thomasson (1978), LaBoube and Yu (1978) and Loughlan (1979). The study
carried out by the author for the development of the unified approach
reported here used the results of tests on 49 locally stable columns and
beam-columns, 140 locally unstable beams, 213 locally unstable stub
columns, columns, and beam-columns, more than 60 angle section columns
and 46 perforated columns and stub columns.

In the implementation of the unified approach in the 1986 AISI
Specification several new features were introduced in format as well as
the technical content. The changes in format include the determination
of allowable loads by applying a factor of safety to the calculated
nominal load-carrying capacity rather than through the use of allowable
stresses.

This feature will simplify conversion to a load and resistance factor
design approach. Another change in format is the formulation of all non-
dimensionalized equations that can be used with any consistent system of
units.

CHAPTER 2

BEHAVIOR OF COMPRESSION ELEMENTS

2.1 INTRODUCTION

The approach developed in this chapter unifies the design procedures

for stiffened and unstiffened compression elements, compression elements

with intermediate or edge stiffeners as well as webs of flexural

members. The 1980 AISI Specification treated these elements with mixed

approaches involving effective widths and allowable average stresses. In

some instances the 1980 AISI Specification was overly conservative thus

putting cold-formed steel members at an unnecessary disadvantage. The

unified approach for compression elements will make some cold-formed

steel products more competitive and improve the procedures for calcula-

tions.

The effective width equation used in cold-formed steel design at

the present time is a slightly modified form of the one derived by Winter

(1947) for elements supported by webs along the two longitudinal edges.

In the unified approach the behavior of compression elements and webs

with various edge support conditions is represented by an effective width

approach.

The effective width approach has been extended in Kalyanaraman,

Peköz and Winter (1972, 1977); Kalyanaraman and Peköz (1978); Desmond,

Peköz and Winter (1978, 1981a, 1981b) to unstiffened elements and to

elements with an edge stiffener or an intermediate stiffener of any

size. The application of the approach to webs was studied by Mulligan

and Peköz (1983, 1984); Cohen and Peköz (1987) and other researchers. In

the course of the studies conducted by the author for the preparation of

the 1986 AISI Specification some modifications were introduced to improve

accuracy or to simplify the expressions.

2.2 STIFFENED ELEMENTS

Cold-formed steel sections are, in general, made up of thin plate

elements. It is well known that the post-buckling behavior of longi-

tudinally compressed elements supported by webs on longitudinal edges can

be represented by an effective width approach. The effective width

equation proposed by Winter (1947) and later modified by him slightly,

serves as the basis of the AISI Specification for the Design of Cold-

Formed Steel Members (1980). The effective width, b, can be written in a

nondimensional form as

$$b = \rho w$$
Eq. 2.2-1

where w is the actual flat element width and ρ is a reduction factor

determined as follows

$$\rho = (1 - 0.22/\lambda)/\lambda$$
Eq. 2.2-2

where

$$\lambda = \sqrt{\frac{f}{F_{cr}}}$$
Eq. 2.2-3

F_{cr} is the plate buckling stress calculated as

$$F_{cr} = \frac{k \pi^2 E}{12(1 - \mu^2)(w/t)^2}$$
Eq. 2.2-4

λ can be written as

$$\lambda = \frac{1.052}{\sqrt{k}} \left(\frac{w}{t}\right) \sqrt{\frac{f}{E}}$$
Eq. 2.2-5

where t is the element thickness, f is the actual stress in the

element,   E is the modulus of elasticity, μ is Poisson's ratio, and k is

the plate buckling coefficient.

For a fully effective element $w = b$ and $\rho = 1$. Substituting $\rho = 1$ into Eq. 2.2-2, the values of λ for which an element is fully effective can be found. These values are 0.327 and 0.673. The value of ρ cannot exceed unity. For values of λ between .327 and .673, the value of ρ determined from Eq. 2.2-2 is larger than unity. Therefore, $\lambda = .673$ is the limiting value of λ below which an element is fully effective.

Section B2.1 of the 1986 AISI Specification gives the effective width expression in the above form. This equation can be shown to be the same as the effective width equation for deflections in the 1980 AISI Specification. The form of the effective width equation in Eqs. 2.2-1 and -2 were used for two reasons. It is in nondimensional form and hence can be used with any consistent unit system, and identifying the plate buckling coefficient k explicitly shows the consistent nature of the treatment for all types of elements.

The stress, f, to be used for the element being considered depends on the way the load carrying capacity is determined. The load carrying capacity calculation may be based on either the initial yield or in some cases the reaching of the ultimate inelastic moment determined according to the procedures of Reck, Peköz and Winter (1975) provided certain conditions are met.

If the initial yield is the basis of design, then f is the yield stress if the yielding initiates in the element being considered, as seen in Fig. 2.2-2a. If the yielding does not initiate in the element being considered as shown in Fig. 2.2-2b, then the stress f should be calculated on the basis of the effective section when yielding initiates. This, in general, results in an iterative procedure.

If the load carrying capacity is determined on the basis of the
ultimate strength, then the stress f is to be determined according to
Reck, Peköz and Winter (1975). In this case the stress f is equal to the
yield stress, F_y, as shown in Figs. 2.2-2c and -2d, except for unusual
cases such as the one shown in Fig. 2.2-2e. Further considerations for
the selection of f in computations for design of beams are discussed in
Chapter 6; those for columns are explained in Chapters 4 and 5.

The unified approach involves the determination of the effective
widths of elements with all edge conditions and stress gradients using
Eqs. 2.2-1 and -2. Special conditions of these cases are accounted for
by using the appropriate plate buckling coefficient, k. For unstiffened
and stiffened elements, the plate buckling coefficients of 0.43 and 4 are
used, respectively. These coefficients are for the cases when the
longitudinal edge or edges are simply supported. It is, in general,
conservative to take these values of k. As discussed in Mulligan and
Peköz (1983, 1984) it is also possible that for exceptional cases such as
for sections having large width-to-depth ratios -- for example, channel
section columns (without stiffening lips) having ratios in excess of 6
-- the unstiffened element may destabilize the stiffened flange. For
this reason the conservative values of k were judged to be appropriate.
Further information on this subject can be found in Mulligan and Peköz
(1983, 1984).

The 1980 AISI Specification contains two types of effective width
equations, one for deflection calculations and one for load carrying
capacity calculations. The 1986 AISI Specification contains only one
effective width equation for load capacity and deflection calculations
since the factor of safety is applied to the nominal load capacity rather

than the yield stress. Although the above equation can be used con-
servatively for deflection calculations, an alternate, more accurate
expression is discussed in the next section.

The 1980 AISI Specification also gives two sets of effective width
equations, one for flanges of square and rectangular tubes and another
one for all other sections. Since the difference between the results
that can be obtained between these two sets is quite small, the 1986
Specification stipulates only one effective width equation.

2.2.1 EFFECTIVE WIDTHS FOR DEFLECTION CALCULATIONS

The effective width equation in the 1986 AISI Specification has been
shown to be very satisfactory for determining ultimate loads. As was
observed by Winter (1947), the above equation underestimates effective
widths at loads below ultimate, namely in calculating deflections. The
same conclusion was reached by Kalyanaraman, Peköz and Winter (1972,
1977), Kalyanaraman and Peköz (1978), Desmond, Peköz and Winter (1978,
1981a, 1981b), Mulligan and Peköz (1983, 1984) as well as by Dawson and
Walker (1972), Graves-Smith (1969) and Thomasson (1978).

The subultimate behavior, namely the deflections and stresses at
service loads, can be studied by casting the above effective width equa-
tion into a more convenient format as follows. The average stress, F_{av},
on the full section area, A, can be written as

$$F_{av} = (b/w) \, F_{max} \qquad\qquad \text{Eq. 2.2.1-1}$$

where F_{max} is the maximum edge stress, which is taken to be uniform over
the effective area. Using Eqs. 2.2-2 and 2.2-3 and taking $f = F_{max}$, Eq.
2.2.1-1 can be rewritten as

$$F_{av}/F_{cr} = \lambda - 0.22 \qquad\qquad \text{Eq. 2.2.1-2}$$

when λ is greater than 0.673. When λ is equal to or less than 0.673, the
element is fully effective, namely $b = w$, and Eq. 2.2.1-1 becomes

$$F_{av}/F_{cr} = \lambda^2 \qquad\qquad \text{Eq. 2.2.1-3}$$

Test results can be compared with the equations in the above form.
For a test the stress, F_{av}, for a compressed element can be calculated
based on the full section and the applied moment. F_{cr} and λ can be
calculated using Eq. 2.2-4 and -5, respectively. Then the test results
can be plotted having as the vertical axis F_{av}/F_{cr} and as the horizontal
axis λ as done in Fig. 2.2.1-1. In this figure, the curve designated
Mulligan and Peköz (1983, 1984) is typical of many test observations.
This curve was derived so that the slope at $\lambda = 0.673$ would be equal to
that for the curve for a fully effective section. The curve also has
zero slope as it intersects the curve for Eq. 2.2-2. The resulting
equation for the curve given in Mulligan and Peköz (1983, 1984) is a
rather complicated one. Based on regression analysis, the two straight
lines designated Weng and Peköz (1986) were obtained to fit the curve of
Mulligan and Peköz (1983, 1984). Based on these two straight lines, Weng
and Peköz (1986) derive the following equations for λ for determining
effective widths for deflection calculations:

$$\rho = 1 \text{ when } \lambda \le 0.673 \qquad\qquad \text{Eq. 2.2.1-4}$$

$$\rho = (1.358 - .461/\lambda)/\lambda \text{ when } 0.673 < \lambda < \lambda_c \qquad\qquad \text{Eq. 2.2.1-5}$$

$$\rho = 0.41 + 0.59 \sqrt{\overline{F_y/f}} - .22/\lambda)/\lambda \text{ when } \lambda \ge \lambda_c \qquad\qquad \text{Eq. 2.2.1-6}$$

where

$$\lambda_c = 0.256 + 0.328(w/t) \sqrt{\overline{F_y/E}} \qquad\qquad \text{Eq. 2.2.1-7}$$

Additional supporting evidence for the above expressions can be
found in Thomasson (1978). The expressions of Thomasson are compared

with the results of analytic studies of Graves-Smith (1969) in Fig.

2.2.1-2. Thomasson concludes that though the analytical curves of

Graves-Smith agree well with his curves qualitatively, the analytical

solution fails to compare well with the test results. In contrast,

expressions of Thomasson agree very well with his test results. The

expressions of Mulligan and Peköz (1983, 1984) and consequently the

expressions of Weng and Peköz (1986) agree well with those of Thomasson.

Section B.2.1 of the 1986 AISI Specification gives Eqs. 2.2.1-4

through -6 for an alternative approach for calculating deflections. The

use of these equations may result in significant benefits in the calcula-

tion of deflections. Deflection requirements for cold-formed steel

members frequently do govern the calculated load capacities. The

difference between the results obtained with above equations and the

results obtained using Eq. 2.2-2 depend on the stress at which the

effective width is calculated, the w/t ratio, yield stress and the

section geometry. The value of ρ is plotted against λ in Fig. 2.2.1-4a.

Whether Eq. 2.2.1-5 or -6 governs can be determined with the aid of

Fig. 2.2.1-4b. These figures can be used as design aids.

The ratios of the effective widths calculated using the Eqs. 2.2.1-4

through -6 which are the equations given as an alternate procedure in the

1986 AISI Specification, to those calculated using Eq. 2.2-2 which is the

equation for deflection calculation in the 1980 AISI Specification,   are

plotted in Fig. 2.2.1-3 versus λ/λ_y where λ_y is the value of λ when $f =$

F_y. In these figures it is seen that the increase in the calculated

effective widths can be up to about 30 percent. Moments of inertia used

for calculating deflections for most sections depend almost linearly on

the effective width of the flange. Thus it is possible to have load

capacities as determined by deflection requirements to increase by up to

about 30 percent.

The 1986 AISI Specification contains more accurate deflection

determination effective width equations discussed above, for stiffened

elements only. For other types of elements Eq. 2.2-2 is stipulated.

However, Kalyanaraman, Peköz and Winter (1972, 1977), Kalyanaraman and

Peköz (1978), Desmond, Peköz and Winter (1978, 1981a, 1981b), Mulligan

and Peköz (1983, 1984) found that Eq. 2.2-2 can be conservative also for

unstiffened elements and for elements with an edge or intermediate

stiffener. Examples of the behavior of beams with unstiffened flanges

are illustrated in Fig. 2.2.1-5.

2.2.2 EFFECTIVE WIDTHS FOR PERFORATED ELEMENTS

The post buckling behavior of elements containing circular perfora-

tions can also be represented by an effective width approach. The

approach used in the 1986 AISI Specification is based on Ortiz-Colberg

and Peköz (1981). This approach involves the modification of Eqs. 2.2-1

and -2 to calculate the effective width b as follows:

$$b = w[1 - (0.22/\lambda) - (0.8d_h/w)]/\lambda \qquad \text{Eq. 2.2.2-1}$$

where d_h is the perforation diameter and λ is as defined in Eq. 2.2-5.

The upper limit for effective width thus calculated is taken conserva-

tively as the net effective width $(w - d_h)$. The applicability of the

above experimentally obtained equation is limited by the range of the

values of the parameters involved in the experiments. These limits are

specified in the 1986 Specification Section B2.2a. The limitations and

other considerations for perforated elements and some of the supporting

experimental evidence are discussed in Chapter 9.

2.3 WEBS

The unified approach developed here includes the treatment of
webs with an effective width approach as well. The development in this
section is based on the test results reported in LaBoube and Yu (1978),
Cohen and Peköz (1987), Kallsner (1977), Johnson (1976), He (1981) and
van Neste (1983). All the test results were evaluated in Cohen and
Peköz (1987) using the proposed procedure for webs connected to stiff-
ened, unstiffened and partially stiffened compression flanges. Some
statistical data on the correlation are given in Table 2.3-1. To unify
the treatment of webs and compression flanges, it was decided the
generalized effective width equations in *Section* B2.3 of the 1986 AISI
Specification would be used for webs rather than the allowable stress
approach of the 1980 AISI Specification.

An illustration of the effective width approach is given in Fig.
2.3-1. For a web with stresses f_1 and f_2, as shown in the figure, the
effective widths b_2 and b_1 are determined as follows:

$$b_2 = b_e/2$$ Eq. 2.3-1

$$b_1 = b_e/(1 - \psi)$$

where $\psi = f_2/f_1$ and b_e is equal to b determined according to the Eqs.
2.2-1 through -5 by taking the theoretical value of k determined as
follows:

$$k = 4 + 2(1 - \psi)^3 + 2(1 - \psi)$$ Eq. 2.3-3

f_2 and f_1 have to be compression (+) and tension (-), respectively. The
case of both f_1 and f_2 being compression is rather unusual except in
columns and beam-columns. However, for columns the stresses are assumed
to be uniform in the web and for beam-columns the axial load and the

moments are treated separately and, thus, there is no need for provisions

for webs for the case when f_1 is compression. Nevertheless, the above

equations may give conservative results for compressive f_1.

The flat width w used in the equation λ is the flat width of the

web. The limiting values of w/t and λ above which the web is not fully

effective can be obtained from Fig. 2.3-2. This figure can be used as

design aids as well.

As will be discussed in Chapter 7, if lateral buckling is involved,

the stress f_2 is to be determined on the basis of full section. The

stress f_1 is to be determined on the basis of effective section taking f_2

as fixed.

2.4 UNSTIFFENED ELEMENTS

2.4.1 UNIFORM STRESS

An example of the motivation for the extension of the effective

width concept to unstiffened elements can be seen in Fig. 2.4.1-1 taken

from DeWolf, Peköz and Winter (1973). In this figure, the results of

some stub column tests on specimens designated S and U are plotted. The

cross-sectional geometry is illustrated in Fig. 2.4.1-2 and the

dimensions are given in Table 2.4.1-1. It is seen that the value of Q,

namely the ratio of the effective area at failure to the full area as

defined in the 1980 AISI Specification, is conservative and satisfactory

for stiffened elements, whereas the effective width implied in the 1980

AISI Specification is grossly conservative for unstiffened elements. The

shortcomings of the Q-factor for column design will be discussed further

in Chapter 4.

The extension of the concept of effective widths to unstiffened

elements has been tried previously by Winter (1947) and others. Winter

proposed the following effective width equation for such elements:

$$\rho = 1.19(1 - 0.30/\lambda)/\lambda \qquad\qquad\qquad\qquad \text{Eq. 2.4.1-1}$$

where λ is as defined in Eq. 2.2-3. This equation was not used pre-

viously because of lack of extensive experimental verification and the

concern for out-of-plane distortions. In the research reported in

Kalyanaraman, Peköz and Winter (1972, 1977) and Kalyanaraman and Peköz

(1978) the applicability of the effective width concept to unstiffened

elements with uniform stress was studied in depth. The results of some

of the tests used in this study are plotted in Fig. 2.4.1-3. In this

figure, both Eq. 2.4.1-1 and Eq. 2.2-2 are plotted with a buckling

coefficient of .43. It is seen that Eq. 2.2-2 gives a conservative lower

bound to the test results. Therefore, Eq. 2.2-2 is also used with the

proper plate buckling coefficient for unstiffened elements. The

correlation of other test data with the unified approach predictions is

summarized in Table 2.3-1.

The out-of-plane deformations in unstiffened elements was studied by

Kalyanaraman, Peköz and Winter (1972, 1977) and Kalyanaraman and Peköz

(1978). An idea about the out-of-plane deformations can be obtained from

Fig. 2.4.1-4 taken from Kalyanaraman, Peköz and Winter (1972). The

results of theoretical calculations and test results on sections having

unstiffened elements with flat width to thickness ratios up to 60 are

presented in this figure. Maximum amplitude of the out-of-plane

deformations at failure divided by the thickness can approach 2 as the

flat-width to thickness ratio approaches 60. However at service loads

the deformations may be significantly less as the figure indicates.

The unified approach incorporated into *Section* B3.1 of the 1986

AISI Specification results in a significant increase in the calculated

load carrying capacity of unstiffened elements and sections having

such elements. For purposes of comparison the 1980 AISI Specification

approach of allowable stress can be cast into an effective width equa-

tion. In Fig. 2.4.1-5 the ratio of the effective width to the effective

width calculated according to the unified approach implied by the 1980

AISI Specification is plotted against flat width to thickness ratios. It

is seen that the benefit can be well in excess of 100 percent.

2.4.2 UNSTIFFENED ELEMENTS WITH STRESS GRADIENT

There is very little conclusive data available on this subject.

This subject is being studied at Cornell University. It was decided to

recommend that the unstiffened compression element with a stress gradient

be treated as a uniformly compressed unstiffened element until further

information becomes available. In this approach, the stress f is assumed

to be the maximum stress in the element.

2.5 COMPRESSION ELEMENTS WITH EDGE AND INTERMEDIATE STIFFENERS

The motivation for the extension of the effective width concept to

elements with edge and intermediate stiffeners is obvious when one con-

siders the fact that for an element with a stiffener slightly smaller

than the minimum required by the 1980 AISI Specification, the stiffener

is completely ignored and the calculated capacity as a result can be only

a small percentage of the actual capacity. Again, further examples of

the improvements obtained by the unified approach that have been

incorporated into *Section* B4 of the 1986 AISI Specification are given

below.

Illustrative Examples 4 and 5 of the 1980 AISI Cold-Formed Steel

Design Manual Part IV can be used to show the shortcomings of 1980

AISI Specification provisions. The cross-sectional dimensions of the two

sections considered are shown in Fig. 2.5-1. Except for the intermediate
stiffener these sections are identical. The intermediate stiffener
added   in Example 5 results in an increase of 60 percent over the
section without the intermediate stiffener. If the intermediate
stiffener is slightly smaller than the one shown in the example, the load
capacity according to the 1980 AISI Specification drops by 60 percent.
However the unified approach of the 1986 AISI Specification shows only a
slight loss in capacity. Thus the unified approach for this case will
result in a significant improvement.

A more significant increase in the predicted capacity according to
the 1986 AISI Specification can be obtained for the case of edge
stiffened sections. For example, for a 0.06-inch thick lipped C-section
7 inches deep, 1.5 inches wide with 0.48-inch long lips made of 50 ksi
steel the allowable major axis bending moment is 38.1 kip-in. If the
lips are 0.47 inches long the allowable moment drops down to 14.3
kip-in. However the proposed approach would predict an insignificant
drop in the calculated capacity, thus resulting in a dramatic 166 percent
increase in the calculated design moment compared to that calculated
according to the 1980 AISI Specification.

It may be noted when the edge stiffener has a moment of inertia
slightly more than the minimum required by the 1980 AISI Specification,
the unified approach may give capacities up to 10 percent lower. Test
results have shown that for these cases the 1980 AISI Specification could
be unconservative up to about 10 percent.

In both of the above examples the proposed version gives a better
representation of the actual performance by far. In cases where the
neutral axis is closer to the compression flange than the tension flange

the increase in the calculated capacity may be less.

Stiffeners present two problems to be considered. First is evalu-
ating the adequacy and effectiveness of the stiffener in restraining the
element to be stiffened. Second is how the stiffener itself should be
considered in calculating the overall section properties such as the
moment of inertia, area and the section modulus.

The effective width approach given in the 1986 AISI Specification
for compression elements with an edge or intermediate stiffener is based
on the work reported in Desmond, Peköz and Winter (1978, 1981a, 1981b).

The provisions of *Section* B4.2 of the 1986 AISI Specification for
elements with edge stiffeners are illustrated in Fig. 2.5-2. In this
figure qualitative plots of the longitudinal stresses in the elements are
also illustrated. The cross-sectional notation is shown in Fig. 2.5-3.
In *Section* B4.2 three cases are identified. The first case is for
elements that do not need an edge stiffener; namely, for elements that
are fully effective as an unstiffened element. For this case the
longitudinal stresses are uniform except for the case when the edge
stiffener is so long (D/w > 0.25) as to destabilize the flange to which
it is attached. There is no provision for this exceptional case in the
1986 AISI Specification.

The second case is when the element can be fully effective as a
stiffened element when it has an adequate stiffener $(I_s > I_a)$ that is not
too long (D/w < 0.25). The expressions for the moment of inertia for an
adequate stiffener were derived in Desmond, Peköz and Winter (1978,
1981a, 1981b). Again the stiffener can be so long (D/w > 0.25) that it
can destabilize the flange to which it is attached. For this case the
provisions reflect the decrease in the efficiency of the element by

reducing the plate buckling coefficient.

The third case is when the element is not fully effective even with an adequate stiffener. Again, for this case the special considerations discussed above, such as the effect of a stiffener that is too long, are applicable.

The correlation of some of the available test data with those predicted by the unified approach is summarized in Table 2.3-1. Further correlations can be found in Desmond, Peköz and Winter (1978).

Similar considerations except for the local instability of the stiffener are valid for elements with intermediate stiffeners. Local instability of the stiffener is of a different nature in intermediate stiffeners. Due to lack of sufficient data, the design of element with locally unstable intermediate stiffeners is not included in the unified approach. Further information on the design of elements with intermediate stiffeners can be found in Desmond, Peköz and Winter (1978, 1981a and 1981b).

In the formulation of Desmond, Peköz and Winter (1978, 1981a, 1981b) for the edge stiffeners made of a simple lip, the effective portion of the edge stiffener and the corner was taken as the stiffener. Their data base for this decision was rather limited. The evidence collected since this work, including the hand calculations and computer parametric studies carried out by the author and J. M. Cohen, supported taking the flat portion of the lip as the stiffener and ignoring the round corner in evaluating the adequacy of the stiffener. The results obtained with this approach are summarized in Table 2.3-1. Taking just the effective part of the stiffener for this purpose would be too conservative because it implies using the effective width equation for

determining the flexural stiffness of the stiffener about its axis
parallel to the plane of the flange. The slight weakening effect of the
stress gradient in the stiffener due to local buckling would be offset in
the computations by ignoring the corner radius. It may also be noted
that if the corner radius is large, its beneficial effect is doubtful,
and if the corner is sharp, the corner is negligible. The effects of
large corner radii are being studied at Cornell University at the present
time.

The parametric studies on beams and beam-columns, as discussed in
Chapter 4 show that the effective stiffener properties need to be used in
calculating the overall section properties of the member. For a plain
lip stiffener which is less than adequate, a simplification to the
computation of the overall section properties was obtained by further
reducing the effective width of the stiffener. This reduction is needed
to represent the reduction of the stress in the stiffener as seen in Fig.
2.5-1 for such cases. Again, the result of this simplification was
checked against the test results and was found to be satisfactory.

The available data for the intermediate stiffeners is not yet
studied from the point of view of ignoring the transition corner between
the stiffener and the element to be stiffened. However, it seemed
reasonable to base the stiffener properties on the actual stiffener
rather than the effective stiffener area in judging the stiffener
adequacy and effects.

The topic of multiple stiffeners was not covered in the research
reported in Desmond, Peköz and Winter (1978, 1981a, 1981b). Therefore,
the 1986 AISI Specification has the same provisions as the 1980 AISI
Specification for the case of multiple stiffeners.

CHAPTER 3

LOCALLY STABLE OPEN SECTION COLUMNS AND BEAM-COLUMNS

3.1   INTRODUCTION

This chapter deals with thin-walled doubly and singly symmetric open

sections subjected to biaxial loading. The formulation also applies to

tubular sections. Though singly symmetric open section cold-formed steel

members are frequently subjected to biaxial loading, general design

provisions did not exist in the 1980 AISI Specification. The design

problem is often complicated because the plate elements making up such

sections may buckle locally below loads causing overall failure. The

subject is relevant to several practical applications including

thin-walled square or rectangular tubes, end wall columns in metal

buildings, many typical industrial storage rack columns and, possibly,

purlins in the end bays of metal buildings. Sections with locally

buckled plate elements will be covered in Chapter 7.

3.2   COLUMNS

At present research is under way at Cornell University on the

flexural behavior of cold-formed steel columns. It was decided by the

AISI Specification Advisory Committee to wait for the completion of this

work before any changes are made in the provisions for flexural buckling

of columns. Therefore, the equations for flexural buckling in *Section* C4

of the 1986 AISI Specification are the same as those in Section 3.6.1.1

of the previous Specification. However, in format the provisions for

flexural and torsional-flexural buckling are unified as follows. First,

the elastic flexural and torsional-flexural buckling stresses are found.

Then, the smaller of these stresses is designated F_e. If F_e is greater

than $F_y/2$ then the inelastic buckling stress, F_n, is found by the usual

equation

$$F_n = F_y(1 - F_y/4F_e)$$ Eq. 3.2-1

A simplified equation is introduced in the 1986 AISI Specification

for torsional-flexural buckling under concentric loading. This

simplified equation is based on Peköz and Winter (1969). In that

reference the following simple interaction equation was derived

$$\frac{1}{P_{tfo}} = \frac{1}{P_{ex}} + \frac{1}{P_t}$$ Eq. 3.2-2

where P_{tfo} is the concentric torsional-flexural buckling load, P_{ex} is the

concentric buckling load about the x axis which, is the axis of symmetry,

and P_t is the torsional buckling load. This equation was further studied

by Loh and Peköz (1985). This equation is expressed in terms of stresses

and proposed for adoption in *Section* C4.2 of the 1986 AISI Specification.

3.3 BEAM-COLUMNS

For sections with fully effective plate elements, the studies by the

author Peköz (1979) show that interaction equations can be used. This

approach was adopted in the RMI Specification for Design, Testing and

Utilization of Industrial Storage Racks (1979). The validity of the

approach was further confirmed in Loh and Peköz (1985) on the basis of

extensive analytical and experimental studies. The interaction equation

for failure between the inflection points is

$$\frac{P}{P_o} + \frac{M_x C_{mx}}{M_{xo}(1 - P/P_x)} + \frac{M_y C_{my}}{M_{yo}(1 - P/P_y)} = 1$$ Eq. 3.3-1

P, M_x and M_y are the axial force and the moments about the x and y

axes, respectively, due to the applied loading. P_o is the failure load

in the absence of any moment. M_{xo} is the failure moment for bending

about the x axis in the absence of an axial load or bending about the y
axis. Similarly, M_{yo} is for bending about the y axis. P_o, M_{xo} and M_{yo}
are determined considering both flexural and torsional-flexural
buckling. C_{mx} and C_{my} are corrections to reflect the moment gradient in
the member. P_x and P_y are the flexural-buckling loads about the x and y
axes, respectively.

The above interaction equation expressed in terms of allowable loads
and moments is the basis of Eq. C5-1 of the 1986 AISI Specification.
Equations C5-2 and -3 were adopted from the previous Specification.

The use of the above equation for axial loading in the plane of
symmetry of singly symmetric sections simplifies the provisions of the
1980 AISI Specification for this case. The approximation involved in
this simplification is shown qualitatively in Fig. 3.3-1.

The ultimate loads observed in tests with various axial load eccen-
tricities are compared with those predicted by Eq. 3.3-1 in Tables 3.3-1
through -4. The cross sectional notation is illustrated in Fig. 3.3-2.
The comparison is made by calculating the ultimate load by the two
approaches. P_{na} is obtained by disregarding any inelastic reserve capac-
ity, while P_{nb} is calculated considering inelastic reserve capacity. The
correlation is considered to be satisfactory. For eccentricities of load
between the centroid and the shear center, the approach is seen to be
quite conservative as one can see from Fig. 3.3-1. However, it is con-
sidered desirable to use the interaction equation above because it is
simpler than the provisions of the 1980 AISI Specification.

The above interaction equation will be shown in Chapter 7 to be
applicable to the case of locally unstable beam-columns if certain modi-
fications are made in the definitions of various terms. Thus it was

possible to unify the approaches for locally stable and unstable beam-

columns.

Further studies and design formulations for angle sections and

perforated columns will be discussed in Chapters 8 and 9, respectively.

CHAPTER 4

INTERACTION OF LOCAL AND FLEXURAL COLUMN BUCKLING

4.1   INTRODUCTION

The effect of local buckling on overall buckling behavior has been

studied in several research projects at Cornell University and elsewhere.   It

has been shown repeatedly that the Q-factor approach may not be in good

agreement with the test results.   On the basis of tests and analytical

studies, DeWolf, Peköz and Winter (1973, 1974) and Kalyanaraman, Peköz and

Winter (1972, 1977) conclude that the overall buckling load can be calculated

using the effective radius of gyration and the effective area, both

calculated at the overall buckling stress.   This results in an iterative

procedure because the buckling stress depends on the effective section

properties which in turn depend on the buckling stress.   As will be discussed

in Chapter 5, the iterative approach has been extended in Loh and Peköz

(1985) to the treatment of torsional-flexural buckling.

The approach of Canadian Specification for Cold-Formed Steel Structural

Members (1984) formulated by John Springfield for flexural buckling was tried

by the author for a variety of sections and failure modes.   This approach is

very similar to the one proposed by Peköz (1979) for perforated columns, and

beam-columns subject to torsional-flexural buckling.   For these members, the

allowable stress is found for an unperforated column and the allowable load

is found by multiplying this stress by the net area.   This approach was

adopted by the Rack Manufacturers Institute (RMI) Specification for Design,

Testing and Utilization of Industrial Storage Racks (1979).

The studies summarized below show that proposed approach approximates

the iterative approach very closely for flexural, torsional-flexural and

lateral buckling and will be used for all these types of behavior. For this

reason this approach will be referred to in the rest of this report as the

unified approach. This is also the approach adopted in the 1986 AISI

Specification.

The unified approach consists of the following steps:

a) The elastic flexural buckling stress, F_e, is calculated for

the full unreduced section:

$$F_e = \pi^2 E / (KL/r)^2$$ Eq. 4.1-1

b) Then the (nominal) failure stress, F_n, is determined:

$$F_n = F_e$$ if $F_n \leq F_y/2$ Eq. 4.1-2

$$F_n = F_y (1 - F_y/4F_e)$$ if $F_n > F_y/2$ Eq. 4.1-3

c) and the ultimate column load, P_n, is calculated as

$$P_n = A_e F_n$$ Eq. 4.1-4

where A_e is the effective area computed at stress F_n.

The remarkable accuracy of the proposed approach can be explained

as follows: The reduction in the value of the radius of gyration resulting

from local buckling is rather small. For small slenderness ratios where the

column buckling stresses are high compared to the yield stress, the buckling

stress is quite insensitive to the changes in the radius of gyration.

However, the effective area is influenced directly and significantly by local

buckling. For small stresses, namely large slenderness ratios, the local

buckling is not significant. Therefore, for both cases the behavior is well

represented by ignoring the reduction in the effective radius of gyration,

but taking into account the reduction in the effective area in finding the

ultimate load of the column.

For locally buckled C and other singly symmetric sections, concentric

axial loading with respect to the centroid of the effective section is an

exceptional situation.   The centroid of the effective section depends on the

magnitude of loading.   The location of the centroid moves as the load is

increased.   However, the allowable concentric loading is important as a

parameter in the interaction equation.

4.2   COMPARISON OF THE Q-FACTOR APPROACH WITH THE ITERATIVE APPROACH

Some results taken from DeWolf, Peköz and Winter (1973, 1974) and

Kalyanaraman, Peköz and Winter (1972, 1977) are illustrated in Figs. 4.2-1 to

-13.   A comparison of the experimentally observed ultimate values and the

ultimate values computed according to the Q-factor approach of the 1980 AISI

Specification can be made on the basis of these figures.   The specimens

designated U and S were discussed in Chapter 2.   The dimensions for these

sections were given in Fig. 2.4.1-2 and Table 2.4.1-1.   In these figures

ultimate loads are predicted using the Q-factor determined according to the

1980 AISI Specification, (Q_{AISI}), as well as the experimentally determined

Q-factor(Q_{test}).

It is seen in Fig. 4.2-3 and -4 that the Q-factor approach can be

unconservative for S-sections even when the experimentally determined value

of Q is used.   On the other hand, as can be seen in Figs. 4.2-5 through -13,

the predicted ultimate loads for U-sections and LC-sections that contain

unstiffened flanges are grossly conservative when the Q-values are computed

according to the 1980 AISI Specification.   The tests on LC-sections which are

basically the same shape as U-sections are reported by Kalyanaraman, Peköz

and Winter (1972).   The correlation is better when experimentally determined

values of Q are used.   However, as mentioned above, even the experimentally

observed Q-values give unsatisfactory results for S-sections.   In contrast

the iterative approach gives satisfactory results for S-, U- and LC-sections.

The iterative approach though satisfactory for S-, U- and LC- sections

is tedious to use. This was the motivation for adopting the unified approach

that does not involve iteration and that is shown to agree well with the

iterative approach.

4.3 COMPARISON OF THE ITERATIVE APPROACH
WITH THE UNIFIED APPROACH

The dimensions of several sections used in evaluating the proposed

approach are given in Table 4.3-1. Sections C1-1, C2-1 and C3-1 are the same

as those used by Loh and Peköz (1985). The results of the computations are

given in Figs. 4.3-1 and -2. The ratios of the ultimate load to the yield

load (P_n/P_y) versus the slenderness ratio based on full section weak axis

radius of gyration (KL/r_y) are plotted in Fig. 4.3-1. Curve 0 is the curve

for the ultimate load if the section is assumed to be fully effective. Curve

1 is for the present AISI Specification approach with the Q-values calculated

according to Chapter 2, namely effective widths are used for unstiffened

elements as well. Curve 2 is for the iterative approach described above.

The iterative approach agrees best with the test results and is to be taken

as the most accurate approach against which the other approaches will be

judged. Curve 3 is for the approach proposed here. The ratios, R, of the

ratio (P_n/P_y) calculated by different procedures to that obtained by the

iterative approach, R_2, are plotted in Fig. 4.3-2.

It is seen that the agreement between the proposed approach and the

iterative approach is excellent. It is seen further that for the sections

considered, the present AISI approach with the Q-values calculated according

to Chapter 2 may give results that are up to about 35 percent uncon-

servative. If Q-values were calculated according to the 1980 AISI

Specification, the errors would be even larger.

The results of computations on other C-sections that have rather high

width to thickness ratios and exaggerated geometries are given in Fig. 4.3-3

for the sake of demonstration. Here the notation is the same as in Fig.

4.3-2. The same trend is also evident in this figure. Here the uncon-

servatism of the 1980 AISI Specification approach with the Q- values

calculated according to Chapter 2 is up to 80 percent. Again, if Q-values

were calculated according to the present AISI Specification, the errors would

be even larger.

Comparisons similar to those of Figs. 4.3-1 and -2 are presented for

tubular sections in Figs. 4.3-4 through -7. Here again the correlation

between the iterative approach and the unified approach is excellent. Again,

the 1980 AISI approach can be very unconservative. For example the 1980 AISI

approach can give results that are more than 60 percent unconservative for

Tube T1-1, which has quite typical dimensions.

CHAPTER 5

INTERACTION OF LOCAL AND TORSIONAL-FLEXURAL
COLUMN BUCKLING

5.1 INTRODUCTION

Extensive studies on post-local buckling torsional-flexural behavior
of open sections has been reported in Loh and Peköz (1985). An analyti-
cal model for this behavior was developed on the basis of the torsional-
flexural theory for the effective section, and the theory was confirmed
by correlating the results with the test results. The approach involves
iterations and, hence, is referred to as the iterative approach in the
discussion below. Again, in this case, the concentric load is not a
typical load for a locally buckled section, but the concentric ultimate
load is a parameter used in the proposed interaction equations.

The approach proposed for calculating the allowable load of a
locally buckled column subject to torsional-flexural buckling is exactly
the same for those subject to flexural buckling in Chapter 4. It
consists simply of determining the torsional-flexural buckling stress for
the fully effective section and multiplying this stress by the effective
area at the buckling stress calculated to obtain the ultimate load.
Thus, in Eqs. 4.1-1 through -4, only the determination of F_e changes.
For torsional-flexural buckling, F_e is determined according to the
torsional-flexural buckling theory for the full unreduced section.

5.2 PARAMETRIC STUDIES

Some of the studies conducted are presented in Fig. 5.2-1a and
5.2-1b. The sections used in these parametric studies are described in
Table 4.3-1. The designation of the curves is the same as those in the
figures of Chapter 4. The iterative curves were taken from Loh and Peköz

(1985). The results for Sections C1-1 and C2-1 are shown in Fig.

5.2-1a. The results for Section H3-LU-3 of Loh and Peköz (1985) are

shown in Fig. 5.2-1b. This section is a hat-section with very pronounced

torsional-flexural behavior. The dimensions are the same as those of

Section C3-1 except that the lips are turned outwards to form a hat

section.

The correlation between the proposed approach and the iterative

approach is seen to be excellent. The results of the approach proposed

here is much better than those of the simplified approach of Loh and

Peköz (1985).

5.3 EXPERIMENTAL VERIFICATION

As mentioned above, a concentric loading, with respect to the

centroid of the effective section, is an exceptional situation. When the

elements buckle locally, the location of the neutral axis changes.

Therefore, all the members that were tested as pin-ended columns were

actually beam-columns. The experimental verification for these members

is described in Chapter 7. Several of the tests reported in Chapter 7

are with axial loading at the centroid of the full section.

CHAPTER 6

INTERACTION OF LOCAL AND LATERAL BEAM BUCKLING

6.1   INTRODUCTION

The unified approach for calculating the effect of local buckling on
lateral buckling is consistent with that for columns. First, the elastic
lateral buckling stress, F_e, is calculated on the basis of the torsional-
flexural buckling theory for the full unreduced section using the equa-
tions of Peköz and Winter (1969). Then the failure stress, F_n, is deter-
mined using Eqs. 4.1-2 and -3. The lateral buckling moment is determined
by multiplying F_n by the effective section modulus calculated for an
outer fiber stress of F_n.

Further details will be discussed and developed in Section 6.5.

6.2   LATERAL BUCKLING OF LOCALLY STABLE BEAMS

Expressions for lateral buckling moments for singly symmetric
sections derived on the basis of the torsional-flexural theory can be
found in several references. Lateral buckling possibility exists for
bending about both principal axes of a singly symmetric section (Peköz
and Winter 1969). Then the failure stress F_n is determined using Eqs.
4.1-2 and -3. The lateral buckling moment is determined by multiplying
F_n by the effective section modulus calculated for an outer fiber stress
of F_n.

The author proposed the use of the equations derived on the basis of
the torsional-flexural buckling theory for the RMI Specification (1979).
Furthermore, the author proposed to use the same inelastic buckling
correction for lateral buckling as the one used for columns. These
expressions are specified to be used to determine the parameters for the

interaction equations for biaxial bending in the present RMI

Specification.

Comparisons of the AISI and the RMI approaches are given in Figs.

6.2-1 and 6.2-2 taken from Loh and Peköz (1985) for Sections C1-1 and

C2-1 of Table 4.3-1. Basically, the primary reason for the difference

between the two approaches is the way the inelastic correction is

applied. Comparisons of the elastic lateral buckling moments according

to the AISI Specification and those computed according to the

torsional-flexural buckling theory can be seen in Fig. 6.2-3. The two

approaches give verysimilar results when the section bends about the

strong axis as in the case of C1-1. The correlation is still acceptable

for C2-1 but not as good. The two moments of inertia are close to each

other for this section. For Section C3-1 the 1980 AISI approach predicts

results too low compared to those from the torsional-flexural buckling

theory. For this section the bending is about the weak axis. The

buckling load for pure bending even in the plane of the weak axis is

needed as a parameter for the beam-column interaction equations.

6.3 LATERAL BUCKLING OF LOCALLY UNSTABLE BEAMS

The unified approach described in Section 6.1 was tried for several

sections and the results were virtually identical with those of the

analytical approach developed in Loh and Peköz (1985) on the basis of

torsional-flexural buckling theory.

6.4 EXPERIMENTAL VERIFICATION

There are no direct test data on the lateral buckling of cold-formed

steel beams. However some data exist on the behavior of sections loaded

axially by eccentric loading in Peköz (1967) and Loh and Peköz (1985).

The data, which are admittedly indirect show that the RMI Specification

approach that is now incorporated into the unified approach and hence the

1986 AISI Specification, is quite satisfactory.

6.5   DEVELOPMENT OF A DESIGN APPROACH
      FOR FLEXURAL MEMBERS

The load carrying capacity of a beam subjected to pure bending

should be checked for the section strength and lateral buckling. The

section strength can be defined as either reaching the yield stress on

the effective section or reaching the failure yield strain as defined and

discussed by Reck, Peköz and Winter (1975). These two definitions may,

in certain cases, give the same result. For example, for a section with

a compression flange that cannot sustain more than the yield strain and,

at the same time, yields in compression first, the initial yield also

means the reaching of the failure strain.

The 1986 AISI Specification uses a factor of safety of 1.67 against

section failure and lateral buckling. The factor of safety is applied to

the nominal moment capacity or the calculated failure moment M_n, which

is taken as the smaller of the nominal section moment capacity or the

nominal lateral buckling moment.

The nominal section moment is determined either by defining the

failure moment as the moment that will cause initial yield in the

effective section or the moment at which compressive yield strain in the

effective section is reached. According to the 1980 AISI Specification,

when the latter definition is used, the allowable moment is the smaller

of 0.75 times the nominal moment determined for initial yield or 0.6

times the moment that causes the reaching of the compressive failure

strain. Since in the 1986 AISI Specification, a factor of safety of 1.67

is applied to the nominal moment, the nominal moment should be taken as

the smaller of 1.25(= 0.75/0.60) times the nominal moment determined for

initial yield or the nominal moment determined for reaching of the
compressive failure strain, M_u.

As discussed in Section 6.1 above, according to the unified
approach, the nominal lateral buckling moment, M_c, is calculated assuming
the section to be fully effective. M_c can be either the elastic lateral
buckling moment, M_e, or the inelastic buckling moment depending on the
ratio of M_e to the yield moment, M_y, for the full section. The lateral
buckling stress, M_c/S_f, is determined on the basis of the full section
modulus, S_f, for the extreme compression fiber. The nominal lateral
buckling moment is determined by multiplying the lateral buckling stress,
M_c/S_f, by the effective section modulus, S_c, for the fiber in question.
The effective section modulus is determined with the effective widths
formulated in Chapter 2. It is assumed that the stress in the fiber in
question remains fixed and the stresses in other fibers in the section
can be determined on the basis of the effective section.

CHAPTER 7

BIAXIALLY LOADED LOCALLY UNSTABLE OPEN SECTION
BEAM-COLUMNS

7.1 INTRODUCTION

The use of interaction equations for cold-formed steel beam-columns
was studied extensively and extended to locally unstable sections in Loh
and Peköz (1985). Though the interaction equation of Loh and Peköz
(1985) is in the same form as Eq. 3.1-1, the definition of several terms
of the interaction equation have been changed for the unified approach.

The unified approach for beam-columns developed here and adopted by
the 1986 AISI Specification is basically different from that of Loh and
Peköz (1985). It involves the use of Eq. 3.1-1 for singly or doubly
symmetric open sections and closed tubes with some of the terms redefined
to account for locally buckled plate elements. P_0 is determined as
described above for locally unstable torsional-flexural buckling. M_{xo}
and M_{yo} are determined by the approach described above for lateral buck-
ling. All eccentricities (for example e_x in Fig. 7.1-1) are taken with
respect to the centroid of the effective section for the axial load
alone. The parameters P_x and P_y are the elastic buckling loads for the
full unreduced section.

The unified approach for beam-columns, which is the basis of
Section C5 of the 1986 AISI Specification, was confirmed by theory and
tests on simply supported locally unstable C, channel and hat section
beam-columns. Correlation for angle sections is discussed in Chapter 8.

7.2 PARAMETRIC STUDIES

The unified approach for beam-columns had several points to be
resolved and clarified. This was achieved by means of parametric

studies and comparisons with the test results and the results of
rigorous solutions.

A point to be resolved was the determination of the applied
moments. The moment of the axial loads was stated to be taken about
the centroidal axes of the effective section. There are several possi-
bilities for calculating the effective section. A possible approach
would be to use the effective section for the axial load and the
moments. However, fortunately taking the effective section as that
under axial load alone in combination with the other assumptions gave
very satisfactory results.

Another point to be resolved was the determination of the critical
load terms in the amplification factors. These factors are used to
amplify the beam moments to determine the beam-column moments. Beam
moments are determined ignoring the axial loads. The beam-column
moment at a point is the sum of the beam moment and the increase in the
moment due to the axial load. This increase can be determined by
multiplying the axial load by the deflection at the point in
question.   It is customary to determine this deflection on the basis
of elastic behavior. The critical load in the magnification factor is,
therefore, the elastic buckling load about the bending axis.

The computation of the buckling load contained in the
amplification factor should include the effects of local buckling on
the stiffness. This would involve an iterative procedure. Several
different schemes were tried. These schemes in combination with
various ways of calculating the eccentricities required parametric
studies and comparisons with the test results. The simplest approach,
namely using the buckling load for the full section, gave the most

satisfactory results.

7.3 CORRELATION WITH TEST RESULTS

The correlation of the test results with those computed according

to the unified approach is presented in Tables 7.3-1 through -5. In

these tables, P_n and P_{uexp} are the calculated and observed failure

loads, respectively. Considering the complex nature of the problem,

the correlation is seen to be satisfactory. An exceptional case is the

correlation with test results of Loughlan (1979). In this case the

unified approach appears to be too conservative. The details of his

test could not be verified.

The correlation of the calculated results with those observed is

summarized in Fig. 7.3-1. This figure presents the results of all the

tests with loads with uniaxial or biaxial eccentricities. The figure

on the left illustrates the presentation of the results. In this

figure R_p, R_x and R_x and R_y represent the first, second and the third

terms of Eq. 3.3-1. Equation 3.3-1 defines the plane ABC. For a given

test, the observed values of P, M_x and M_y are substituted into the

equation and a point with the resulting R_p, M_x and M_y values is plotted.

The results that fall outside the volume OABC indicate that the proposed

interaction equation is conservative for those cases. This

three-dimensional situation is represented in the right figure in Fig.

7.3-1 in two dimensions by plotting the projections of the test points on

the R_p-R_o plane. Thus, from geometry R_o is equal to 0.707 $(R_x + R_y)$.

The points that fall outside the area OAD in the figure on the right show

that the Eq. 3.3-1 is conservative. The few points that fall within this

area have been mostly explained and the approach is judged satisfactory.

CHAPTER 8

DESIGN OF ANGLES

8.1 INTRODUCTION

In this chapter the applicability of the unified approach to the design of angle section columns and beam-columns is studied. Due to time constraints, the study reported here has been brief. Several extensions and further verifications are possible. The verification here has been based on the test results reported in Madugula, Prabhu, and Temple (1984) and Wilhoit, Zandonini and Zavellani (1983). The results of 41 tests from Madugula, Prabhu and Temple (1984) were used in the study. The tests of Madugula, Prabhu and Temple (1984) include tests on 16 hot rolled angles.

8.2 TEST SPECIMENS

Both references report nominal dimensions and section properties calculated from actual dimensions. The cross-sectional dimensions and yield stresses are presented in Tables 8.2-1 and -2. Center line length of the angle leg is designated "b." The actual dimensions were not stated clearly in Madugula, Prabhu and Temple (1984). The stated actual dimensions in Wilhoit, Zandonini and Zavellani (1983) did not give the section properties stated. This could have been due to the effect of rounded corners in calculating the section properties. Therefore, an angle leg dimension was calculated for each section from the given section properties as indicated in the tables of Section 8.3.

All the sections were loaded concentrically. It should be noted that all the sections except Section 2 have moderate w/t ratios and hence are not very sensitive to local buckling.

8.3   CORRELATION OF OBSERVED AND CALCULATED RESULTS

A computer program was prepared using the unified design approach.
This program was capable of calculating ultimate loads for an angle
section loaded in the plane of symmetry. By introducing an eccentricity
in the plane of symmetry, the effect of sweep (initial
out-of-straightness) is studied. The sweep in the plane of symmetry
towards the corner of the section has the most influence as opposed to
sweepin other directions.

The observed and calculated ultimate loads of Section 1 are plotted
in Figs. 8.3-1a through -1e. Some of the tests on Section 1 were carried
out with some restraint to force the direction of deflection towards the
corner of the column section. The calculated results when the column is
assumed to be perfectly straight, namely $e_x = 0$, are shown in Fig.
8.3-1a. It is seen that the calculated results provide an upper bound
and, hence, are unconservative. Torsional-flexural buckling governs in
the initial rather flat portion up to a slenderness ratio of about 60.
Beyond this flexural buckling about the minor axis governs.

Wilhoit, Zandonini, and Zavellani (1983) mentions the presence of
sweep and applies an analytical model assuming a sweep equal to L/1000.
The effect of various eccentricities of the axial load or sweep values,
as indicated by e_x, are studied in Figs. 8.3-1b and -1c.

It is seen in Figs. 8.3-1b and -1d that the assumption of an initial
sweep of L/1000 leads to estimates of a lower bound of the test results.
The following ratio is plotted for various sweep values for Section 1 in
Fig. 8.3-1c for Section 1.

$$\text{Ratio} = \frac{\text{Ultimate load calculated assuming } e_x = 0}{\text{Ultimate load calculated assuming an } e_x}$$

As will be discussed similar plots are provided for other sections as well. It is seen in Fig. 8.3-1c that a sweep of L/1000 causes a lowering of the ultimate load of up to 30 percent.

To compare the sensitivity of the angle sections to sweep with the sensitivity of other sections, a study reported in Table 8.3-1 was carried out for a lipped channel with sweep perpendicular to the plane of symmetry. The two sections compared buckled flexurally and torsional-flexurally when loaded concentrically. The results show that the angle sections are much more sensitive to sweep than the lipped sections studied in Table 8.3-1. Studies, as the one shown in this table, need to be carried out for other sections.

Since the angle sections are very sensitive to initial sweep it appears prudent to consider a sweep in the design of angle sections. This conclusion is further supported in the plots for other sections as well.

The comparison of the test results on Section 1 with those obtained from the 1980 AISI Specification are given in Fig. 8.3-1e. This figure is taken from Madugula, Prabhu and Temple (1984). It is seen that the 1980 AISI Specification is unconservative for some of the test specimens.

The results of studies on Section 2 are plotted in Figs. 8.3-2a through -2d. This particular section had a high w/t ratio and, hence, was more susceptible to local buckling effects. The assumption of a per-fectly straight column does not seem to lead to unconservative results. However, the assumption of a sweep in design still seems prudent.

The results of tests on Section 3, which is a hot rolled angle, are

presented in Figs. 8.3-3a through -3d. Again, the assumption of an
initial sweep in design appears needed.

The results of tests on Sections 4 and 5 are reported in Wilhoit,
Zandonini and Zavellani (1983). The initial out-of-straightnesses for
the specimens were measured but not reported. The test results are com-
pared with those calculated in Figs. 8.3-4a through -4c and -5a through
-5c for Sections 4 and 5, respectively. It is quite possible that these
specimens were more straight than others. However the assumption of an
initial sweep does not seem to lead to overly conservative results.

8.4 CONCLUSIONS

The results of the above brief and limited study appear to support
the use of the unified approach outlined. Due to the particular
sensitivity of angle sections to initial sweep, it appears prudent to
consider an initial sweep in design. The magnitude of the initial sweep
equal to L/1000 gave reasonable results for the specimens considered in
this study.

Based on this study, Sections C4c and C5 of the 1986 AISI Specifica-
tion require the use of an out-of-straightness of L/1000 for the design
of angle sections.

A more extensive verification for sections with large flat width to
thickness ratios is needed. The application of the unified approach to
biaxially loaded angle sections, though appearing justified intuitively,
also needs to be verified.

CHAPTER 9

DESIGN OF COLUMNS WITH
CIRCULAR PERFORATIONS

9.1   INTRODUCTION

This chapter presents the results of a brief study on the design of

perforated cold-formed steel columns using the unified design approach.

Some limited data reported in Ortiz-Colberg and Peköz (1981) are used in .

this study.   The provisions of the 1986 AISI Specifications are thus

based on rather limited data, some engineering judgement and intuition.

The brief study reported in Ortiz-Colberg and Peköz (1981) included

stub and long column tests on lipped channel sections with and without

circular perforations.   The dimensions of the stub and long columns used

in the study are given in Tables 9.1-1 and -2, respectively.   Obviously,

the variation of several possible parameters would have resulted in much

more than the 46 members used in the study.   A few of the results

reported in Ortiz-Colberg and Peköz (1981) were not used because they

looked obviously defective.

9.2   STUB COLUMN TEST RESULTS

The ratio of the observed stub column ultimate load to that

calculated using the effective width equations of Chapter 2 for

perforated plate elements is designated R and given in Table 9.1-1.   The

mean and standard deviation of R values are 1.072 and 0.086,

respectively.   This excellent correlation should not be too surprising

since the formulation was based partly on the same data set.

9.3   COLUMN TEST RESULTS

9.3.1   CALCULATION PROCEDURES

The results of the application of the unified approach is presented
in Tables 9.3.1-1 through -4. The following are the different procedures
tried in calculating failure loads:

Procedure 1:

The unified approach procedure is applied assuming the axial load to
be applied at the centroid of the full cross section. In the
evaluation of the test results this assumption is not correct
because the load was centered such that the strains around the cross
section did not deviate from the average by more than 5 percent at
about 25 percent of the expected ultimate load. This means that the
point of application of the load was between the centroid of the
full cross section and the centroid of the effective section at the
failure load. It is possible to estimate the location of the load
in the tests from a calculation of the effective section centroid
location at 25 percent of the ultimate load. This would be rather
approximate, and the time constraint of the present study did not
permit such calculations.

The ratio of the ultimate loads observed to those calcu-
lated,assuming the load to be at the centroid of the full section,
is designated R1 in all the tables. It is seen that since the load
was not applied at the centroid of the full section the calculated
results are significantly below the observed results.

Procedure 2:

The unified approach is applied assuming the load to be applied at
the centroid of the effective section at ultimate load. The ratio

of the observed load to that calculated according to this procedure

is designated R2 in the tables.

Procedure 3:

The unified approach is applied ignoring the perforations and

assuming the load to be applied at the centroid of the full

section. The ratio of the observed load to that calculated

according to this procedure is designated R3 in the tables.

Procedure 4:

The unified approach is applied ignoring the perforation and

assuming the load to be applied at the centroid of the effective

section at ultimate load. The ratio of the observed load to that

calculated according to this procedure is designated R4 in the

tables.

Procedure 5:

Procedures 1 and 2 assume that when there is a perforation, the

section properties are changed throughout the section even if the

perforation is at one point. Even for multiple perforations the

reduction in the section properties are limited to small segments

of the column. Procedure 5 involves weighting the calculations for

perforated and unperforated columns depending on the number and size

of perforations. This is done according to the formula

$$P = P_o - (P_o - P_p) \frac{dn}{L} \qquad \text{Eq. 9.3.1-1}$$

where P_o and P_p are the ultimate loads calculated for unperforated

and perforated columns, respectively, assuming the load to be

applied at the centroid of the effective section at ultimate; d is

the diameter of each perforation; n is the number of perforations; L

is the column length. The ratio of the observed load to that

calculated according to Eq. 9.3.1-1 is designated R5.

9.3.2 CORRELATION OF OBSERVED AND CALCULATED RESULTS

As discussed above, it appears more reasonable to assume that the load is applied close to the centroid of the effective section. Thus the values of R2, R4 and R5 show better correlation than R1 and R3. Procedure 5 is quite a bit more complicated than procedures 2 and 4. For these reasons, the rest of the study will deal with Procedures 2 and 4.

For most of the sections without multiple perforations there is very little or no difference between R2, R4 and R5. This is due to the fact that for the sections without multiple perforations only a small portion of the length of the column has reduced moment of inertia and area due to the perforation. Since there are only nine columns with multiple perforations, an analytical parametric study was carried out. This study is described in the next section.

9.4 BUCKLING LOAD OF NONPRISMATIC SECTIONS

The effect of perforations on a column may be idealized as the reduction of section properties at the regions of perforations. An estimate of the magnitude of this effect can be obtained treating the column as a nonprismatic member with reduced moment of inertia at the regions of perforations. For a column with multiple perforations along its length, this would result in an idealized model with multiple regions of reduced moment of inertia.

An upper bound estimate of the effect of perforations was obtained by concentrating all the regions of reduced moment of inertia along a region at midheight of the column. The length of this region at midheight was taken equal to the sum of the lengths of individual regions along the length of the column.

An analytical model for a column with varying moment of inertia
as described above, can be found in Timoshenko and Gere (1961). The
transcendental equation for the flexural buckling of a column as shown
in Fig. 9.4-1a, can be derived as

$$\tan\left[\frac{\pi r}{2}(1-RL)\right]\tan\left[\frac{\pi r}{2}(RI)(RL)\right]\frac{1}{RI} = 0 \qquad \text{Eq. 9.4-1}$$

In this equation $RI = \frac{I1}{I2}$ \qquad Eq. 9.4-2

I1 is the moment of inertia of the effective section without per-
foration, and I2 is the moment of inertia of the section with
perforation. The regions of I1 and I2 are illustrated in Fig. 9.4-1a

$$RL = \frac{a}{L} \qquad \text{Eq. 9.4-3}$$

L is the length of the column, and a is the length of the region of
reduced moment of inertia taken as (nd). The number of perforations
along the length of a column is designated n.

$$r = \frac{P}{P1} \qquad \text{Eq. 9.4-4}$$

The term r is the ratio of the buckling load for the column of
Fig. 9.4-1a divided by that for the column of Fig. 9.4-1b. P1 is the
buckling load of a column with moment of inertia equal to I1 as shown in
Fig. 9.4-1. P1 can be expressed as

$$P1 = \frac{\pi^2 E I1}{L^2} \qquad \text{Eq. 9.4-5}$$

P is the buckling load of the nonprismatic column.

The buckling load P can be written as

$$P = r P1 \qquad \text{Eq. 9.4-6}$$

The term r indicates the reduction in the value of the elastic
buckling load due to the presence of perforations. As described above

the concentration of the perforations at midheight should overestimate the effect of perforations.

A computer program was written to determine the value of P using the above transcendental equation. The results are presented in Table 9.4-1. It is seen that for a wide range of values of the ratios RI and RL the column buckling load is quite insensitive to the presence of perforations. It should also be noted that the discussion so far has been limited to elastic buckling. For inelastic buckling, namely overall buckling stresses more than one-half of the yield stress, the effect of perforations on the buckling stress is even more insignificant.

The accuracy of Eq. 9.3.1-1 is studied in Table 9.4-2. The buckling load ratio given in this figure is the buckling load determined according to the transcendental equation Eq. 9.4-1 divided by the buckling load determined using Eq. 9.3.1-1.

It is instructive to examine the ratios RI and RL of the test specimens, which are listed in Table 9.4-3. In this table RI is the ratio of the moment of inertia of the effective section through a perforation, and the moment of inertia of the full unreduced section. It is seen that most of the sections without multiple perforations have RL and RI ratios such that there should be little difference between perforated and unperforated columns. The values of R2, R4 and R5 as well as RI and RL are tabulated in Tables 9.4-4 through -6. The values of these parameters are plotted in Figures 9.4-2 through 9.4-7.

In Tables 9.4-4 through 9.4-6 and Fig. 9.4-6a, it is seen that when RL is less than 0.015, the value of R4 is not in general below one except when the column is unperforated. If R4 is not below one, the capacity of the column can be calculated ignoring the perforations. The values of R4

below one for unperforated columns is attributed to test data scatter.
However it appears prudent and conservative to account for the
perforations in accordance with the unified approach when RL is larger
than 0.015. The value of RL is easy to calculate.

A similar demarcation can be formulated for the value of RI.
However, the calculation of RI is almost as tedious as the calculation of
the capacity using the unified approach. Therefore such a formulation
would not result in a significant design simplification.

9.5 LIMITATIONS OF THE EFFECTIVE WIDTH EQUATIONS

The effective width equations for perforated plate elements given in
Chapter 2 were obtained from tests on lipped-channel sections reported in
Ortiz-Colberg and Peköz (1981) with the following ranges of dimensions:

d/w from 0 to 0.50 where w is the flat width and d is the hole
diameter.

w/t up to 64.

spacing of holes greater than 0.50w and 3d.

These should be the range of applicability of the effective width equa-
tions given in Chapter 2 for perforated plate elements.

9.6 CONCLUSIONS

Based on the limited test data and the studies above, it has been
shown that the design formulation given in this chapter can be used until
further studies are completed. The limitations stipulated in Section 9.5
above are included in *Section* B2.2 of the 1986 AISI Specification.
Section C4 of the 1986 AISI Specification contains a provision for
perforated columns that allows one to ignore perforations if the number
of holes in the effective length region times the hole diameter divided
by the

effective length does not exceed 0.015. This provision is based on the

discussion of Section 9.4 above.

CHAPTER 10

STUB COLUMN TESTS AND EVALUATION
OF STUB COLUMN TEST RESULTS

10.1 INTRODUCTION

The unified approach necessitates an expression for the effective
area, A_e, as a function of the stress, f, on the effective area. The
stress f is taken as F_n in calculating column strength. When A_e cannot
be calculated, such as when the column has dimensions or geometry outside
the range of applicability of the generalized effective width equations
of the 1986 AISI Specification, a functional relation between f and A_e
can be obtained by stub column tests as described in this chapter.

A draft for test and evaluation procedures is given in Appendix A.

10.2 EVALUATION OF TEST RESULTS

10.2.1 TESTS WHERE AXIAL SHORTENING IS ACCURATELY MEASURED

An expression for the relationship between the stress on the effec-
tive section versus the effective area for axially loaded members can be
obtained directly by measuring the axial shortening versus the axial load
in a stub column test. From these measurements, an expression for the
relationship between the effective area at that stress, A_e, and the
stress, f, on the effective area can be derived as described below. In
finding the ultimate load for an actual column, f is to be taken as F_n
which is the column buckling stress calculated on the basis of full
unreduced cross-section.

Denoting the axial load on the stub column, P, the effective area at
this load is

$$A_e = P/f$$ Eq. 10-1

The axial shortening, D, at load P can be expressed as

$$D = f \, L/E$$ Eq. 10-2

where L is the length of the stub column and E is the modulus of
elasticity.

It is usually assumed that at the ultimate stub column load, P_u, the
stress on the effective section is equal to the yield stress, F_y. The
effective area and the axial shortening at P_u will be designated A_{eu} and
D_u, respectively. Thus

$$P_u = A_{eu} \, F_y$$ Eq. 10-3

and

$$D_u = F_y \, L/E$$ Eq. 10-4

From Eqs. 10-2 and -4

$$D/D_u = f/F_y$$ Eq. 10-5

and

$$f = F_y \, D/D_u$$ Eq. 10-6

Substituting Eq. 10-6 into Eq. 10-1

$$A_e = P \, D_u/(F_y \, D)$$ Eq. 10-7

If axial shortening measurements are taken and F_y is known, then all
the terms of Eq. 10-7 are known, and the effective area, A_e, at each
stress level, f, and the axial load level, P, can be determined. A_e
should not be taken larger than the full unreduced area of the section, A.

Even though the axial shortening is measured accurately, if the
evaluation of multiple stub column tests and any interpolations are
needed (as given in Eq. 10-13, -15, -16 and -17 below), the approach
derived in the following section is definitely more convenient. For
this reason it is given as the primary procedure in Appendix A. The

approach of the next section underestimates effective areas and hence

is conservative. An alternate procedure for using the measured axial

shortening is given in the Section 10.6.

10.2.2 TESTS WHERE AXIAL SHORTENING IS NOT MEASURED

In this section, expressions for A_e versus f will be derived for

the case when the axial shortening is not measured and only the ultimate

load is measured (as was required according to the 1980 AISI Speci-

fication). These equations can be used for the cases where axial

measurements are taken and the results of multiple tests are to be

evaluated.

It can be observed that for f equal to zero A_e should be equal to

the full unreduced area A. At ultimate load the effective area is equal

to A_{eu}. A_{eu} should not be taken larger than A. A_e may be expressed as

$$A_e = A - (A - A_{eu})(f/F_y)^n$$ Eq. 10-8

The writer carried out rather extensive parametric studies to

determine a proper expression for the exponent n in the above equation.

The following is a brief description of these parametric studies.

For most sections the effective area, A_e, can be calculated

analytically using the unified effective width approach described in the

1986 AISI Specification. Using these calculated results an expression

for n inEq. 10-8 was developed. In this study three square thin-walled

tubes were used. These sections give a *conservative* assessment of the

approach of Eq. 10-8 since all the plate elements are partially

effective. An expression for n based on this type of section would be

conservative for sections that have both partially effective and fully

effective plate elements.

Figure 10-1 shows the plots of calculated P/P_u versus D/D_u curves

for a 8"x8" square tube with .05-inch wall thickness. Curve A is

obtained using the effective width equation of *Section* B2.1b Procedure

(1) of the 1986 AISI Specification. Curve B is obtained using the

effective width equations of Procedure (2). As expected the approach of

Procedure (1) is conservative. Thus in the subsequent plots Procedure

(1) is used.

In Figs. 10-2 through -4 the results using Eq. 10-8 are plotted for

4"x4", 8"x8" and 16"x16" columns each having 0.05-inch-thick walls. In

each of these figures the curves for n = 1/3, 1/5, and the curve obtained

using the present effective width equation for stiffened elements (Curve

A - simulated stub column test result) is plotted. These plots were just

three of many obtained trying different approaches.

If the calculated curve shows a larger axial shortening for a given

axial load, it means that the calculated results are conservative

compared to the simulated test results. It is seen that for sections

having larger width to thickness values, smaller values of n are required

to get better agreement between the curve A and the curve calculated

according to

Eq. 10-8. Consequently, it was decided to have

$$n = A_{eu}/A \qquad\qquad\qquad Eq. 10-9$$

The results of using n according to Eq. 10-9 in Eq. 10-8 are plotted

in Figs. 10-5 through -7. As seen in these figures the agreement with

curve A is excellent.

Figures 10-8 and -9 show comparison of the results obtained by Eqs.

10-8 and 10-9 with two stub column test results reported in Mulligan and

Peköz (1983). Figure 10-8 shows that the Eqs. 10-8 and -9 are slightly

unconservative but quite satisfactory for the Test Specimen CLC/1 60X30.

However, Fig. 10-9 shows that Eqs. 10-8 and -9 are quite conservative for

the test specimen CLC/2 60X90.

It may be noted that Eq. 10-8 can be written in terms of the Q

factor presently used in the 1980 AISI Specification as follows:

$$A_e/A = 1 - (1 - Q)(f/F_y)^Q \qquad \text{Eq. 10-10}$$

The value of A_e for any f can be calculated using the presently

available product properties tables listing values of Q.

If the axial shortening measurements are taken and Eq. 10-8 or -10

is used in the evaluation of multiple stub column test results, then the

procedure developed in Section 10.4 may be used.

10.3 EFFECT OF STUB COLUMN LENGTH

Another question that needs to be resolved is the evaluation of test

results when the length of the column is 3 to 4 times the largest

dimension of the column cross-section (minimum length requirement) and

when this length is larger than 20 times the least radius of gyration of

the section, r_{min} (maximum length requirement). In the opinion of the

writer it is more important to meet the minimum length requirement rather

than the maximum length requirement.

When the length is larger than 20 r_{min}, then the test results can be

evaluated as follows: Having the length larger than 20 r_{min} is expected

to lower the overall buckling load. In this case, the critical stress F_n

for the full section of the column tested can be determined according to

the proposed specification provisions using the full unreduced section

and taking the effective length factor as 0.5. The effective area A_r in

the test at the ultimate load P_u can be calculated as

$$A_e = P_u / F_n$$ Eq. 10-11

If the overall column buckling effects were to be reduced by lateral restraints, the effective area at ultimate load would be A_{eu}. The value of A_{eu} can be determined from Eq. 10-8 on the basis of A_e calculated according to Eq. 10-11. Thus with F_u substituted for f

$$A_{eu} = A - (A - A_e)/(F_n/F_y)^n$$ Eq. 10-12

The value of n depends on A_{eu} and has to be determined by trial and error. As a first try n can be taken as 0.2 and A_{eu} can be determined. This value of A_{eu} can now be used in Eq. 10-9 to determine n. With this value of n a new value of A_{eu} can be determined. The process should be repeated until the assumed value of n equals the calculated value of A_{eu}/A. With the converged-upon value of A_{eu}, Eq. 10-8 can be used to obtain A_e at any stress level f. The above minimum length requirements are for unperforated columns. For perforated columns, since there can be a wide variety of configurations, general guidelines should be used carefully and with consideration of special conditions. The applicability of the unified approach and the use of stub columns for results in the unified approach for columns with significant perforations have not yet been verified. In the meantime, some guidelines have been obtained mostly based on engineering intuition. The following are the guidelines given in Appendix A.

"For perforated columns with the largest dimension of the cross section W, the following guidelines will be used in deciding the length of the specimen to be used:

If a complete perforation pattern (single or multiple group of perforations) has a length along the column less than W then the specimen length may be chosen with the guidelines for unperforated columns (as in Figs. 10-26b, c, g).

If a complete perforation pattern (single or multiple group of
perforations) has a length along the column larger than W (as in
Figs. 10-26d, e, f) then the specimen length should be not less than
3 times the perforation pattern length if the ends are not welded
and 4 times the perforation pattern length if the ends are welded.
In this case it is desirable to have the more significant
perforation at midheight of the stub column (compare Figs. 10-26d
and e).

If the perforations are such that a cut cannot be made without going
through a perforation as in Fig. 10-26i, then a special section may
be fabricated as in Fig. 10-26j. In some instances it is
conceivable to have tests carried out even when the cut goes through
a perforation to evaluate performance in the actual member if the
member has a similar configuration in actual application."

10.4 USE OF THE RESULTS OF MULTIPLE TESTS IN DESIGN

The results of several tests are to be used to determine the

expression for calculating A_e for a stress level f. One needs to

consider how this can be achieved for design purposes. Several

approaches come to mind. These may include the following:

1. Use of the lowest or a statistically weighted value of A_{eu}

    obtained in a series of tests in Eq. 10-8. Obviously this would

    necessitate the use of Eq. 10-8, which is conservative compared

    to the use of plots of stub column axial shortening versus axial

    load.

2. If one wants to use such plots then one may use a lower envelope

    to the different curves obtained in different tests.

3. Another approach again for the case of using plots would be

    a weighted curve obtained from the results of several tests.

The first possibility is adopted in the procedures outlined in

Appendix A. Using this approach it is possible to carry out various

interpolations outlined below.

The procedure for choosing the value of A_{eu} is in general agreement

with the present AISI Specification Section 6.2. According to this

section, three specimens are tested first. If the results of any test
does not differ from the mean of all the tests by more than 10 percent
then the mean value is used. If the deviation from the mean is more than
10 percent then three more tests are conducted. The average of the three
lowest are regarded as the result of the series of tests.

It is possible to carry out evaluations of the multiple test results
using the equations derived in this report directly from the plots of A_{eu}
versus f. This procedure would be much more complicated.

10.5 INTERPOLATIONS

10.5.1 INTERPOLATIONS BETWEEN THICKNESSES TESTED

Using the first approach of Section 10.4, it is possible to carry
out various interpolations. For example, where a series of sections with
identical cross-sectional dimensions and hole dimensions and locations
are produced in a variety of thicknesses, with t_1 and t_2 being the
minimum and maximum thicknesses, the value of A_{eu} for a given thickness t
can be calculated as follows:

$$\frac{A_{eu}}{A} = \frac{A_{ue1}}{A_1} + \frac{(A_{eu1}/A_2) - (A_{eu1}/A_1)}{t_1 - t_2} (t_1 - t) \qquad \text{Eq. 10-13}$$

where A_1 and A_2 are the full unreduced areas of the sections with minimum
and maximum thicknesses. A_{eu1} and A_{eu2} are the effective areas of the
sections with minimum and maximum thicknesses at ultimate stub column
loads.

Some results of the parametric studies on the validity of Eq. 10-13
are presented in Fig. 10-10. This figure shows that a straight line
drawn between any two points for two different thicknesses would under-
estimate the value of A_{eu} between the two points. This leads to a con-
servative estimate of the A_e versus f relationship. These curves were

drawn for a 4"x4" tubular section. Because the thicknesses are varied

over a wide range, the results are typical of other tubular sections as

well. Since the square tube gets affected by local buckling

significantly, other sections with combinations of effective and

partially effective plate elements should behave in a similar manner.

The same reasoning is used in the interpolations and extrapolations

studied below.

10.5.2 EXTRAPOLATION FOR YIELD STRENGTH

In using the above interpolation equation as well as in other

situations, a procedure is needed for adjusting the test results for

variations in the yield strength. Making straight-line interpolations

between two yield strengths for a given thickness can be studied on the

basis of Figs. 10-11 and -12. It is seen that straight-line

interpolations would be unconservative. In Fig. 10-12 it is seen that

the following equation with $m = 0.8$ gives a good approximation of the A_{eu}

values:

$$A_{eu} = A_{eu1} - (A_{eu1} - A_{eu2})[F_y - F_{y1})/(F_{y2} - F_{y1})]^m \qquad \text{Eq. 10-14}$$

where A_{eu1} and A_{eu2} are the values for the same section with yield

stresses F_{y1} and F_{y2}, respectively. Straight line with $m = 1$ gives

unconservative results.

A more typical situation is to determine the value of A_{eu} for a

yield stress F_y from a test where A_{eut} was obtained on a specimen with

yield stress F_{yt}. On the basis of a rather extensive numerical study,

the following procedure was obtained. The results of this parametric

study are presented in Figs. 10-13 through -20. For yield strength F_y

smaller than F_{yt}, the value of A_{eu} can be taken as the lower of the two

values obtained from Eqs. 10-15 and -16:

$$A_{eu}/A = 1 - (1 - A_{eut}/A)(F_y/F_{yt}) \qquad \text{Eq. 10-15}$$

$$A_{eu}/A = (A_{eut}/A)(F_{yt}/F_y)^{0.4} \qquad \text{Eq. 10-16}$$

The variation in the yield strength between 30 ksi and 65 ksi appears to
be acceptable. Positive errors indicate conservative estimates of test
results.

10.5.3 EXTRAPOLATION FOR THICKNESS

It is possible that multiple specimens tested may have small
differences in thickness. In that event it is reasonable to adjust the
test results linearly provided that the differences in the thicknesses
are of the order of 20 percent. For example, if the nominal thickness is
T_n and the tested specimen with an observed A_{eut} has thickness T_t, then
the A_{eu} for the nominal thickness can be calculated as

$$A_{eu}/A = (A_{eut}/A)(T_n/T_t) \qquad \text{Eq. 10-17}$$

The accuracy of extrapolations using Eq. 10-17 can be seen in Figs. 10-21
through -25. Positive errors indicate conservative estimates of test
results.

10.6 USE OF AXIAL SHORTENING MEASUREMENTS IN DESIGN

The procedure of using Eq. 10-8 with Eq. 10-9 can be conservative,
and a procedure enabling the use of observed axial shortening values when
measured is desirable. The following is a development of a procedure for
this purpose. The procedure will be illustrated through use of two
examples.

Two examples of test results are plotted in Figs. 10-27 through -30
along with the result of calculations according to Eqs. 10-8 and -9 as
well as the equations developed below. It is seen that Eqs. 10-8 and -9
predict reduction of the effective area starting with zero stress. This

was intentionally devised to make the approach conservative for a wide

range of section geometries. It is seen in these figures that a function

as

$$A_e/A = 1 - (1 - A_{eu}/A)[f - f_o)/(F_y - f_o)]^b \qquad \text{Eq. 10-18}$$

can be fitted through the test data consisting of n number of readings

taken from which f and A_e/A can be calculated for reading number i by

Eqs. 10-6 and -7 as f_i and A_{ei}/A. In this equation f_o is the value of

stress above which the section is not fully effective. The exponent b

can be determined by a least squares approach as

$$b = \frac{\sum\limits_{i=1}^{n} (X_i)(Y_i) - a \sum\limits_{i=1}^{n} X_i}{\sum\limits_{i=1}^{n} (X_i)^2} \qquad \text{Eq. 10-19}$$

where n is the number of measurements taken

$$X_i = \ln [(f_i - f_o)/(F_y - f_o)]$$

$$Y_i = \ln (1 - A_{ei}/A)$$

ln designates natural logarithm

The error in various equations can be seen in Fig. 10-27 for one of

the tests. For the same test, the error is magnified through the use of

different scales in Figs. 10-28 and -29. Similar information is

presented in Fig. 10-30 for another test. There the fitted curve is

identical with the observed curve.

It is not possible to express a simple averaging process for obtain-

ing a design curve. The number of tests may be decided upon the basis of

A_{eu}, but the values may be selected as the lowest of the values obtained

form multiple tests for each value of f.

It is interesting to compare the values of A_e obtained in the two

tests with those calculated in Figs. 10-31 through -34. It is seen that

the effective width equations of the 1986 AISI Specification *Section*

B2.1b Procedure (1) are quite conservative at subultimate loads. The

effective width equations of Procedure (2) for deflection calculations

give closer and very satisfactory estimate of subultimate effective

areas. Since the corner radii were not specified, the corners were

assumed to be sharp. This could have led to the slight underestimate

seen in the figures. It may be noted that the vertical scales in Figs.

10-31 and -33 are convenient for seeing the percentage of error, whereas

the scales in Figs. 10-32 and -34 exaggerate the error.

10.7 SUMMARY OF EVALUATION PROCEDURE

For a single thickness and configuration either three or six tests

are carried out in accordance with the 1986 AISI Specification. The

results of these multiple tests are adjusted to the nominal thickness and

yield stress using Eqs. 10-15 through -17. The means and deviations used

in deciding whether three or six tests are to be carried out will be

based on the adjusted values of A_{eu} for variations in yield stress and

thickness. The resulting A_{eu} value is a property of the section that may

be tabulated for different sections. Extrapolations of this value for

properties varying, as discussed above, from those of the test specimens

appear reasonable.

If the same section configuration (including perforation patterns

and dimensions if any) is used for different thicknesses, a series of

tests can be carried out and evaluated as described in the preceding

paragraph for the thinnest and the thickest sections. Then interpola-

tions may be carried out using Eq. 10-13 for intermediate thicknesses.

10.8 SPECIMEN PREPARATION TOLERANCES AND TESTING RATES

The study presented by Peköz (1979b) and other experience at Cornell University indicates that for industrial purposes the specimens can be saw cut to a tolerance of ± 0.002 inch. If such tolerances cannot be maintained because of the shape of the cross-section, the ends may be machined as flat as possible and bearing plates welded to each end.

The application of the load at a rate of about 1.5 ksi per minute appears to be satisfactory. This rate was used in the tests reported by Peköz (1979b).

10.9 FURTHER STUDIES NEEDED

Using the approaches developed in this report, the author has carried out a statistical study of the determination of the number of tests required and the evaluation of the test results on the basis of the number of tests. This study will be published in the near future.

To a large degree, mostly analytical approaches were used to develop the approaches given in this report. It is very desirable to verify these approaches experimentally. Some work is in progress at Cornell University on this subject.

The applicability of the unified approach and the use of the stub column test results for members with significant perforations need to be studied.

THIS PAGE INTENTIONALLY LEFT BLANK

A P P E N D I X   A

DRAFT OF POSSIBLE STUB COLUMN TEST

AND EVALUATION PROCEDURES

A1.   OBJECTIVES OF STUB COLUMN TESTS

The primary objective of the stub column test of prismatic cold-formed steel sections is to determine the variation of the effective area of a compression member with the stress on the effective area when it cannot be calculated. The results of the procedure described below also include the effects of residual stresses and work hardening due to cold-forming. In the 1986 AISI Specification, the ultimate column load is determined by multiplying the column buckling stress based on full unreduced section by the effective area calculated at that stress.

A secondary objective is the determination of the extent of local deformations with axial load when the appearance of the member is important.

A2.   TEST SPECIMEN AND ITS PREPARATION

A2.1   GENERAL

If possible, stub column specimens shall be cut from a member formed by the same procedure as used or contemplated for use in the prototype. If this is not possible, the amount of cold work in producing the specimens shall be less than that for the contemplated prototype. If the prototype is made by a forming procedure different than that used to fabricate the specimens, it is advisable to confirm the test results later by using specimens cut from the commercially produced member.

A2.2 LENGTH OF SPECIMEN

To insure proper representation of local buckling and post-buckling behavior the following minimum lengths shall be used:

- If end plates are not welded, the length of the specimen shall be not
  less than 3 times the largest dimension of the section.

- If end plates are welded, the length of the specimen shall be not less
  than 4 times the largest dimension of the section.
- If the member has a repeating perforation pattern the minimum length
  of column shall be chosen so that the local buckling and post-buckling
  behavior is properly represented.

For perforated columns with the largest dimension of the cross sec-
tion W, the following guidelines will be used in deciding the length of
the specimen to be used:

If a complete perforation pattern (single or multiple group of per-
forations) has a length along the column less than W, the specimen length
may be chosen with the guidelines for unperforated columns (as in Figs.
A1b, c, g).

If a complete perforation pattern (single or multiple group of
perforations) has a length along the column larger than W (as in Figs.
A1d, e, f), then the specimen length should be not less than 3 times the
perforation pattern length if the ends are not welded and 4 times the
perforation pattern length if the ends are welded. In this case it is
desirable to have the more significant perforation at midheight of the
stub column (compare Figs. A1d and e).

If the perforations are such that a cut cannot be made without going
through a perforation as in Fig. A1i, a special section may be fabricated
as in Fig. A1j. Tests may be carried out with the cut going through a
perforation if the member has a similar configuration in actual
application and if the effect of such an end condition is to be evaluated.

It is desirable to have the length of the specimen not more than 20
times the least radius of gyration. For members with perforations, the
least radius of gyration of the net section shall be used. This

requirement is to ensure that the overall column-buckling behavior will

not affect the stub column behavior. If this requirement cannot be met

because of the requirement for minimum length, then the influence of the

overall column behavior shall be accounted for as described in Section

A4.2.

A2.3 PREPARATION OF THE TEST SPECIMEN

The stub column specimen shall be cut from the member without

causing annealing that would change the properties of the stub column

significantly. The specimens can be saw cut to a tolerance of + or -

0.002 inch out of the plane of the ends. Careful saw cutting should give

such a tolerance if the plate elements are not too slender. If the plate

elements are very slender, the vibrations of the section during saw

cutting can be reduced by clamping wooden blocks to the section. The end

planes shall be perpendicular to the axis of the specimen.

If such tolerances cannot be maintained because of the shape of the

cross section, the ends shall be machined as flat as possible and bearing

plates shall be welded to each end. (The above tolerance and the require-

ment regarding the welded end plates are based on the study reported in

Appendix B.) A welding procedure that minimizes residual stresses (such

as sequential welding, with time allowed between short segments of

welding to allow cooling, etc.) shall be used. The resulting weld should

be continuous around the section. The welded end plates shall be at

least 1/2-inch thick and ground to plane a tolerance of .0015 inch.

A2.4 NUMBER OF TESTS

The number of tests shall be in accordance with the AISI Specifi-

cation.

A2.5   TESTING APPARATUS

The tests shall be performed in a testing machine complying with the requirements prescribed in ASTM Methods E4, Verification of Testing Machines.

A2.6   INSTRUMENTATION

Displacement measuring devices with 0.0001-inch divisions shall be used to measure the axial shortening. For this purpose the displacement measuring device shall be supported firmly on the inner surface of one end plate and bear against the inner surface of the other end plate.

Local distortions of the stub column may be measured with devices with 0.001-inch divisions.

A2.7   TEST SET-UP AND ALIGNMENT

A quarter inch layer of gypsum based capping compound (such as Hydrostone) of sufficient viscosity shall be placed on the center of the testing machine table. A ground end plate shall be placed on top of the capping compound if no end plates are welded. If end plates are welded the specimen will be seated directly on the capping compound. The capping compound should cover completely the underside of the plate.

The specimen shall be placed on top of the base plate and centered with respect to the axis of the test machine. Levels shall be used to align the specimen, vertically by pressing on the base plate. Before the capping compound hardens, the other ground end plate shall be placed on the top of the specimen and a layer of capping compound shall be spread entirely over the top plate. If end plates are welded, the capping compound shall be placed directly on the top end plate. There shall be no direct contact between the machine head and the stub

column. While the capping compound hardens some load may be developed on

the stub column.

Testing shall not be started until after the capping compound

hardens (after about 40 minutes). The test shall begin with the load

developed as a result of the hardening process of the capping compound.

A2.8 TEST PROCEDURE

After alignment as described above, the axial load shall be applied

in increments not exceeding one-tenth of the estimated yield or local

buckling load. If axial shortening measurements are taken, they shall be

recorded at each load increment after the readings stabilize. It is a

good practice to plot the results and record all observations as the test

progresses.

A3. PRESENTATION OF TEST DATA

The report on each test shall contain the following:

- A description of the test specimen with all relevant dimensions

  including base material thickness exclusive of coating

- A description of the steel used

- A sketch of the test setup showing all relevant details

- The results of the tension tests according to ASTM A370 on

  specimens taken from the flats of the section or from the virgin

  material

- The magnitude of the maximum load observed and description of any

  events during the test such as the appearance of local buckles

- A plot and a table of axial shortening values versus axial load

  if such readings are taken

- Plot of local distortions if measured.

A4. EVALUATION OF TEST RESULTS

The effective area A_e or the effective area at ultimate load A_{eu} determined in any of the subsections of this section shall not be taken larger than the unreduced area A.

A4.1 LENGTH SHORTER THAN 20 TIMES r_{min}

If the length of the column is not longer than 20 times minimum radius of gyration of the section, r_{min} (net minimum section for perforated sections), the effective area A_e for a given stress f on the effective section shall be calculated as follows:

$$A_e = A - (A - A_{eu})(f/F_y)^n \qquad \text{Eq. A4.1-1}$$

where

$$n = A_{eu}/A \qquad \text{Eq. A4.1-2}$$

A = full unreduced area of an unperforated section and the net minimum area of a perforated section.

Alternatively, the value of A_e can be calculated on the basis plots of observed axial shortening versus stress on the effective area as described in Section A4.4.

A4.2 LENGTH LONGER THAN 20 TIMES r_{min}

When the length is larger than 20 r_{min}, the test results can be evaluated using the proposed provisions and the following procedure shall be used:

1. Determine failure stress F_n using the Specification

2. Determine A_e

$$A_e = P_u/P_n \qquad \text{Eq. A4.2-1}$$

3. Calculate A_{eu} with the following equation:

$$A_{eu} = A - (A - A_e)/F_n/F_y)^n \qquad\qquad \text{Eq. A4.2-2}$$

where $n = A_{eu}/A$ $\qquad\qquad\qquad\qquad$ Eq. A4.2-3

For the first try take $n = .2$

4. Using the value of A_{eu} obtained determine a new value of n and
    A_{eu} by Eqs. A4.2-3 and -2, respectively

5. Repeat step 3 until the value of A_{eu} used in Eq. A4.2-3 equals
    the value of A_{eu} calculated by Eq. A4.2-2

6. With the value of A_{eu} converged upon in step 5 use Eq. A4.1-1 of
    Section A4.1 to obtain A_e for any value of f.

A4.3 EVALUATION OF MULTIPLE COLUMN TEST RESULTS

For a given geometry and thickness the value of the number of tests
to be carried out shall be determined in accordance with the present AISI
Specification Section 6.2. According to this section, first three
specimens are tested. The values of A_{eu} determined for any test does not
differ from the mean of all the tests by more than 10 percent then the
mean value A_{eu} is used. If the deviation from the mean is more than 10
percent three more tests are conducted. Then the average of the three
lowest are regarded as the result A_{eu}.

The results of multiple tests shall be adjusted to the nominal
thickness and yield stress using Sections A4.3.2 and .3 below. The means
and deviations used in deciding whether three or six tests are to be
carried out will be based on the values of A_{eu} adjusted for variations in
yield stress and thickness. The resulting A_{eu} value is property of the
section that may be tabulated for different sections. Extrapolations of
this value for properties varying from those of the test specimens may be
carried out according to Sections A4.3.2 and .3.

If the same section configuration (including perforation patterns and dimensions if any) is used for different thicknesses, a series of tests can be carried out and evaluated for the thinnest and the thickest sections. Then interpolations may be carried out using Section A4.3.1 for intermediate thicknesses.

A4.3.1   INTERPOLATION FOR THICKNESSES NOT TESTED

For sections with identical cross-sectional dimensions and hole dimensions and locations produced in a variety of thicknesses, A_{eu} for a thickness t can be determined by interpolation from the results of tests on specimens with the minimum and maximum thicknesses, t_1 and t_2, respectively, as follows:

$$\frac{A_{eu}}{A} = \frac{A_{eu1}}{A_1} + \frac{\frac{A_{eu2}}{A_2} - \frac{A_{eu1}}{A_1}}{(t_1 - t_2)} (t_1 - t) \qquad \text{Eq. A4.3.1-1}$$

where A_1 and A_2 are the full unreduced areas of the sections with minimum and maximum thicknesses. A_{ue1} and A_{eu2} are the effective areas of the sections with minimum and maximum thicknesses at ultimate stub column loads.

A4.3.2   EXTRAPOLATION FOR YIELD STRESS

If a specimen with yield stress F_{yt} is tested and A_{eu} equal to A_{eut} is obtained, A_{eu} for a given F_y can be calculated using the following procedure:

For yield strength F_y smaller than F_{yt}, the value of A_{eu} can be taken as the lower of the two values obtained from Eqs. A4.3.2-1 and -2:

$$A_{eu}/A = 1 - (1 - A_{eut}/A)(F_y/F_{yt}) \qquad \text{Eq. A4.3.2-1}$$

$$A_{eu}/A = (A_{eut}/A)(F_{yt}/F_y)^{0.4} \qquad \text{Eq. 4.3.2-2}$$

For yield strength F_y larger than F_{yt}, the value of A_{eu} can be

obtained from Eqs. A4.3.2-2.

A4.3.3 EXTRAPOLATION FOR THICKNESS

If a specimen of thickness t_t is tested and A_{eu} equal to A_{eut} is

obtained, the value of A_{eu} for a thickness t varying by not more than 20

percent from t_t can be calculated by the following equation:

$$A_{eu}/A = (A_{eut}/A)(t/t_t)$$ Eq. A4.3.3-1

A4.4 USE OF AXIAL SHORTENING MEASUREMENTS IN DESIGN

At any axial, P, in a stub column test, the effective area, A_e, and

the stress on the effective area, f, can be calculated using the

equations below. In all cases the value of A_e or the value of A_{eu} at

ultimate load should not be taken greater than A, full unreduced area of

the section.

$$A_e = P D_u/F_y D)$$ Eq. A1

$$f = F_y D/D_u$$ Eq. A2

where F_y is the yield stress of the material, D is the axial shortening

at load P and D_u is the axial shortening at ultimate load.

If n number of readings are taken A_e and f for the reading number i,

A_{ei} and f_i, respectively, can be calculated using Eqs. A1 and A2. The

following expression can be used for determining A_e for any stress f:

$$A_e/A = 1 - (1 - A_{eu}/A)[(f - f_o)/(F_y - f_o)]^b$$

where f_o is the value of stress above which the section is not fully

effective.   The exponent b can be determined by a least squares approach

as

$$b = \frac{\sum\limits_{i=1}^{n} (X_i)(Y_i) - a \sum\limits_{i=1}^{n} X_i}{\sum\limits_{i=1}^{n} (X_i)^2}$$

where $X_i = \ln [f_i - f_o)/(F_y - f_o)]$

$Y_i = \ln (1 - A_{ei}/A)$

$a = \ln (1 - A_{eu}/A)$

ln designates natural logarithm

It is not possible to express a simple averaging process for

obtaining a design curve. The number of tests may be decided upon the

basis of A_{eu}, but the values should be selected as the lowest of the

values obtained from multiple tests for each value of f.

Page intentionally left blank.

REFERENCES

American Iron and Steel Institute (1986), "Specification for the Design of Cold-Formed Steel Structural Members", Washington, D.C.

Canadian Standards Association (1984), "Cold Formed Steel Structural Members - A National Standard of Canada"

Chilver, A. H. (1953), "The Stability and Strength of Thin-Walled Steel Struts", The Engineer, Vol. 196, August, 1953.

Cohen, J. M. and Peköz, T., Project Director (1987), "Local Buckling Behavior of Plate Elements", Research Report, Department of Structural Engineering, Cornell University, Ithaca, N.Y. (to be published).

Dawson, R. G. and Walker, A. C. (1972), "Postbuckling of Geometrically Imperfect Plates", Journal of the Structural Division, ASCE, January 1972.

Desmond, T. P., Peköz, T. and Winter, G. (1981a), "Edge Stiffeners for Thin-Walled Members", Journal of the Structural Division, ASCE, February 1981.

Desmond, T. P., Peköz, T. and Winter, G. (1981b), "Intermediate Stiffeners for Thin-Walled Members", Journal of the Structural Division, ASCE, April 1981.

Desmond, T. P., Peköz, T. and Winter, G. (1978), "Local and Overall Buckling of Cold Formed Compression Members", Department of Structural Engineering Report, Cornell University.

DeWolf, J. T., Peköz, T. and Winter, G. (1973), "Local and Overall Buckling of Cold Formed Compression Members", Department of Structural Engineering Report, Cornell University.

DeWolf, J. T., Peköz, T. and Winter, G. (1974), "Local and Overall Buckling of Cold Formed Steel Members", Journal of the Structural Division, ASCE, October 1974.

Graves-Smith, T. R. (1969), "The Ultimate Strength of Locally Buckled Columns of Arbitrary Length", Thin-Walled Structures, Edited by Rockey, K. C. and Hill, V. H., Crosby Lockwood, London.

He, Bao-Kang (1981), "Purlin Tests", Research Report, Department of Structural Engineering, Cornell University, Ithaca, N.Y.

He, Bao-Kang and Peköz, T., Project Director (1982), "Behavior of Cold-Formed Steel Angle Sections", Research Report No. 82-5, Department of Structural Engineering, Cornell University, Ithaca, N.Y.

Johnson, D. L. (1976), "Buckling of Beam Compression Flanges", A Report Submitted to American Iron and Steel Institute, Butler Manufacturing Company, November 1976.

Kalsner, B. (1977), "Post Buckling Behavior and Load Carrying Capacity of
Thin-Walled Box and Hat Sections", Department of Structural Engineering,
Division of Technology, Lund, Sweden.

Kalyanaraman, V., Peköz, T. and Winter, G. (1972), "Performance of
Unstiffened Compression Elements", Department of Structural Engineering
Report, Cornell University.
öKalyanaraman, V. and Peköz, T. (1978), "Analytical Study of Unstiffened
Elements", Journal of the Structural Division, ASCE, September 1978.

LaBoube, R. A. and Yu, W. W., Project Director (1978), "Structural
Behavior of Beam Webs Subjected to Bending Stress", Final Report, Civil
Engineering Study 78-1, University of Missouri-Rolla, Mo.

Loh, T. S. and Peköz, T., Project Director (1985), "Combined Axial Load
and Bending in Cold-Formed Steel Members", Department of Structural
Engineering Report, Cornell University.

Loughlan, J. (1979), "Mode Interaction in Lipped Channel Columns Under
Concentric and Eccentric Loading," Ph.D. Thesis, Department of Mechanics
of Materials, University of Strathclyde, Glasgow.

Madugula, M. K., Prabhu, T. S. and Temple, M. C. (1983), "Ultimate
Strength of Concentrically Loaded Cold-Formed Angles", Canadian Journal
of Civil Engineering 10.606.

Mulligan, G. P. and Peköz, T. (1984), "Locally Buckled Thin-Walled
Columns", Journal of the Structural Division, ASCE, November 1984.

Mulligan, G. P. and Peköz, T. Project Director (1983), "The Influence of
Local Buckling on the Structural Behavior of Single Symmetric Cold Formed
Steel Columns", Department of Structural Engineering Report, Cornell
University.

Ortiz-Colberg, R. and Peköz, T., Project Director (1981), "Load Carrying
Capacity of Perforated Cold-Formed Steel Columns", Research Report No.
81-12, Department of Structural Engineering, Cornell University, Ithaca,
N.Y.

Peköz, T. and Winter, G. (1967), "Torsional-Flexural Buckling of Thin-
Walled Sections under Eccentric Load", Department of Structural
Engineering Report, Cornell University.

Peköz, T. and Winter, G. (1969), "Torsional-Flexural Buckling of
Thin-Walled Sections under Eccentric Load", Journal of the Structural
Division, ASCE, May 1969.

Peköz, T. (1977), "Post Buckling Interaction of Plate Elements", Progress
Report to Swedish Building Research Council, Department of Structural
Engineering, Cornell University.

Peköz, T. (1979a), "Design of Cold-Formed Steel Racks", Thin-Walled
Structures, Edited by J. Rhodes and A. C. Walker.
Peköz, T. (1979b), "Stub Column Tests", Memorandum, Department of

Structural Engineering, Cornell University.

Rack Manufacturers Institute (1979), "Specification for Design, Testing and Utilization of Industrial Storage Racks".

Thomasson, P. O. (1978), "Thin-Walled C-Shaped Panel in Axial Compression", Document D1:1978, Swedish Council for Building Research, Stockholm, Sweden.

Timoshenko, S. and Gere, J. M. (1961), "Theory of Elastic Stability", Second Edition, McGraw-Hill Book Company, Inc., N.Y.

van Neste, A. J. (1983), "A Practical Method for the Calculation of Steel Sheeting in Bending", Report, Department of Architecture, Building Science and Urban Planning, Structural Engineering, Eindhoven, the Netherlands.

Weng, C. C. and Peköz, T., Project Director (1986), "Subultimate Behavior of Uniformly Compressed Stiffened Plate Elements", Research Report, Department of Structural Engineering, Cornell University, Ithaca, N.Y., (to be published).

Wilhoit, G., Zandonini, R. and Zavellani, A. (1984), "Behavior and Strength of Angles in Compression: An Experimental Investigation", Paper presented in the ASCE Annual Convention and Structures Congress.

Winter, G (1947), "Strength of Thin Steel Compression Flanges", Transactions, ASCE, Vol. 112.

PAGE INTENTIONALLY LEFT BLANK

TABLES AND FIGURES

TABLE 2.3-1
EVALUATION OF TEST RESULTS

Comp. Flange (1)	Web (2)	Test on (3)	Sources (4)	No. (5)	Mean	C.O.V.
U	F	S	A, B	14	1.242	.052
U	F	B	A	16	1.201	.081
E	F	S	C	28	1.013	.060
E	F	F	C	4	1.130	.093
ES	F	B	D	8	1.146	.046
U	P	S	E	8	1.114	.064
U	P	S	F	12	.970	.077
U	P	S	J	7	1.015	.044
U	P	B	G	23 (6)	.951	.105
UW	P	B	H	9	.954	.026
ST	P	B	K	16	1.032	.067
ST	P	B	I	14	.932	.061
ST	P	B	L	54	.891 (7)	.106 (7)
ST	P	B	L	54	.988 (8)	.060 (8)

(1) Compression flange
　　U Unstiffened
　　E Edge stiffened
　　ES Edge stiffened with a sloping stiffener
　　ST Stiffened
　　UW Unstiffened (built-up I section by welding)

(2) Web
　　F Fully effective
　　P Partially effective

(3) Tests on
　　S Stub Columns
　　B Beams

(4) Sources
　　A.　Kalyanaraman, Peköz and Winter (1972)
　　B.　DeWolf, Peköz and Winter (1973)
　　C.　Desmond, Peköz and Winter (1978)
　　D.　Cohen and Peköz (1987)
　　E.　Mulligan and Peköz (1983)
　　F.　Chilver (1953)
　　G.　LaBoube and Yu (1978)
　　H.　Johnson (1976)
　　I.　Kalsner (1977)
　　J.　Peköz (1977)
　　K.　LaBoube (1983)
　　L.　van Neste (1983)

(5) Number of tests

(6) Only specimens without calculated inelastic reserve strength considered.

(7) Sections had large corner radii. Actual corner radius used in calculations.

(8) Same sections as in (7). Corner radii assumed equal to thickness.

TABLE 2.4.1-1
DIMENSIONS OF TEST SPECIMEN SECTIONS[1]

Specimen[2]	W (in)	W (in)	T (in)	Width-Thickness[3] Single Thickness Element	Width-Thickness Double Thickness Element
			(a) Stiffened Sections		
S-1	2.0	3.5	0.058	57.2	16.7
S-2	2.0	5.0	0.058	83.0	16.7
S-3	2.0	7.0	0.058	117.4	16.7
S-4	2.0	9.0	0.058	151.8	16.7
			(b) Unstiffened Sections		
U-1	1.0	3.0	0.058	16.2	24.8
U-2	1.25	3.0	0.058	20.5	24.8
U-3	1.5	3.0	0.058	24.8	24.8
U-4	1.75	3.0	0.058	29.1	24.8

[1] See Fig. 2.4-1 for cross-sectional notation
[2] Inside corner radii of all specimens were extremely small and may be considered as zero.
[3] Width based on distance to inside of adjoining element.

TABLE 3.3-1
LOCALLY STABLE BEAM-COLUMNS
EVALUATION OF TEST RESULTS
Hat Sections of Peköz and Winter (1967)

Specimen	w_1 (in)	w_2 (in)	w_3 (in)	t (in)	L (in)	f_y (ksi)	e_x (in)	e_y (in)	$\dfrac{P_{uexp}}{P_{na}}$	$\dfrac{P_{uexp}}{P_{nb}}$
H1-LS-1	1.200	1.650	.450	.058	53.0	45.0	0.10	0.	1.03	1.03
H1-LS-2	1.200	1.650	.450	.058	53.0	45.0	0.90	0.	1.07	1.03
H1-LS-2	1.200	1.650	.450	.058	53.0	45.0	1.40	0.	0.97	0.97
H2-LS-1	0.950	1.925	.506	.058	53.0	45.0	0.	0.	0.91	0.91
H2-LS-2	0.950	1.925	.506	.058	53.0	45.0	1.33	0.	1.05	1.05
H2-LS-3	0.950	1.925	.506	.058	53.0	45.0	1.86	0.	0.90	0.90
H3-LS-1	0.950	1.450	.450	.058	53.0	45.0	0.	0.	0.91	0.91
H3-LS-2	0.950	1.450	.450	.058	53.0	45.0	0.76	0.	1.07	1.07
H3-LS-3	0.950	1.450	.450	.058	53.0	45.0	1.26	0.	1.00	1.00
H4-LS-1	1.296	1.719	.445	.048	53.0	45.0	0.	0.	1.03	1.03
H4-LS-2	1.296	1.719	.445	.048	53.0	45.0	0.95	0.	1.03	1.03
H4-LS-3	1.296	1.719	.445	.048	53.0	45.0	1.45	0.	1.11	1.11
H5-LS-1	0.968	1.969	.460	.048	53.0	45.0	0.	0.	1.06	1.06
H5-LS-2	0.968	1.969	.460	.048	53.0	45.0	1.02	0.	1.05	1.05
H5-LS-3	0.968	1.969	.460	.048	53.0	45.0	1.52	0.	1.08	1.08
H6-LS-1	0.968	1.484	.460	.048	53.0	45.0	0.	0.	1.06	1.06
H6-LS-2	0.968	1.484	.460	.048	53.0	45.0	0.76	0.	1.13	1.13
H6-LS-3	0.968	1.484	.460	.048	53.0	45.0	1.27	0.	1.14	1.14
Mean									1.03	1.03
Standard Deviation									0.07	0.07
Coefficient of Variation (%)									7	7

TABLE 3.3-2
LOCALLY STABLE BEAM-COLUMNS
EVALUATION OF TEST RESULTS
Lipped Channel Sections of Loh and Peköz (1985)

Specimen	w_1 (in)	w_2 (in)	w_3 (in)	t (in)	L (in)	r_i (in)	f_y (ksi)	e_x (in)	e_y (in)	$\dfrac{P_{uexp}}{P_{na}}$	$\dfrac{P_{uexp}}{P_{nb}}$
LC1-LS-1	2.922	2.922	.711	.078	39.0	.145	45.5	1.50	0.	1.13	1.13
LC1-LS-2	2.922	2.922	.711	.078	51.0	.145	45.5	1.50	0.	1.05	1.05
LC1-LS-3	2.922	2.922	.711	.078	63.0	.145	45.5	1.50	0.	0.94	0.94
LC2-LS-1	2.868	2.868	.684	.132	36.6	.212	41.9	-2.00	0.	1.33	1.27
LC2-LS-2	2.868	2.868	.684	.132	49.8	.212	41.9	-2.25	0.	1.27	1.21
LC2-LS-3	2.868	2.868	.684	.132	60.6	.212	41.9	-2.25	0.	1.25	1.19
Mean										1.16	1.13
Standard Deviation										0.15	0.12
Coefficient of Variation (%)										13	11

TABLE 3.3-3
LOCALLY STABLE BEAM-COLUMNS
EVALUATION OF TEST RESULTS
Lipped Channel Sections of Loh and Peköz (1985)

Specimen	w_1 (in)	w_2 (in)	w_3 (in)	t (in)	L (in)	r_i (in)	f_y (ksi)	e_x (in)	e_y (in)	$\dfrac{P_{uexp}}{P_{na}}$	$\dfrac{P_{uexp}}{P_{nb}}$
LC3-LS-1	2.900	1.600	.700	.073	52.0	.164	40.9	0.	1.45	1.16	1.04
LC3-LS-2	2.927	1.552	.713	.073	39.1	.161	39.1	0.	2.00	1.23	1.10
LC3-LS-3	2.927	1.552	.713	.073	51.1	.161	39.1	0.	2.00	1.19	1.05
LC3-LS-4	2.927	1.552	.713	.073	63.4	.161	39.1	0.	2.00	1.25	1.10
LC4-LS-1	2.910	1.566	.705	.090	39.1	.145	59.4	0.	2.50	1.18	1.03
LC4-LS-2	2.910	1.566	.705	.090	51.2	.145	59.4	0.	2.50	1.14	1.00
LC5-LS-1	2.868	2.868	.684	.132	51.2	.220	47.5	0.	2.03	1.01	0.93
LC5-LS-2	2.868	2.868	.684	.132	69.2	.220	47.5	0.	2.00	1.00	0.92
LC6-LS-1	2.925	2.925	.712	.075	51.5	.214	39.3	0.	2.38	1.21	1.18
LC6-LS-2	2.925	2.925	.712	.075	63.5	.214	39.3	0.	2.13	1.21	1.17
LC7-LS-1	3.868	2.868	.684	.132	50.2	.208	37.4	0.	2.25	1.22	1.12
LC7-LS-2	2.868	2.868	.684	.132	69.0	.208	37.4	0.	2.22	1.19	1.09
LC8-LS-1	3.923	2.923	.711	.077	40.1	.236	41.6	0.	1.50	1.02	1.00
LC8-LS-2	3.923	2.923	.711	.077	51.1	.236	41.6	0.	1.50	1.02	0.99
LC8-LS-3	3.923	2.923	.711	.077	63.8	.236	41.6	0.	1.50	1.02	0.99
LC8-LS-4	3.924	2.924	.712	.076	75.6	.236	42.5	0.	1.66	1.00	0.96
LC8-LS-5	3.924	2.924	.712	.076	87.6	.236	42.5	0.	2.00	1.04	0.99

Mean										1.12	1.04
Standard Deviation										0.10	0.08
Coefficient of Variation (%)										9	8

TABLE 3.3-4
LOCALLY STABLE BEAM-COLUMNS
EVALUATION OF TEST RESULTS
Lipped Channel Sections from Loh and Peköz (1985)

Specimen	w_1 (in)	w_2 (in)	w_3 (in)	t (in)	L (in)	r_i (in)	f_y (ksi)	e_x (in)	e_y (in)	$\frac{P_{uexp}}{P_{na}}$	$\frac{P_{uexp}}{P_{nb}}$
LC9-LS-1	3.396	2.334	.604	.104	39.5	.201	58.2	1.50	2.00	1.18	1.08
LC9-LS-2	3.396	2.334	.604	.104	52.8	.201	58.2	1.50	2.00	1.13	1.08
LC9-LS-3	3.396	2.334	.604	.104	64.8	.201	58.2	1.50	2.00	1.05	1.00
LC9-LS-4$	3.395	2.395	.603	.105	62.6	.192	65.3	-2.00	2.50	0.91	0.85
LC10-LS-1*	3.899	2.899	.949	.101	39.2	.235	54.9	-2.00	2.50	1.36	1.31
LC10-LS-2*	3.899	2.899	.949	.101	51.2	.235	54.9	-2.00	2.50	1.33	1.27
LC10-LS-3	3.899	2.899	.949	.101	63.2	.235	54.9	-2.00	2.50	1.30	1.24
LC11-LS-1	2.924	2.924	.712	.076	39.0	.205	48.8	2.00	2.50	1.28	1.27
LC11-LS-2	2.924	2.924	.712	.076	49.5	.205	48.8	2.50	2.00	1.27	1.25
LC11-LS-3	2.924	2.924	.712	.076	61.3	.205	48.8	2.00	2.50	1.16	1.14
Mean										1.23	1.18
Standard Deviation										0.10	0.11
Coefficient of Variation (%)										8	9

$ Premature failure of welds joining
end plates to column. Excluded
from statistical evaluation.

* Premature failure of welds joining
end plates to column. Included in
statistical evaluation.

TABLE 4.3-1

SECTIONS FOR PARAMETRIC STUDIES
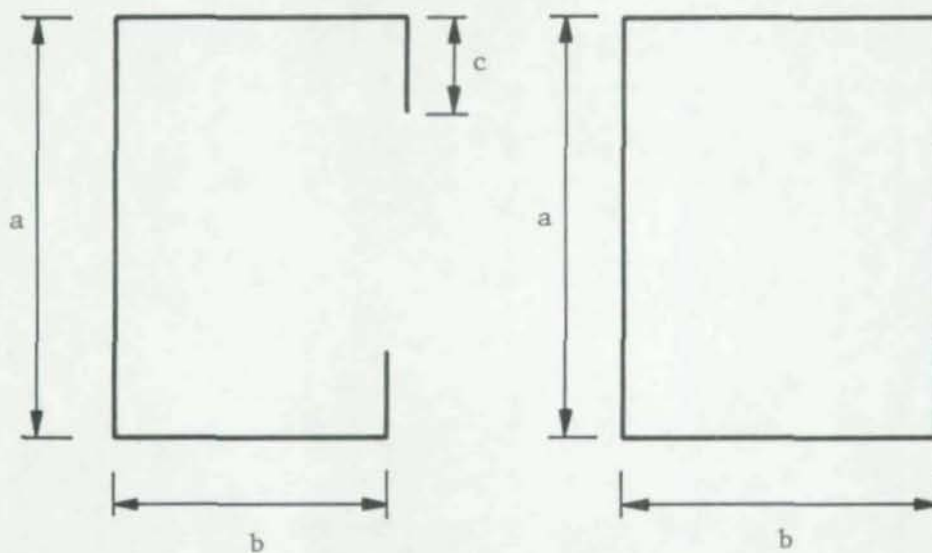
C- Section (C)   Tube (T)

Section	a (in)	b (in)	c (in)	t (in)	Fy (ksi)	a/t	b/t
C1-1	8.886	3.374	1.029	.061	62.9	145.67	55.31
C1-2	17.772	6.748	1.029	.061	62.9	291.34	110.62
C2-1	4.000	4.000	.750	.050	50.0	80.	80.
C2-2	8.000	8.000	.750	.050	50.0	160.	160.
C3-1	2.593	5.025	.793	.046	33.0	56.37	109.24
C3-1	5.186	10.060	.793	.046	33.0	112.74	218.98
T1-1	8.886	3.374		.061	62.9	145.67	55.31
T1-2	17.772	6.748		.061	62.9	291.34	110.62
T1-3	26.658	10.122		.061	62.9	937.02	165.93
T2-1	4.000	4.000		.050	50.0	80.	80.
T2-2	8.000	8.000		.050	50.0	160.	160.
T2-3	12.000	12.000		.050	50.0	320.	320.
T3-1	2.593	5.025		.046	33.0	56.37	109.24
T3-2	5.186	10.050		.046	33.0	112.11	218.48
T3-3	7.779	15.075		.046	33.0	169.11	372.72

TABLE 7.3-1
LOCALLY UNSTABLE BEAM-COLUMNS
EVALUATION OF TEST RESULTS
Lipped Channel Sections of Mulligan and Peköz (1983)

Specimen	w_1 (in)	w_2 (in)	w_3 (in)	t (in)	L (in)	r_i (in)	f_y (ksi)	e_x^* (in)	e_y^* (in)	$\dfrac{P_{uexp}}{P_n}$
GM1	6.119	3.148	.691	.045	63.0	.109	32.4	0.	0.	1.186
GM2	5.096	3.147	.649	.045	75.0	.107	32.0	0.	0.	1.323
GM3	6.134	3.146	.648	0.46	121.1	.109	32.0	0.	0.	1.189
GM4	6.072	3.152	.672	.045	121.0	.111	32.0	0.	0.	1.247
GM5	6.116	3.121	.696	.048	75.0	.116	32.5	0.	0.	1.323
GM6	9.072	3.154	.658	.045	72.0	.107	32.6	0.	0.	1.321
GM7	9.088	3.149	.666	.045	95.1	.111	32.4	0.	0.	1.291
GM8	9.097	3.150	.662	.044	118.0	.106	32.4	0.	0.	1.271
GM9	9.030	3.151	.702	.048	95.0	.116	33.1	0.	0.	1.399
GM10	4.468	4.432	.754	.048	99.2	.118	34.3	0.	0.	0.983
GM11	8.694	4.448	.761	.048	75.1	.114	31.8	0.	0.	1.256
GM12	8.725	4.428	.742	.048	99.1	.118	35.4	0.	0.	1.211
GM13	8.718	4.440	.729	.048	99.2	.118	33.9	0.	0.	1.213
GM14	6.125	3.124	.687	.047	75.0	.121	31.8	0.54	0.	1.136
GM15	6.108	3.134	.704	.048	75.7	.118	31.8	0.53	0.	0.927
GM16	6.100	3.135	.688	.048	75.7	.118	31.8	-0.98	0.	1.318
GM17	6.092	3.143	.690	.048	75.0	.116	32.5	0.21	0.	1.153
GM18	8.671	4.436	.742	.048	99.0	.105	33.1	0.52	0.	0.983

Mean	1.207
Standard Deviation	0.131
Coefficient of Variation (%)	10.85
Number of Specimens	18

* With respect to the centroid of the full section.

TABLE 7.3-2
LOCALLY UNSTABLE BEAM-COLUMNS
EVALUATION OF TEST RESULTS
Lipped Channel Sections of Thomasson (1978)

Specimen	w_1 (in)	w_2 (in)	w_3 (in)	t (in)	L (in)	f_y (ksi)	e_x* (in)	e_y* (in)	$\frac{P_{uexp}}{P_n}$
A71	11.775	3.949	.771	.025	105.9	56.7	0.	0.	1.029
A74	11.795	3.965	.811	.025	105.9	57.3	0.	0.	1.029
A75	11.775	3.957	.787	.025	105.9	57.7	0.	0.	0.985
A76	11.814	3.944	.795	.026	105.9	41.8	0.	0.	0.972
A101	11.803	3.957	.795	.037	105.9	67.3	0.	0.	1.082
A102	11.803	3.957	.787	.037	105.9	66.7	0.	0.	1.031
A103	11.783	3.961	.771	.037	105.9	66.7	0.	0.	1.094
A104	11.742	9.921	.768	.038	105.9	68.9	0.	0.	0.964
A151	11.783	3.937	.799	.057	105.9	55.4	0.	0.	1.402
A152	11.814	3.937	.795	.056	105.9	55.0	0.	0.	1.316
A153	11.806	3.929	.819	.054	105.9	57.3	0.	0.	1.364
A154	11.835	3.952	.921	.055	105.9	57.0	0.	0.	1.347
A156	11.785	3.926	.803	.055	105.9	55.3	0.	0.	1.322

Mean	1.149
Standard Deviation	0.171
Coefficient of Variation (%)	14.84
Number of Specimens	13

* With respect to the centroid of the full section.

TABLE 7.3-3
LOCALLY UNSTABLE BEAM-COLUMNS
EVALUATION OF TEST RESULTS
Lipped Channel Sections of Loh and Peköz (1985)

Specimen	w_1 (in)	w_2 (in)	w_3 (in)	t (in)	L (in)	r_i (in)	f_y (ksi)	e_x* (in)	e_y* (in)	$\dfrac{P_{uexp}}{P_n}$
LC1-LU-1	6.870	2.461	.710	.073	76.0	.240	55.9	0.	2.1	1.155
LC1-LU-2	6.870	2.461	.710	.073	76.0	.240	55.9	0.	12.0	1.037
LC1-LU-3	6.870	2.461	.710	.073	76.0	.240	55.9	0.	6.0	1.202
LC2-LU-1	9.086	3.136	.684	.050	99.9	.128	35.1	0.	6.0	1.158
LC2-LU-2	9.071	3.129	.717	.050	99.9	.128	35.8	0.	9.0	1.048
LC3-LU-1	7.958	3.900	.624	.058	99.9	.098	43.4	0.	4.0	0.905
LC3-LU-2	8.001	3.919	.620	.058	99.9	.098	44.4	0.	8.0	1.006
LC3-LU-3	7.930	3.927	.631	.058	99.9	.098	43.2	0.	4.0	0.962
LC4-LU-1	8.881	3.379	1.023	.061	99.9	.283	62.1	0.	12.0	1.107
LC4-LU-2	8.881	3.379	1.023	.061	99.9	.283	62.1	0.	18.0	0.989
LC4-LU-3	8.873	3.383	1.026	.058	99.9	.301	62.9	0.	6.0	1.108
LC5-LU-1	7.882	3.399	1.028	.061	99.9	.283	58.5	0.	4.0	1.181
LC5-LU-2	7.882	3.399	1.028	.061	99.9	.283	58.5	0.	8.0	1.151
LC5-LU-3	7.884	3.394	1.032	.062	99.8	.297	58.6	0.	6.0	1.200
LC5-LU-4	7.884	3.394	1.032	.062	99.8	.297	58.6	0.	10.0	1.101
LC6-LU-1	9.351	3.436	1.222	.090	99.9	.269	71.7	0.	5.0	1.131
LC6-LU-2	9.351	3.436	1.222	.090	99.8	.269	71.7	0.	10.0	1.098

Mean	1.091
Standard Deviation	0.087
Coefficient of Variation (%)	7.95
Number of Specimens	17

* With respect to the centroid of the full section.

TABLE 7.3-4
LOCALLY UNSTABLE BEAM-COLUMNS
EVALUATION OF TEST RESULTS
Lipped Channel Sections of Loh and Peköz (1985)

Specimen	w_1 (in)	w_2 (in)	w_3 (in)	t (in)	L (in)	r_i (in)	f_y (ksi)	e_x* (in)	e_y* (in)	$\frac{P_{uexp}}{P_n}$
LC8-LU-1	8.887	3.379	1.031	.060	98.9	.284	61.2	−1.0	2.0	1.206
LC8-LU-2	8.887	3.379	1.031	.060	99.2	.284	61.2	−1.0	2.0	1.222
LC8-LU-3	8.886	3.374	1.029	.061	98.9	.298	62.9	−1.0	4.0	1.217
LC8-LU-4	8.886	3.374	1.029	.061	98.9	.298	62.9	−1.0	4.0	1.195
LC8-LU-5	8.879	3.375	1.021	.060	99.1	.299	63.2	−1.0	6.0	1.177
LC8-LU-6	8.879	3.375	1.021	.060	98.7	.299	63.2	−1.0	6.0	1.235
LC9-LU-1	7.874	3.400	1.031	.062	93.4	.282	69.9	0.38	3.94	1.011
LC9-LU-2	7.874	3.400	1.031	.062	93.1	.282	69.9	0.38	6.0	0.905
LC9-LU-3	7.885	3.404	1.031	.062	93.1	.251	70.3	0.38	6.0	0.945
LC9-LU-4	7.885	3.404	1.031	.062	93.1	.251	70.3	0.63	3.94	0.922
LC10-LU-1	9.375	3.439	1.221	.089	98.9	.286	70.6	0.	5.5	1.144
LC10-LU-2	9.375	3.439	1.221	.089	98.9	.286	70.6	0.	5.5	1.154
Mean										1.111
Standard Deviation										0.127
Coefficient of Variation (%)										11.45
Number of Specimens										12

* With respect to the centroid of the full section.

TABLE 7.3-5
LOCALLY UNSTABLE BEAM-COLUMNS
EVALUATION OF TEST RESULTS
Lipped Channel Sections of Loughlan (1979)

Specimen	w_1 (in)	w_2 (in)	w_3 (in)	t (in)	L (in)	f_y (ksi)	e_x^* (in)	e_y^* (in)	$\frac{P_{uexp}}{P_n}$
L1	3.998	1.991	.742	.032	75.	35.1	-0.29	0.	1.022
L2	3.981	1.988	.757	.031	51.	35.1	-0.29	0.	1.078
L3	4.045	2.471	1.001	.031	75.	35.1	-0.40	0.	0.987
L4	4.014	2.472	1.000	.032	63.	35.1	-0.40	0.	0.961
L5	4.001	2.480	1.013	.031	51.	35.1	-0.41	0.	1.065
L6	5.034	1.992	.735	.031	75.	35.1	-0.07	0.	1.138
L7	4.976	1.987	.742	.031	63.	35.1	-0.07	0.	1.103
L8	4.980	1.991	.753	.031	51.	35.1	-0.07	0.	1.125
L9	5.031	2.469	1.000	.031	75.	35.1	-0.18	0.	1.115
L10	5.015	2.481	1.004	.031	63.	35.1	-0.19	0.	1.130
L11	4.990	2.477	1.007	.032	51.	35.1	-0.19	0.	1.052
L12	5.981	1.998	.746	.032	75.	35.1	-0.18	0.	1.071
L13	5.992	1.992	.774	.032	63.	35.1	-0.18	0.	1.044
L14	5.974	1.987	.749	.032	51.	35.1	-0.18	0.	1.088
L15	6.061	2.472	.998	.031	75.	34.1	0.	0.	1.157
L16	6.061	2.476	1.008	.032	63.	35.1	0.	0.	1.109
L17	5.985	2.480	1.006	.031	51.	35.1	0.	0.	1.163
L18	7.009	1.976	.742	.031	75.	35.1	-0.22	0.	1.124
L19	6.976	1.987	.745	.031	63.	35.1	-0.22	0.	1.129
L20	6.995	1.988	.771	.032	51.	35.1	-0.22	0.	1.090
L21	7.020	2.478	.992	.031	75.	35.1	-0.16	0.	1.036
L22	7.021	2.480	.996	.031	63.	35.1	-0.16	0.	1.139
L23	6.950	2.481	1.017	.031	51.	35.1	-0.16	0.	1.030
L24	5.997	1.941	.699	.064	75.	33.8	0.	0.	1.638
L25	5.994	2.430	.967	.065	75.	33.8	-0.08	0.	1.669
L26	5.986	2.428	.974	.066	63.	33.8	-0.08	0.	1.594
L27	5.960	2.434	.978	.065	51.	33.8	-0.08	0.	1.563
L28	7.010	1.940	.708	.064	75.	33.8	-0.11	0.	1.562
L29	6.998	1.944	.707	.065	63.	33.8	-0.11	0.	1.550
L30	6.933	1.933	.712	.065	51.	33.8	-0.11	0.	1.561
L31	7.017	2.435	.969	.064	75.	33.8	0.	0.	1.710
L32	7.006	2.426	.975	.064	63.	33.8	0.	0.	1.622
L33	6.958	2.441	.980	.064	51.	33.8	0.	0.	1.636

Mean   1.244
Standard Deviation   0.251
Coefficient of Variation (%)   20.17
Number of Specimens   33

* With respect to the centroid of the full section.

TABLE 8.2-1
CROSS SECTIONAL DIMENSIONS
Specimens of Madugula, Prabhu and Temple (1984)

Spec. No.	b_{nom} (in)	t_{nom} (in)	r_y (in)	b_{used} (in)	w/t	F_y (ksi)
1	1.952751	.15748	.3684	1.803	9.449	67.56
2	2.728341	.11811	.5331	2.611	20.107	67.56
3	1.980311	.16929	.3871	1.896	9.200	59.38

Notes: b_{nom} is the nominal leg length given in the paper
r_y is the least radius gyration given in the paper
b_{used} is the leg dimension calculated from the value of
r_y given in the paper assuming sharp corners.   This
value is used in all calculations
w is the flat width calculated as b–2t
Sections 1 and 2 are cold formed.   Section 3 is hot rolled

Dimensions are given to as many significant figures as
given in the paper

TABLE 8.2-2
CROSS SECTIONAL DIMENSIONS
Specimens of Wilhoit, Zandonini and Zavellani (1983)

Spec. No.	b_{nom} (in)	t (in)	I_y (in)	b_{used} (in)	b/t (in)	F_y (ksi)
4	2.5591	.1575	.1723	2.359	10.59	54.68
5	1.7717	.1181	.0419	1.620	11.26	53.54

Notes: b_{nom} is the nominal leg length given in the paper
I_y is the last moment of inertia given in the paper
b_{used} is the leg dimension calculated from the value
of r_y given in the paper assuming sharp corners. This
value is used in all calculations
b is the flat width calculated based on the information
given in the paper
The dimensions are converted from metric units.

TABLE 8.3-1
EFFECT OF INITIAL SWEEP ON LIPPED CHANNEL COLUMNS

$c = .9$ in.

$F_y = 45$ ksi.

$t = .105$ in.
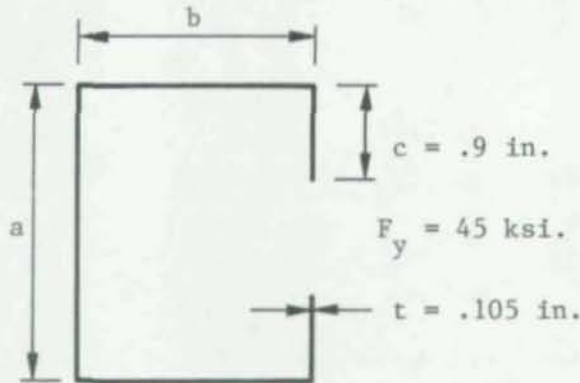
a x b (in)	Length (in)	$e_y = 0$ P_{ult1} (k)	$e_y = L/1000$ P_{ult2} (k)	$\dfrac{P_{ult1}}{P_{ult2}}$
3 x 1	60	19.33	18.42	1.05
	100	7.66	7.35	1.04
3 x 3	60	32.17	30.70	1.05
	100	14.73	14.12	1.04

Note: e_y is the maximum amplitude of sweep perpendicular to
        the plane of symmetry

TABLE 9.1-1
STUB COLUMN TEST RESULTS

Spec. No.	F_y (ksi)	d (in)	P_u (k)	R
1	48.50	.00	15.10	1.019
2	47.10	.00	14.80	1.024
3	49.60	.50	14.50	1.006
4	47.10	.75	14.15	1.054
5	49.60	1.04	14.05	1.028
6	51.55	1.25	13.80	.996
7	48.50	1.50	12.65	.992
8	51.55	1.75	13.60	1.035
9	49.60	.50	15.50	1.075
10	48.50	1.04	14.68	1.097
11	48.50	1.50	14.50	1.137
12	47.00	.00	27.90	1.274
13	47.60	1.04	24.60	1.159
14	47.60	1.50	24.00	1.214

Mean*   1.072
St. Dev.*   0.086

All sections assumed to have the average overall dimensions shown
in Fig. 9.1-1.
Specimens 1-11 t = .05 in, Specimens 12-14 t = 0.076 in

*Excluding result on specimen 12 which is obviously in error.

TABLE 9.1-2
COLUMN TEST SPECIMENS

Spec. No.	F_y (ksi)	d (in)	F_y (ksi)	s (*)	s (*)
1	63.00	.50	51.60	10.05	6.00
2	63.00	.50	45.70	8.50	1.00
3	27.00	1.00	42.90	11.35	1.00
4	27.00	.00	44.90	12.40	.00
5	27.00	1.00	42.90	11.55	6.00
6	63.00	1.00	46.10	8.50	1.00
7	63.00	1.50	45.50	8.45	1.00
8	63.00	1.00	41.90	7.05	6.00
9	39.00	1.00	43.80	9.40	1.00
10	38.90	1.50	42.30	10.10	1.00
11	39.00	.00	43.80	8.65	.00
12	27.00	.00	41.90	11.90	.00
13	63.00	.00	42.90	8.00	.00
14	39.10	.50	42.90	9.60	1.00
15	45.00	.00	48.30	22.40	.00
16	51.00	1.00	48.10	17.20	1.00
17	51.10	1.50	48.10	15.00	1.00
18	45.00	1.00	47.60	18.20	2.00
19	27.00	1.50	51.50	21.20	1.00
20	45.00	1.00	47.60	19.00	8.00
21	45.00	1.00	44.50	15.85	4.00
22	45.00	1.50	46.70	20.00	1.00
23	45.00	1.50	46.70	15.85	6.00
24	45.00	1.00	44.50	16.20	3.00
25	62.50	.00	48.30	13.44	.00
26	45.00	1.00	45.80	19.10	1.00
27	27.00	1.00	48.30	21.90	1.00
28	27.00	1.00	42.30	22.40	1.00
29	27.00	.00	42.30	22.00	.00
30	27.00	.00	42.30	22.40	.00
31	45.00	1.00	46.70	18.10	6.00
32	63.00	1.00	47.90	13.30	1.00

(*) s = 0 for column without perforations
   s = 1 for column with one perforation at midheight
   s > 1 spacing of the perforations along the length of the column in inches

All sections assumed to have the average overall dimensions shown in Fig. 9.1-1.
Specimens 1-14 t = .05 in, Specimens 15-32 t = .076 in

TABLE 9.3.1-1
EVALUATION OF COLUMN TEST RESULTS
(All test results)

Spec. No.	R1	R2	R3	R4	R5
1	1.692	1.275	1.525	1.202	1.208
2	1.469	1.091	1.317	1.028	1.028
3	1.458	1.038	1.186	.936	.939
4	1.258	.986	1.258	.986	.986
5	1.484	1.056	1.207	.952	.970
6	1.628	1.160	1.315	1.026	1.028
7	1.808	1.237	1.311	1.022	1.027
8	1.391	.984	1.113	.869	.887
9	1.318	.922	1.069	.829	.831
10	1.613	1.077	1.170	.912	.917
11	.984	.763	.984	.763	.763
12	1.262	1.000	1.262	1.000	1.000
13	1.257	.980	1.257	.980	.980
14	1.229	.906	1.105	.859	.860
15	1.299	1.155	1.299	1.155	1.155
16	1.570	1.138	1.080	.969	.951
17	1.611	1.089	.943	.846	.852
18	1.518	1.105	1.060	.946	1.021
19	1.584	1.095	.999	.880	.890
20	1.584	1.154	1.107	.988	1.007
21	1.372	1.005	.945	.858	.983
22	1.983	1.342	1.172	1.052	1.059
23	1.571	1.064	.929	.834	.855
24	1.402	1.027	.965	.877	.925
25	.961	.961	.961	.961	.961
26	1.627	1.189	1.127	1.016	1.019
27	1.471	1.103	1.071	.956	.960
28	1.661	1.261	1.183	1.085	1.091
29	1.162	1.066	1.162	1.066	1.066
30	1.183	1.085	1.183	1.085	1.085
31	1.525	1.112	1.061	.952	.977
32	1.545	1.150	.966	.966	.968
MEAN	1.453	1.080	1.134	.964	.975
ST. DEV.	.223	.116	.140	.098	.094

TABLE 9.3.1-2
EVALUATION OF COLUMN TEST RESULTS
(Specimens without perforations)

Spec. No.	R1	R2	R3	R4	R5
4	1.258	.986	1.258	.986	.986
11	.984	.763	.984	.763	.763
12	1.262	1.000	1.262	1.000	1.000
13	1.257	.980	1.257	.980	.980
15	1.299	1.155	1.299	1.155	1.155
29	1.162	1.066	1.162	1.066	1.066
30	1.183	1.085	1.183	1.085	1.085
MEAN	1.171	.999	1.171	.999	.999
ST. DEV.	.130	.116	.130	.116	.116

TABLE 9.3.1-3
EVALUATION OF COLUMN TEST RESULTS
(Specimens with one perforation at midheight)

Spec. No.	R1	R2	R3	R4	R5
2	1.469	1.091	1.317	1.028	1.028
3	1.458	1.038	1.186	.936	.939
6	1.628	1.160	1.315	1.026	1.028
7	1.808	1.160	1.315	1.026	1.028
9	1.318	.922	1.069	.829	.831
10	1.613	1.077	1.170	.912	.917
14	1.228	.906	1.105	.859	.860
16	1.570	1.138	1.080	.969	.971
17	1.611	1.089	.943	.846	.852
19	1.584	1.095	.999	.880	.890
22	1.983	1.342	1.172	1.052	1.059
26	1.627	1.189	1.127	1.016	1.019
27	1.471	1.103	1.071	.956	.960
28	1.661	1.261	1.183	1.085	1.091
32	1.545	1.150	.966	.966	.968
MEAN	1.572	1.120	1.134	.959	.963
ST. DEV.	.181	.116	.120	.080	.080

TABLE 9.3.1-4
EVALUATION OF COLUMN TEST RESULTS
(Specimens with multiple perforations)

Spec. No.	R1	R2	R3	R4	R5
1	1.692	1.275	1.525	1.202	1.208
5	1.484	1.056	1.207	.952	.970
8	1.391	.984	1.113	.869	.887
18	1.518	1.105	1.060	.946	1.021
20	1.584	1.154	1.107	.988	1.007
21	1.372	1.005	.945	.858	.893
23	1.571	1.064	.929	.834	.885
24	1.402	1.027	.965	.877	.925
31	1.525	1.112	1.061	.952	.977
MEAN	1.504	1.087	1.101	.942	.975
ST. DEV.	.105	.089	.183	.111	.102

TABLE 9.4-1
NONPRISMATIC COLUMNS
BUCKLING LOAD RATIOS (*)

RI \ RL	.10	.20	.30	.40	.50	.60
1.00	1.00	1.00	1.00	1.00	1.00	1.00
1.10	.98	.96	.95	.93	.92	.92
1.20	.96	.93	.90	.88	.86	.85
1.30	.94	.89	.86	.83	.80	.79
1.40	.93	.86	.82	.78	.75	.73
1.50	.91	.84	.78	.74	.71	.69
1.60	.89	.81	.75	.70	.67	.65

(*) Ratio of the buckling load for the nonprismatic column shown in Fig. 9.4-2a
to that for the prismatic column shown in Fig. 9.4-2b.

TABLE 9.4-2
NONPRISMATIC COLUMNS
BUCKLING LOAD RATIOS (*)

RI \ RL	.10	.20	.30	.40	.50	.60
1.00	1.00	1.00	1.00	1.00	1.00	1.00
1.10	.99	.98	.97	.97	.97	.97
1.20	.98	.96	.95	.94	.94	.94
1.30	.97	.94	.92	.91	.91	.91
1.40	.95	.92	.89	.88	.88	.89
1.50	.94	.89	.87	.85	.85	.86
1.60	.93	.87	.84	.82	.82	.84

(*) Ratio of the buckling load for the nonprismatic column shown in Fig. 9.4-2a
determined by the transcendental equation to that obtained by the approximate
equation.

TABLE 9.4-3
PARAMETERS FOR COLUMN SPECIMENS

Spec.	RI	RL
1	1.057	.087
2	1.057	.008
3	1.122	.037
4	1.000	.000
5	1.122	.185
6	1.131	.016
7	1.228	.024
8	1.131	.175
9	1.123	.026
10	1.212	.039
11	1.000	.000
12	1.000	.000
13	1.000	.000
14	1.055	.013
15	1.000	.000
16	1.150	.020
17	1.272	.029
18	1.146	.511
19	1.246	.056
20	1.146	.133
21	1.148	.267
22	1.266	.033
23	1.266	.267
24	1.148	.356
25	1.000	.000
26	1.147	.022
27	1.140	.037
28	1.144	.037
29	1.000	.000
30	1.000	.000
31	1.147	.178
21	1.157	.016

TABLE 9.4-4
PARAMETERS AND RESULTS OF CALCULATIONS

ALL COLUMNS

SP. NO.	RI	RL	R2	R4	R5
1	1.057	.087	1.275	1.202	1.208
2	1.057	.008	1.091	1.028	1.028
3	1.122	.037	1.038	.936	.939
4	1.000	.000	.986	.986	.986
5	1.222	.185	1.056	.952	.970
6	1.131	.016	1.160	1.026	1.028
7	1.228	.024	1.237	1.002	1.027
8	1.131	.175	.984	.869	.887
9	1.123	.026	.922	.829	.831
10	1.212	.039	1.077	.912	.917
11	1.000	.000	.763	.763	.763
12	1.000	.000	1.000	1.000	1.000
13	1.000	.000	.980	.980	.980
14	1.055	.013	.906	.859	.860
15	1.000	.000	1.155	1.155	1.155
16	1.150	.020	1.138	.969	.971
17	1.272	.029	1.089	.846	.852
18	1.146	.511	1.105	.946	1.021
19	1.246	.056	1.095	.880	.890
20	1.146	.133	1.154	.988	1.007
21	1.148	.267	1.005	.858	.893
22	1.266	.033	1.342	1.052	1.059
23	1.266	.267	1.064	.834	.885
24	1.148	.356	1.027	.877	.925
25	1.000	.000	.961	.961	.961
26	1.147	.022	1.189	1.016	1.019
27	1.140	.037	1.103	.956	.960
28	1.144	.037	1.261	1.085	1.091
29	1.000	.000	1.066	1.066	1.066
30	1.000	.000	1.085	1.085	1.085
31	1.147	.178	1.112	.952	.977
32	1.157	.016	1.150	.966	.968

TABLE 9.4-5
PARAMETERS AND RESULTS OF CALCULATIONS

UNPERFORATED COLUMNS

SP. NO.	RI	RL	R2	R4	R5
4	1.000	.000	.986	.986	.986
11	1.000	.000	.763	.763	.763
12	1.000	.000	1.000	1.000	1.000
13	1.000	.000	.980	.980	.980
15	1.000	.000	1.155	1.155	1.155
25	1.000	.000	.961	.961	.961
29	1.000	.000	1.066	1.066	1.066
30	1.000	.000	1.085	1.085	1.085

TABLE 9.4-6
PARAMETERS AND RESULTS OF CALCULATIONS

PERFORATED COLUMNS

SP. NO.	RI	RL	R2	R4	R5
1	1.057	.087	1.275	1.202	1.208
2	1.057	.008	1.091	1.028	1.028
3	1.122	.027	1.038	.936	.939
5	1.122	.185	1.056	.952	.970
6	1.131	.016	1.160	1.026	1.028
7	1.228	.024	1.237	1.022	1.027
8	1.131	.175	.984	.869	.887
9	1.123	.026	.922	.829	.831
10	1.212	.039	1.077	.912	.917
14	1.055	.013	.906	.859	.860
16	1.150	.020	1.138	.969	.971
17	1.272	.029	1.089	.846	.852
18	1.146	.511	1.105	.946	.021
19	1.246	.056	1.095	.880	.890
20	1.146	.133	1.154	.988	1.007
21	1.148	.267	1.005	.858	.893
22	1.266	.033	1.342	1.052	1.059
23	1.266	.267	1.064	.834	.885
24	1.148	.356	1.027	.877	.925
26	1.147	.022	1.189	1.016	1.019
27	1.140	.037	1.103	.956	.960
28	1.144	.037	1.261	1.085	1.091
31	1.147	.178	1.112	.952	.977
32	1.157	.016	1.150	.966	.968
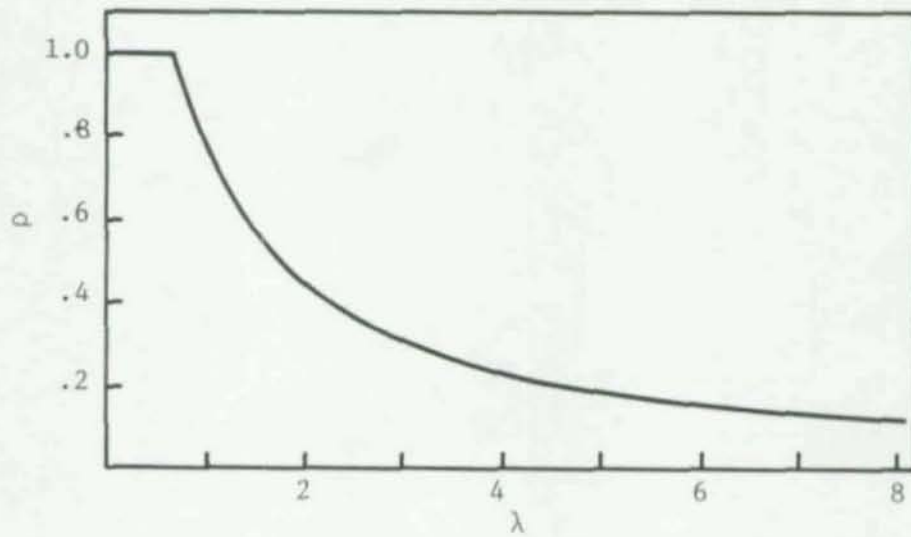
Fig. 2.2-1   Plot of Eq. 2.2-1 and -2

a. Initial yield in compression

b. Initial yield in tension

c. Ultimate state with compression flange $w/t < 190/\sqrt{F_y}$

d. Ultimate state with compression flange $w/t \geq 190/\sqrt{F_y}$

e. Ultimate state with an element where $f < F_y$
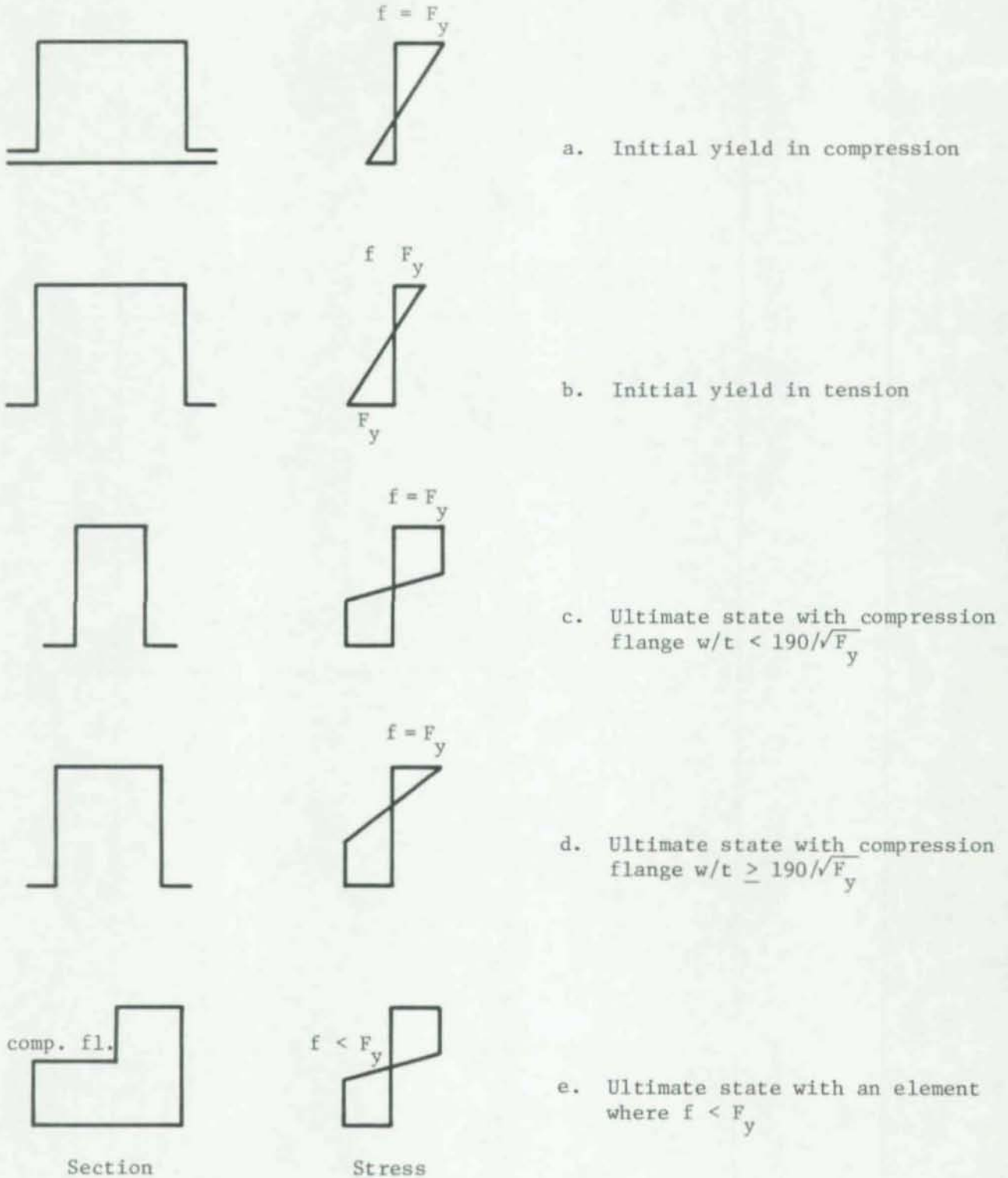
Section   Stress

Fig. 2.2-2   Stress f in Eq. 2.2-2
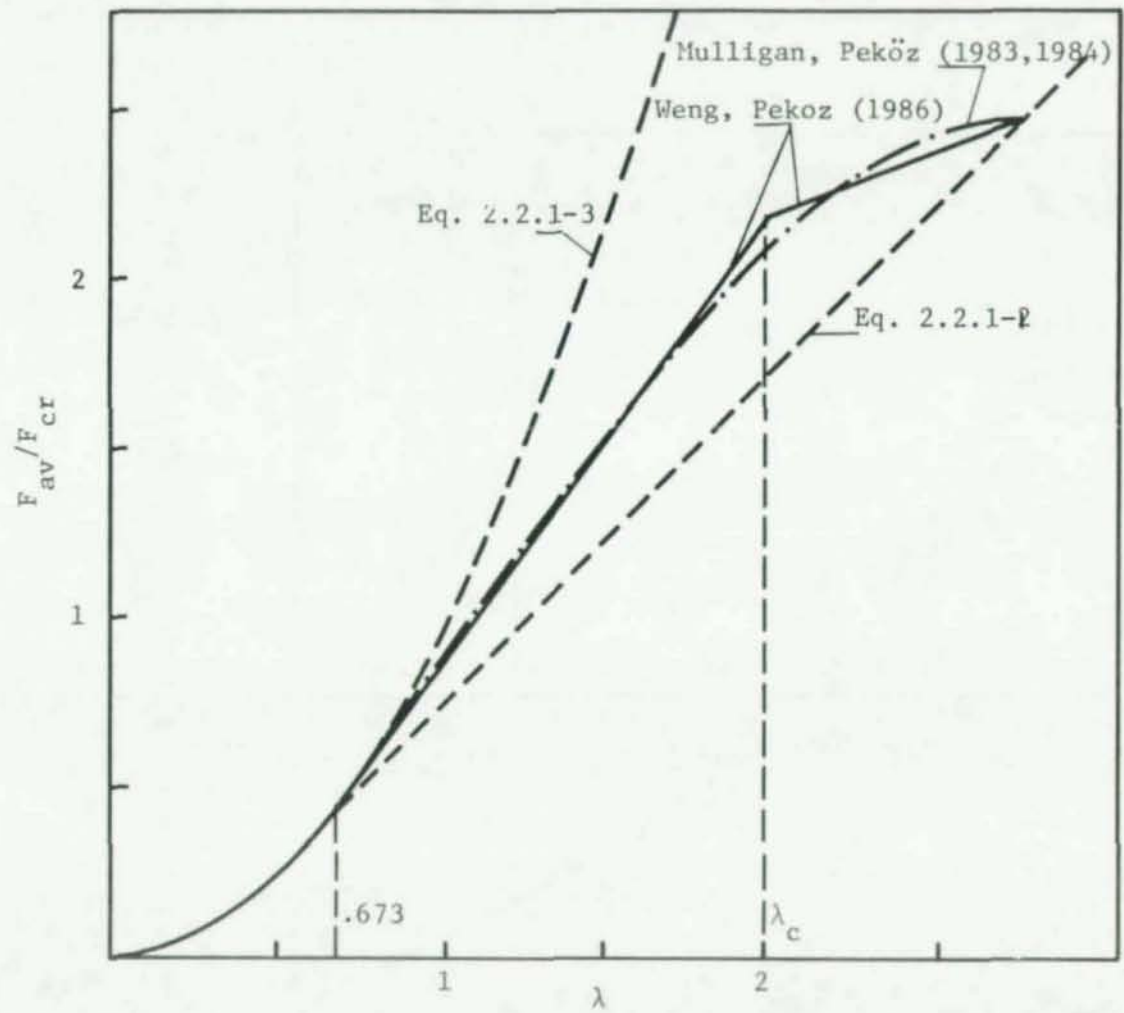
Fig. 2.2.1-1 Subultimate behavior of stiffened compression elements
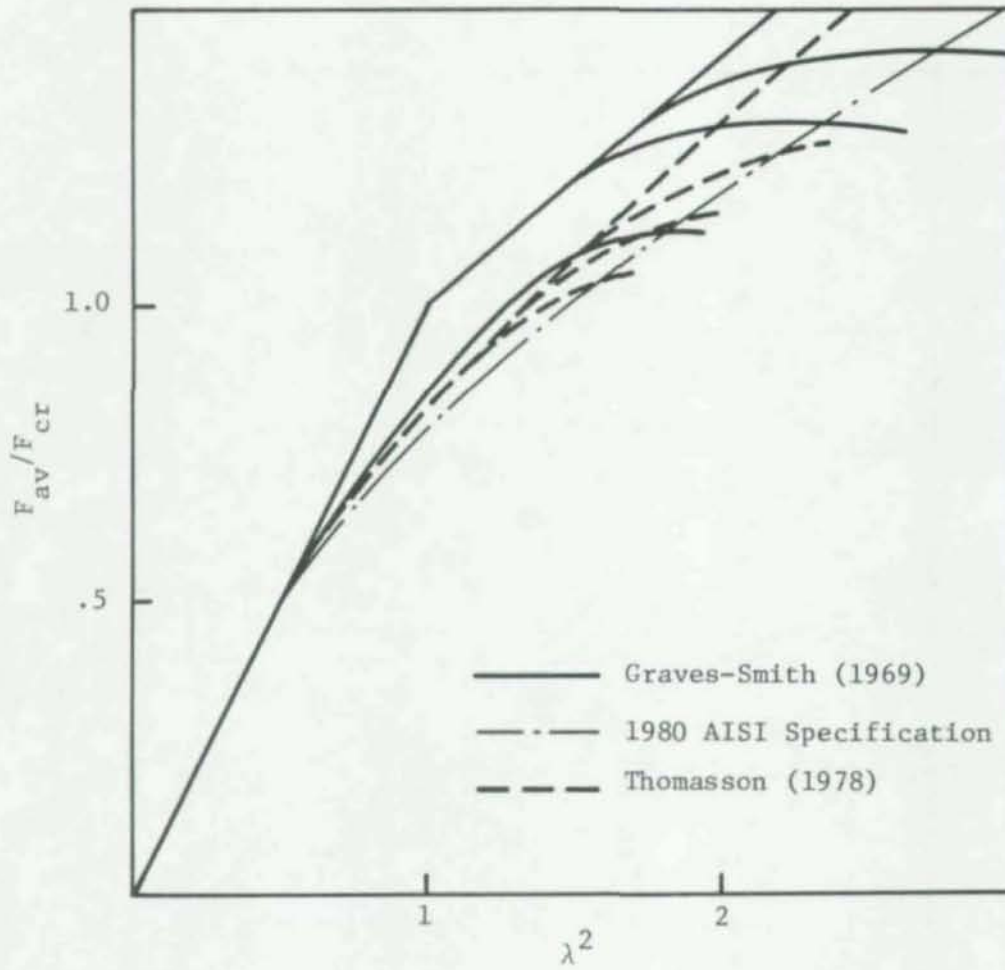
Fig. 2.2.1-2   Comparison of some subultimate behavior predictions
of stiffened compression elements
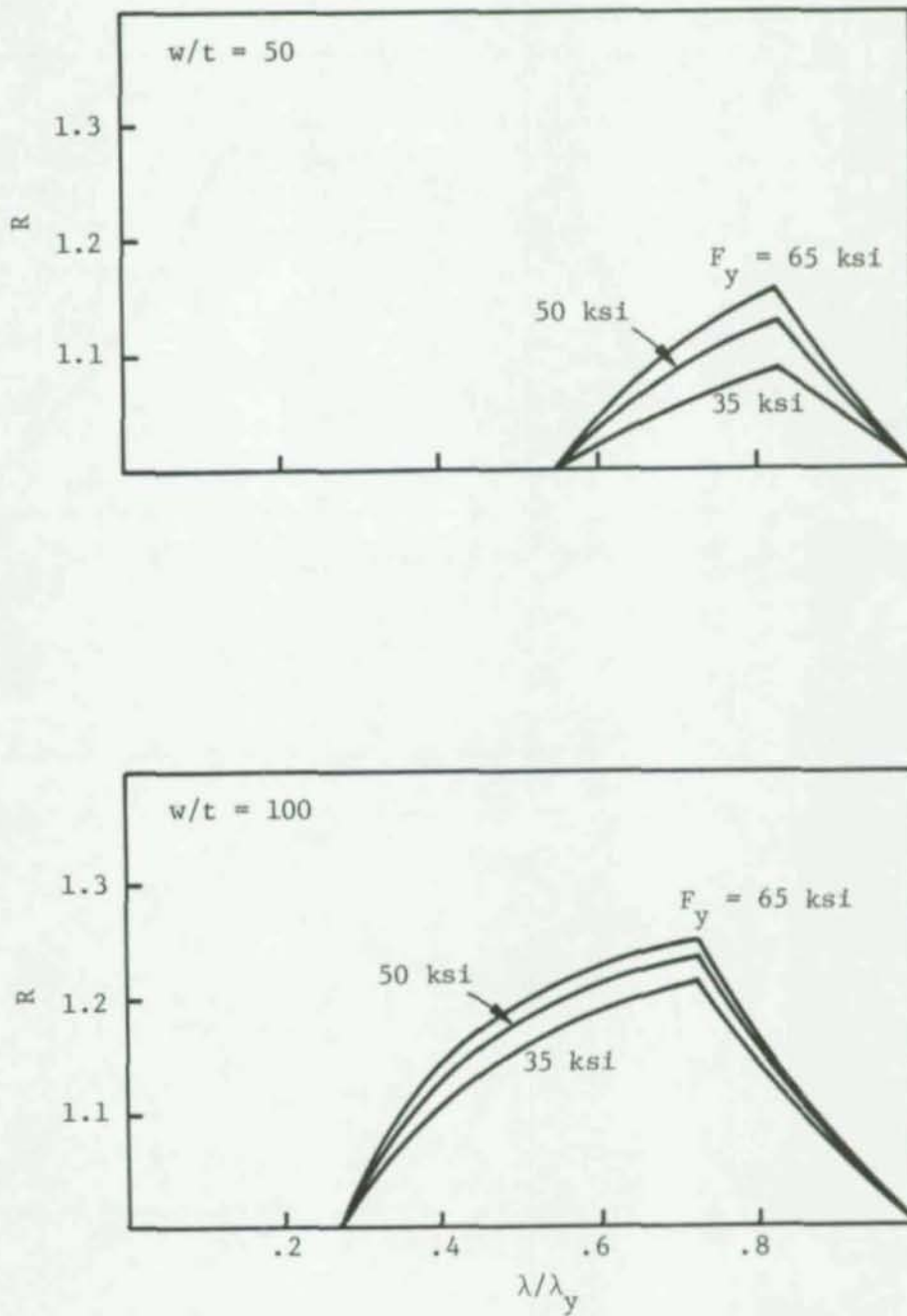
Fig. 2.2.1-3   Ratio, R, of the effective widths calculated
according to Eqs. 2.2.1-4 through -6 to those
calculated according to Eq. 2.2-2
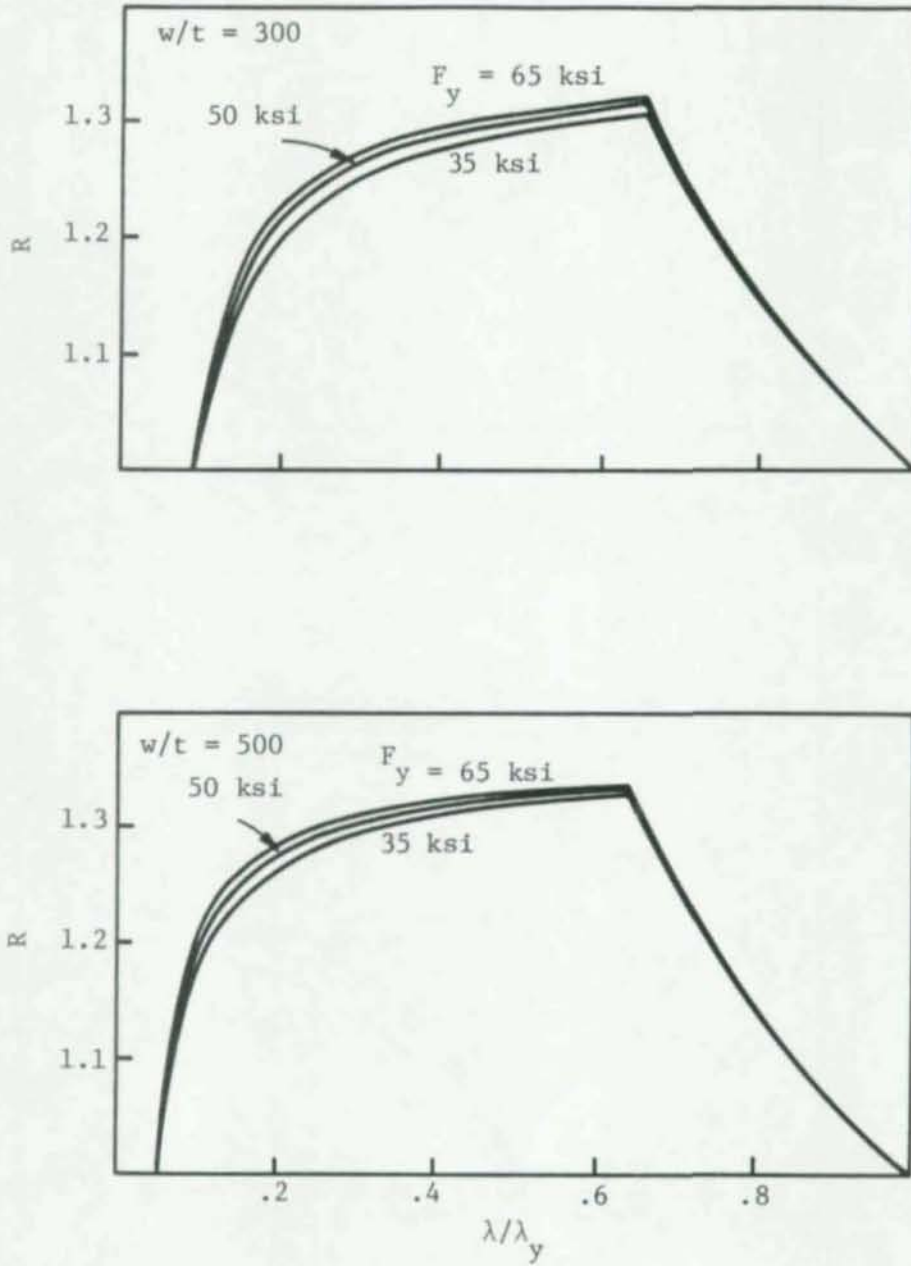
Fig. 2.2.1-3   (cont.)
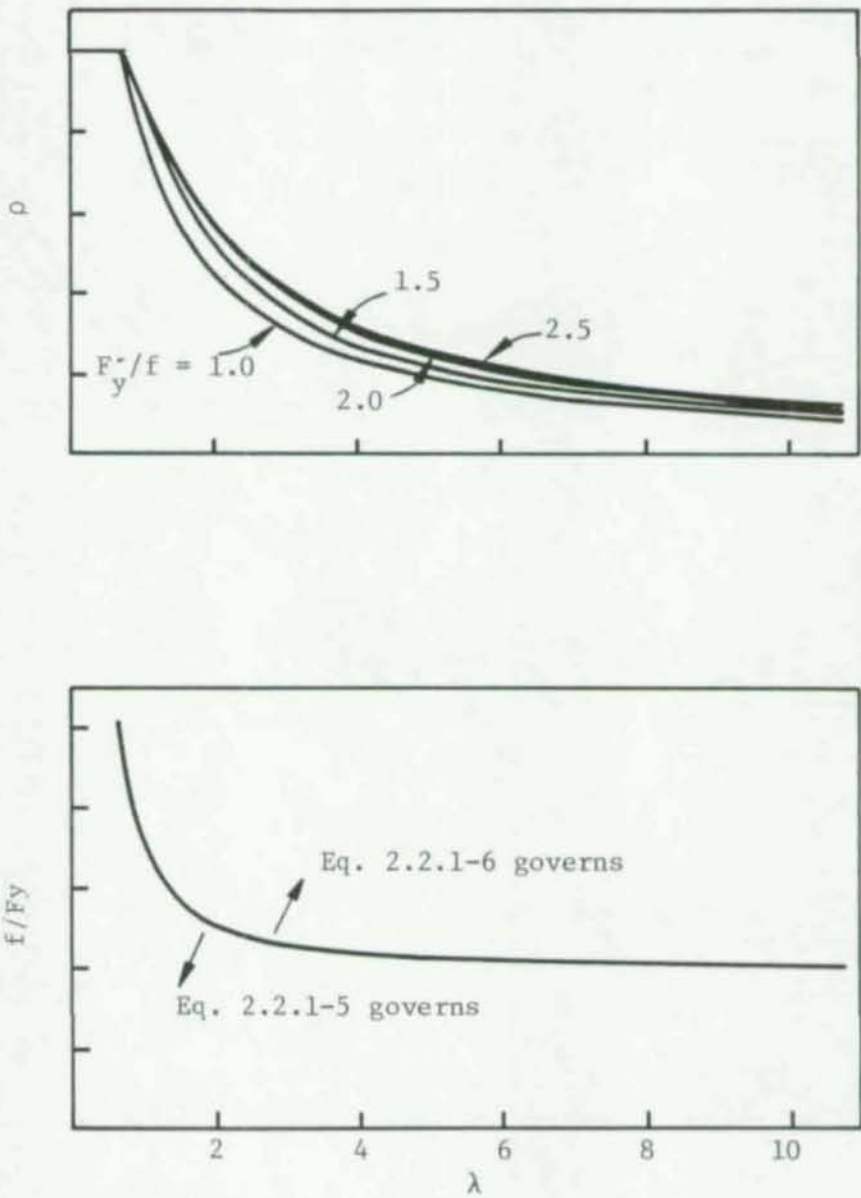
Fig. 2.2.1-4 Possible design aids for webs
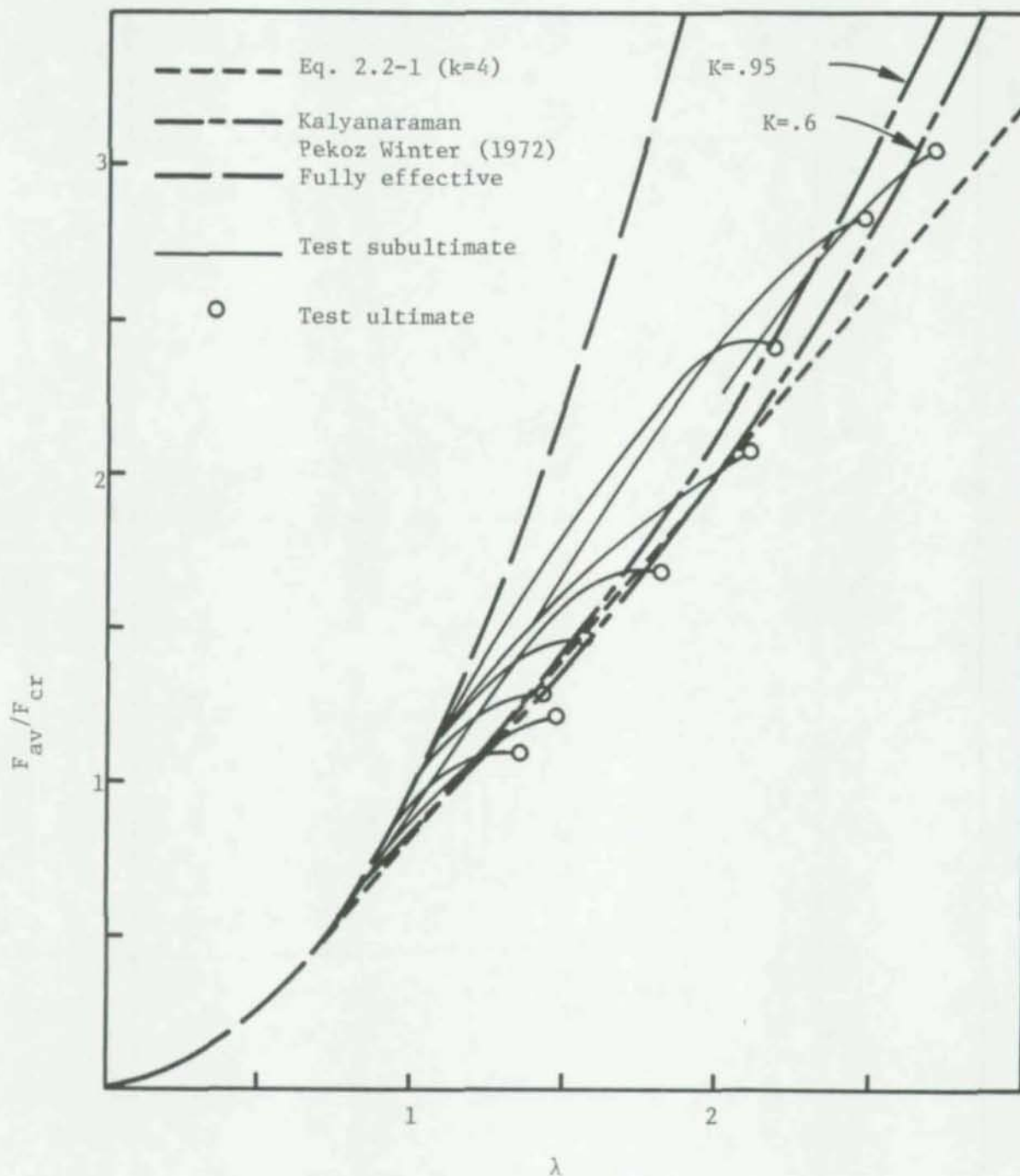
Fig. 2.2.1- 5 Subultimate behavior of beams with unstiffened flanges
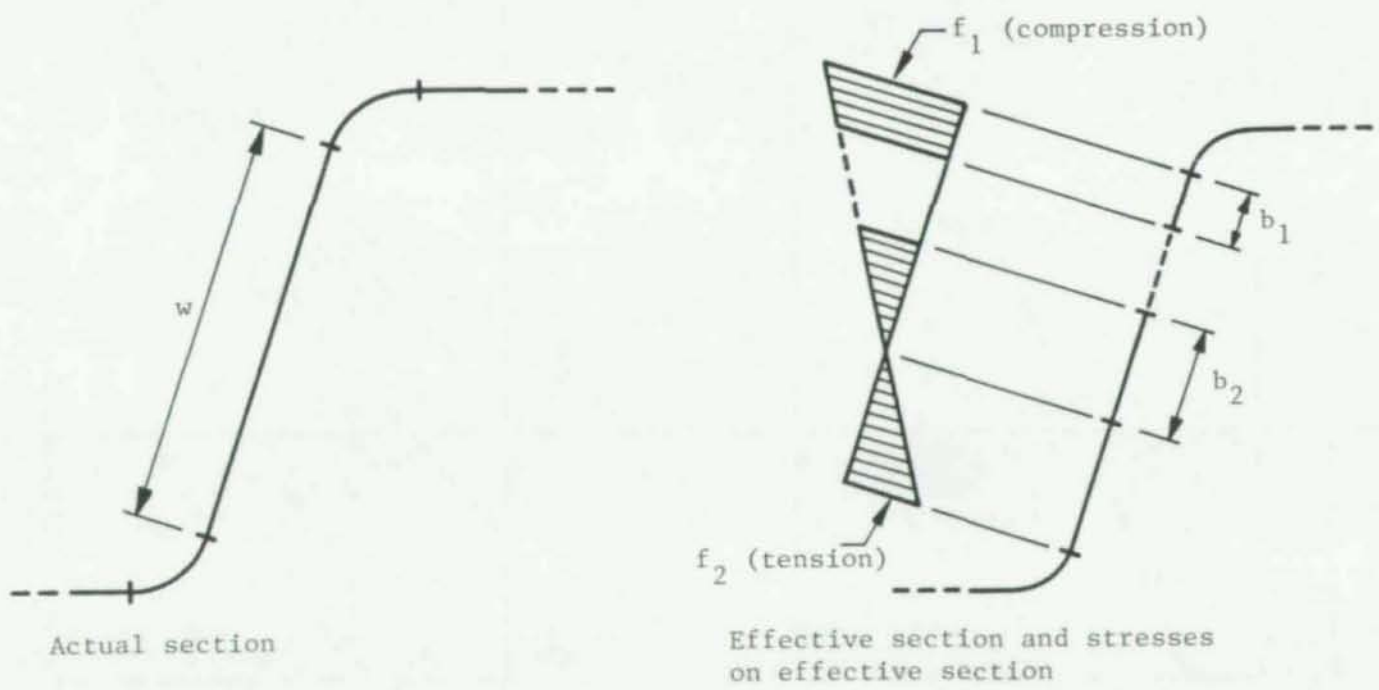
Actual section

Effective section and stresses
on effective section

Fig. 2.3-1 Web effective widths
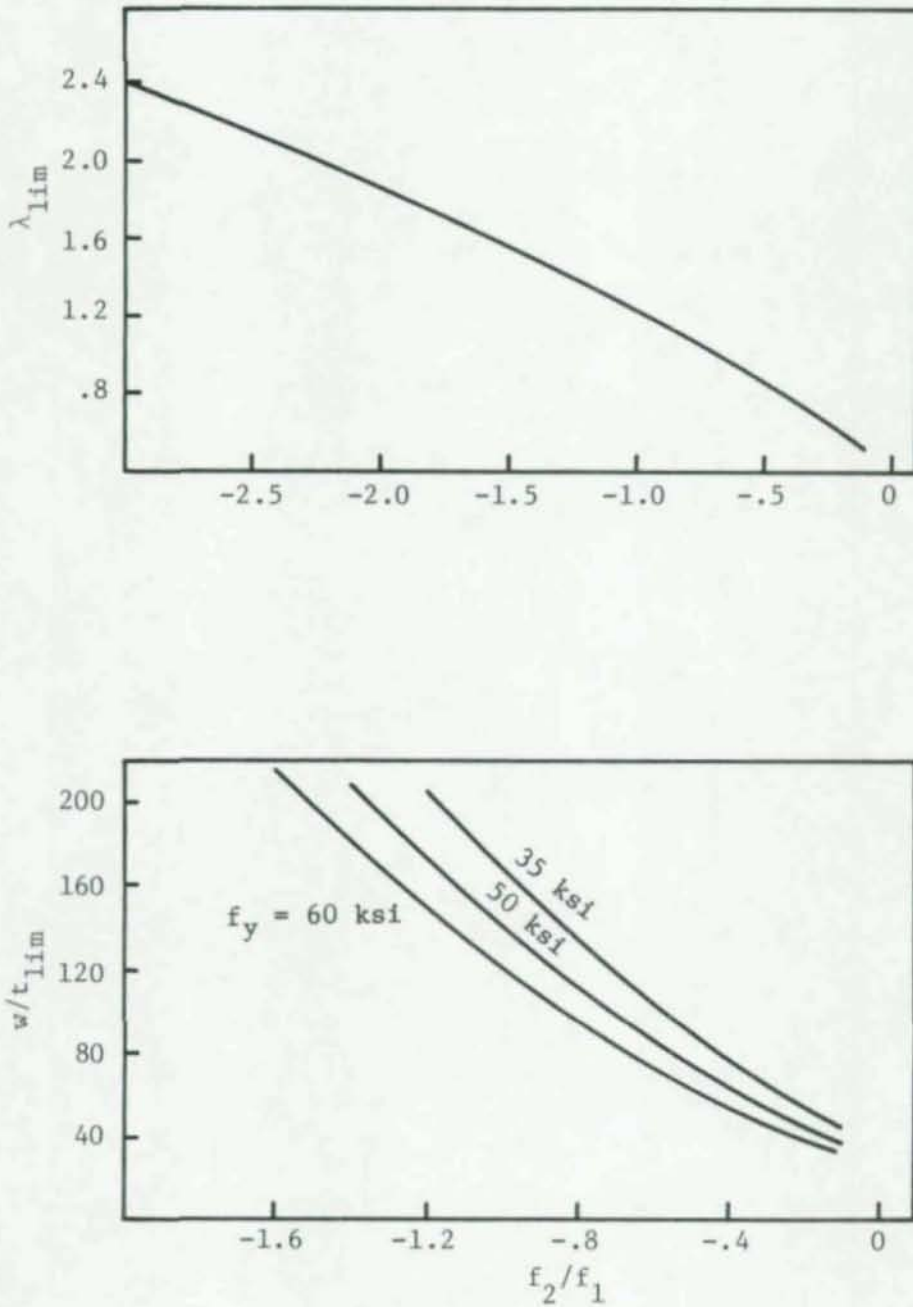
Fig. 2.3-2 Limiting values of λ and w/t above which the
web is not fully effective
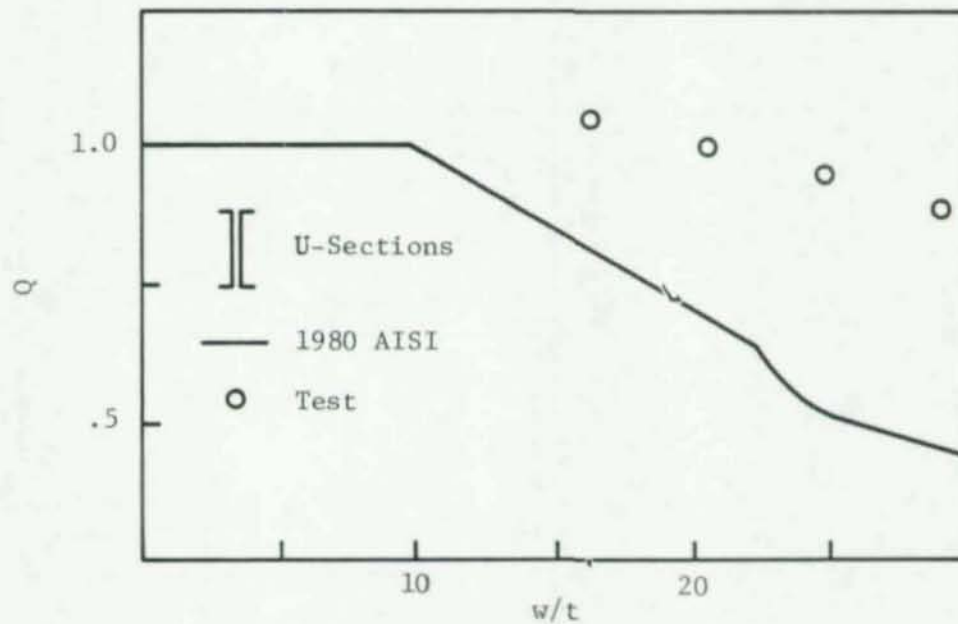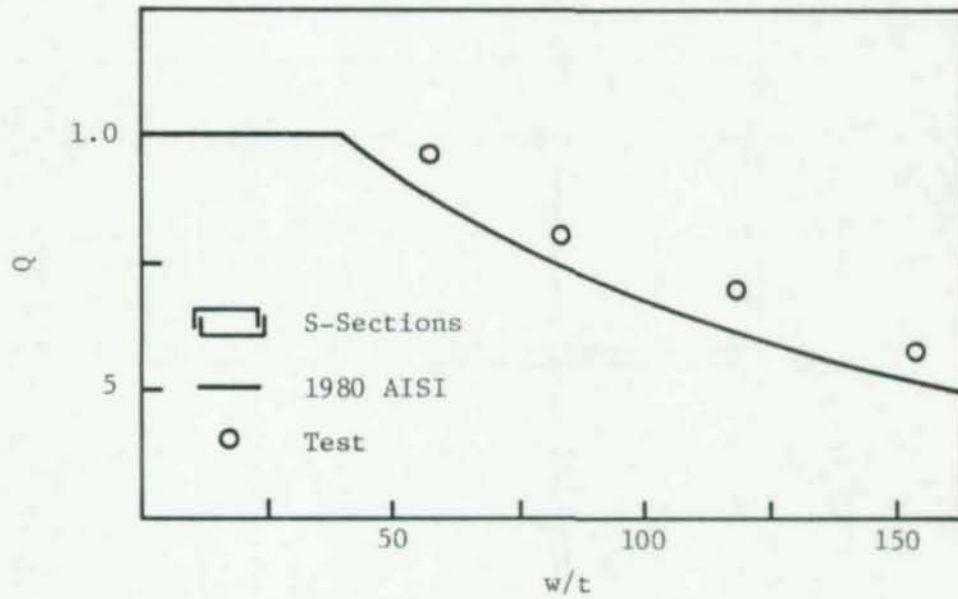
Fig. 2.4.1-1   Values of Q-factor observed in tests and
according to the 1980 AISI Specification

D

W

T

S-Section

D

W

T
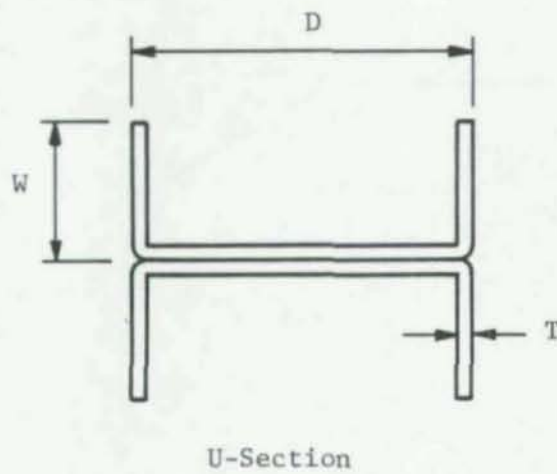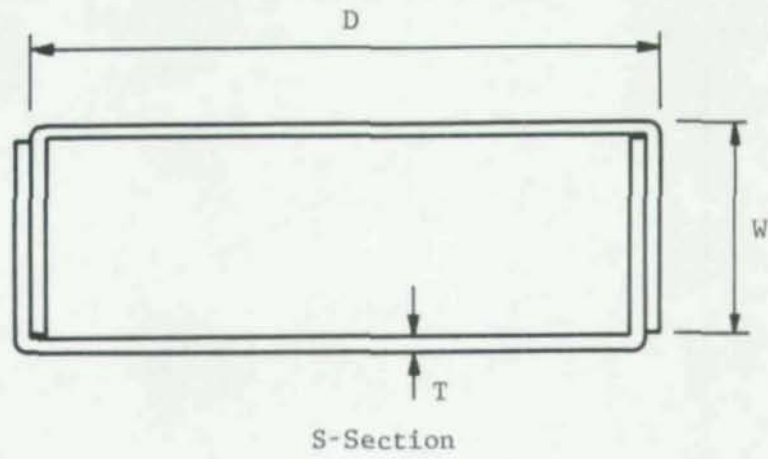
U-Section

Fig. 2.4.1-2   Column specimen sections
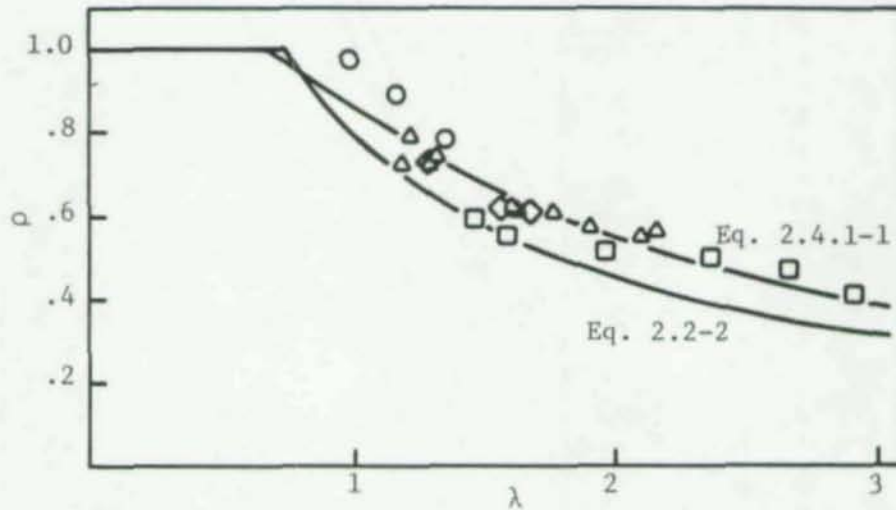
Fig. 2.4.1-3   Some stub column test results on sections
with unstiffened flanges
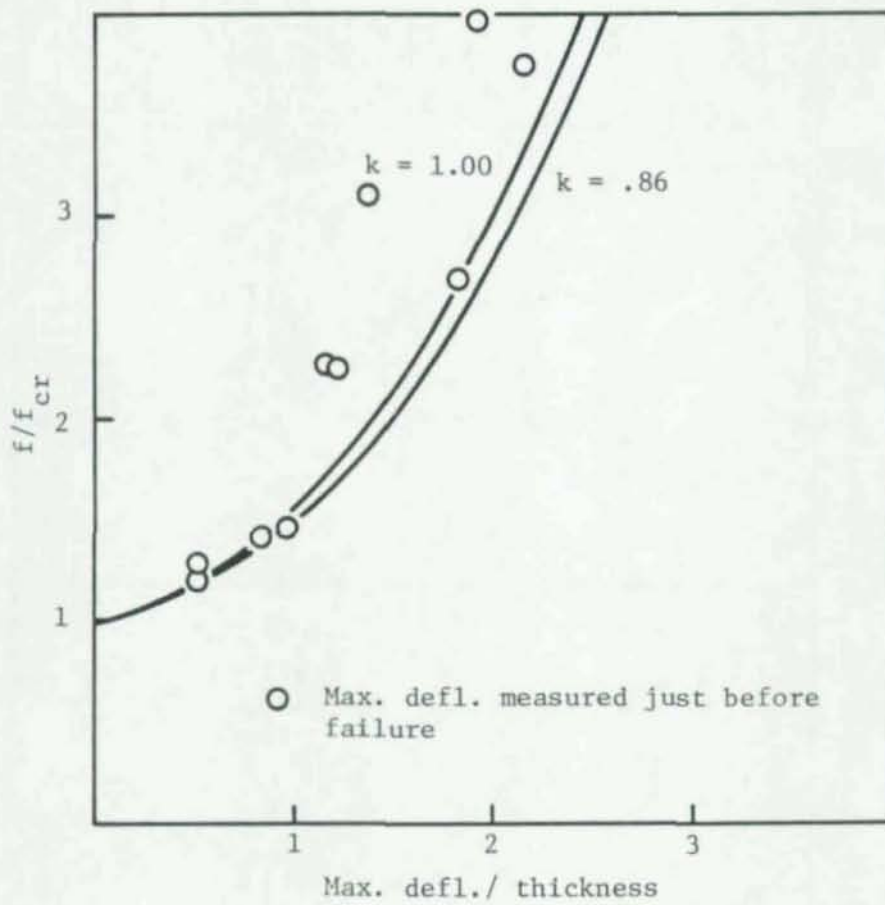
Fig. 2.4.1-4   Maximum out-of-plane deflections of un-
stiffened compression elements
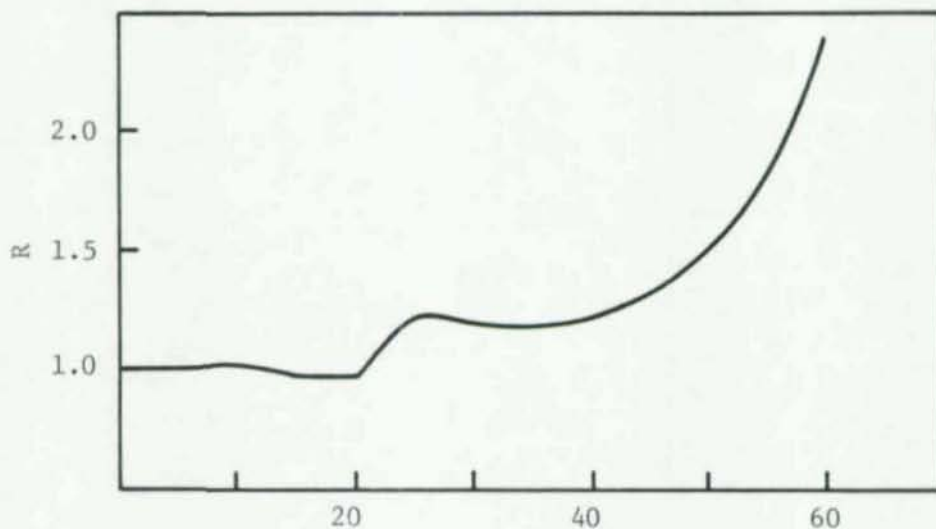
Fig. 2.4.1-5 Ratio, R, of the effective width
given by Eq. 2.2-2 with k = 4.3
to that implied in the 1980 AISI
Specification
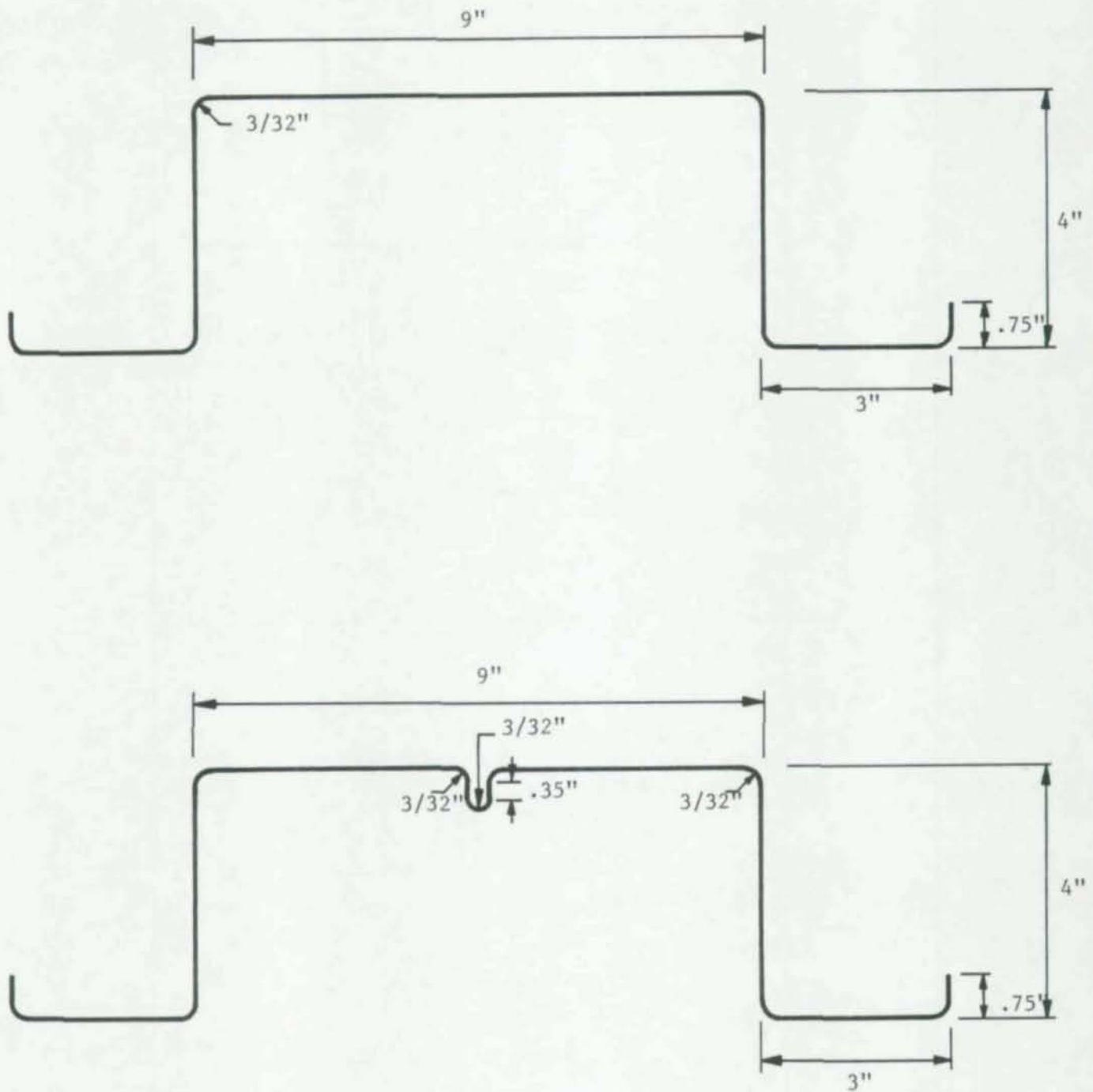
Fig. 2.5-1 Sections for the Numerical Examples 4 and 5 of the 1980 AISI ⌐
          Cold-Formed Steel Design Manual

Case I: $w/t \leq S/3$; $S = 1.28 \sqrt{E/f}$ Flange fully effective without stiffener

no stiffener   with stiffener   stiffener too long

F_y

stress

D

section

w

$D/w \leq .25$ $D/w > .25$

Case II: $S/3 < w/t \leq S$ Flange fully effective with $I_s \geq I_a$ and $D/w \leq .25$

no stiffener   inadequate stiffener   adequate stiffener   stiffener too long

F_y

$D/w \leq .25$ $D/w > .25$

$I_s = 0$ $I_s < I_a$ $I_s \geq I_a$ $I_s > I_a$

Case III: $w/t > S$

no stiffener   inadequate stiffener   adequate stiffener   stiffener too long

F_y

$D/w \leq .25$ $D/w > .25$

$I_s = 0$ $I_s < I_a$ $I_s \geq I_a$ $I_s > I_a$

Fig. 2.5-2 Edge stiffener design criteria
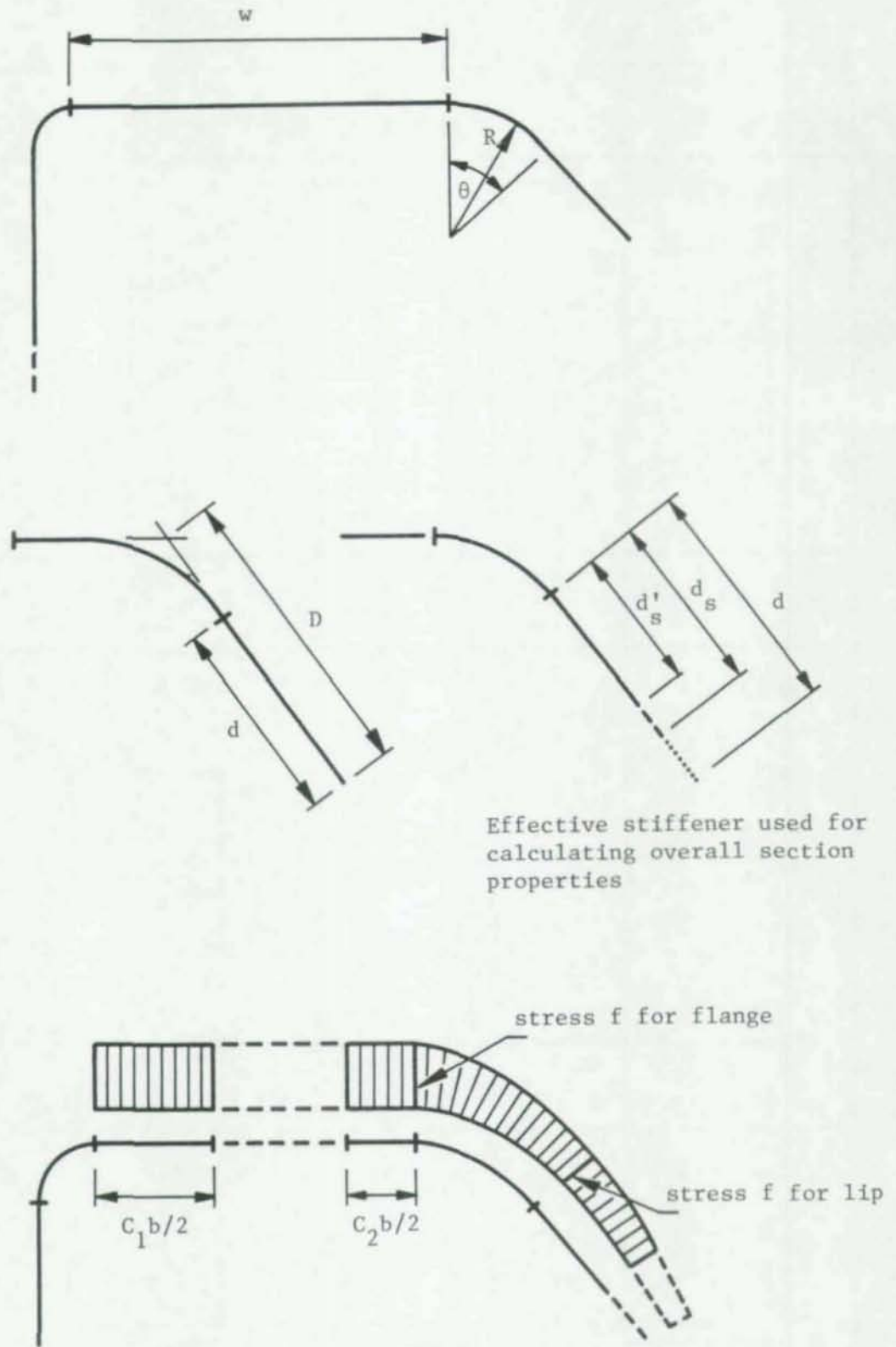
Effective stiffener used for
calculating overall section
properties

stress f for flange

stress f for lip

Fig. 2.5-3 Compression element with edge stiffener
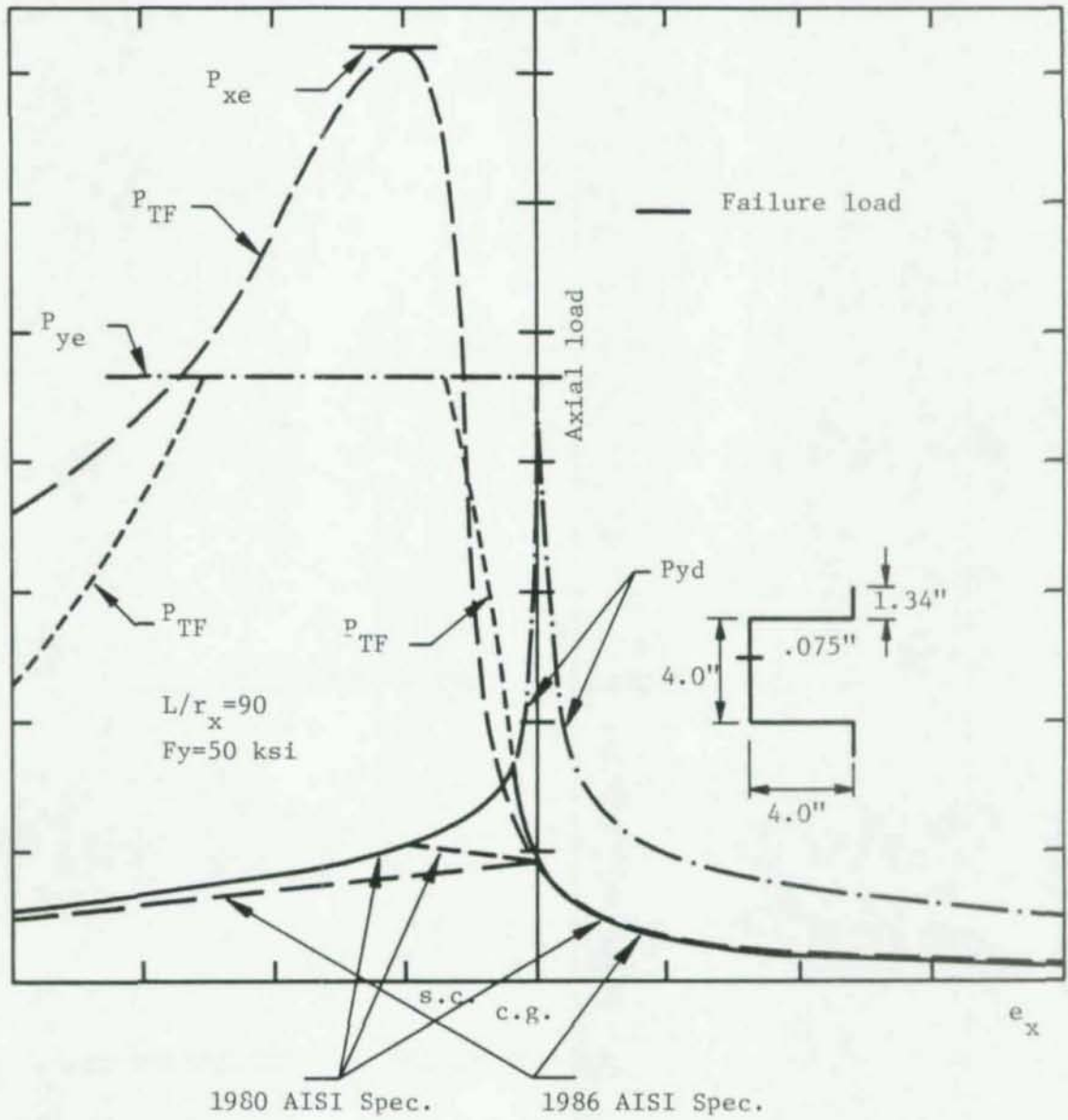
Fig. 3.3-1   Torsional-flexural behavior for axial loads along the axis
of symmetry
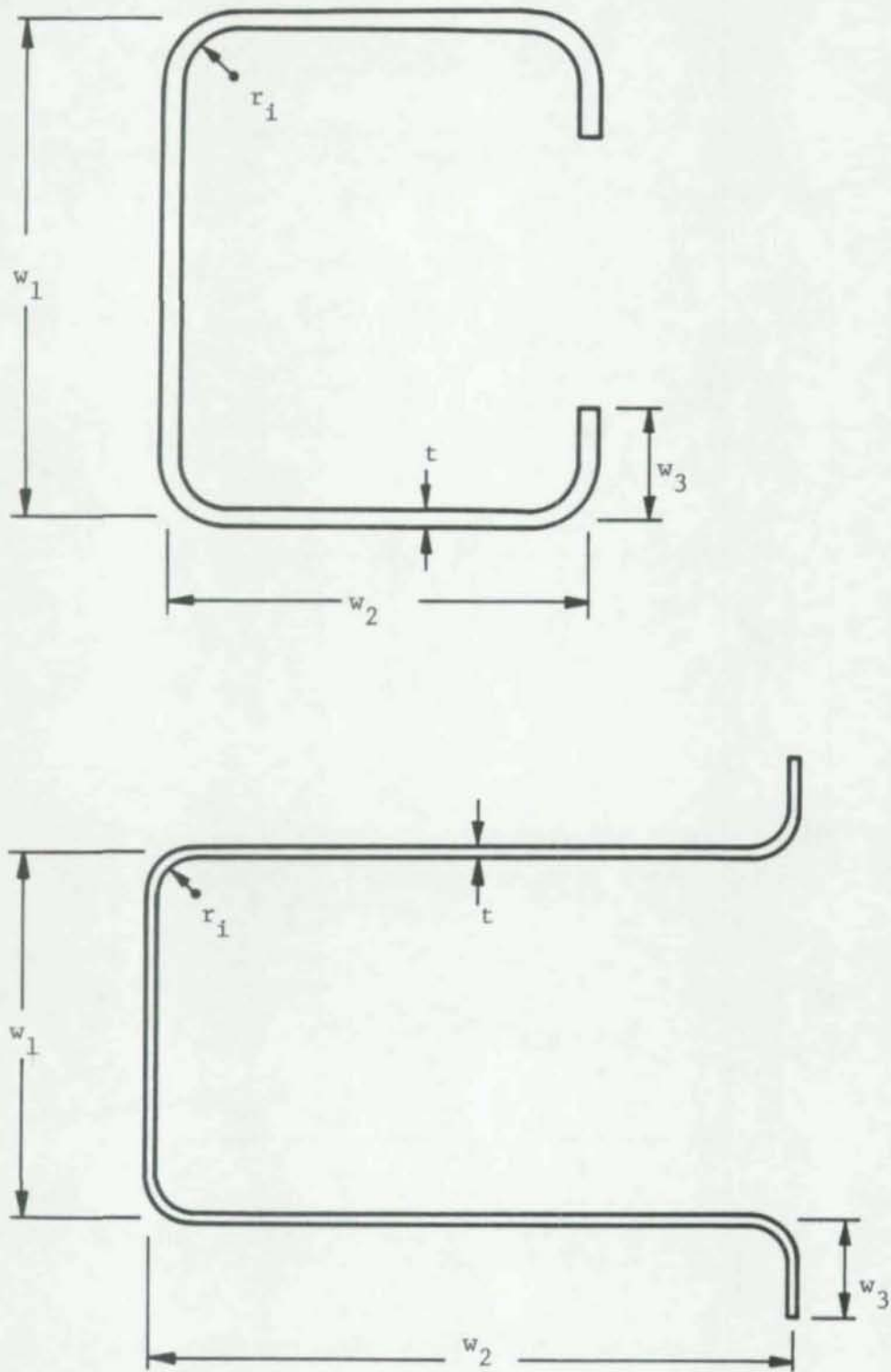
Fig. 3.3-2 Cross sectional geometry
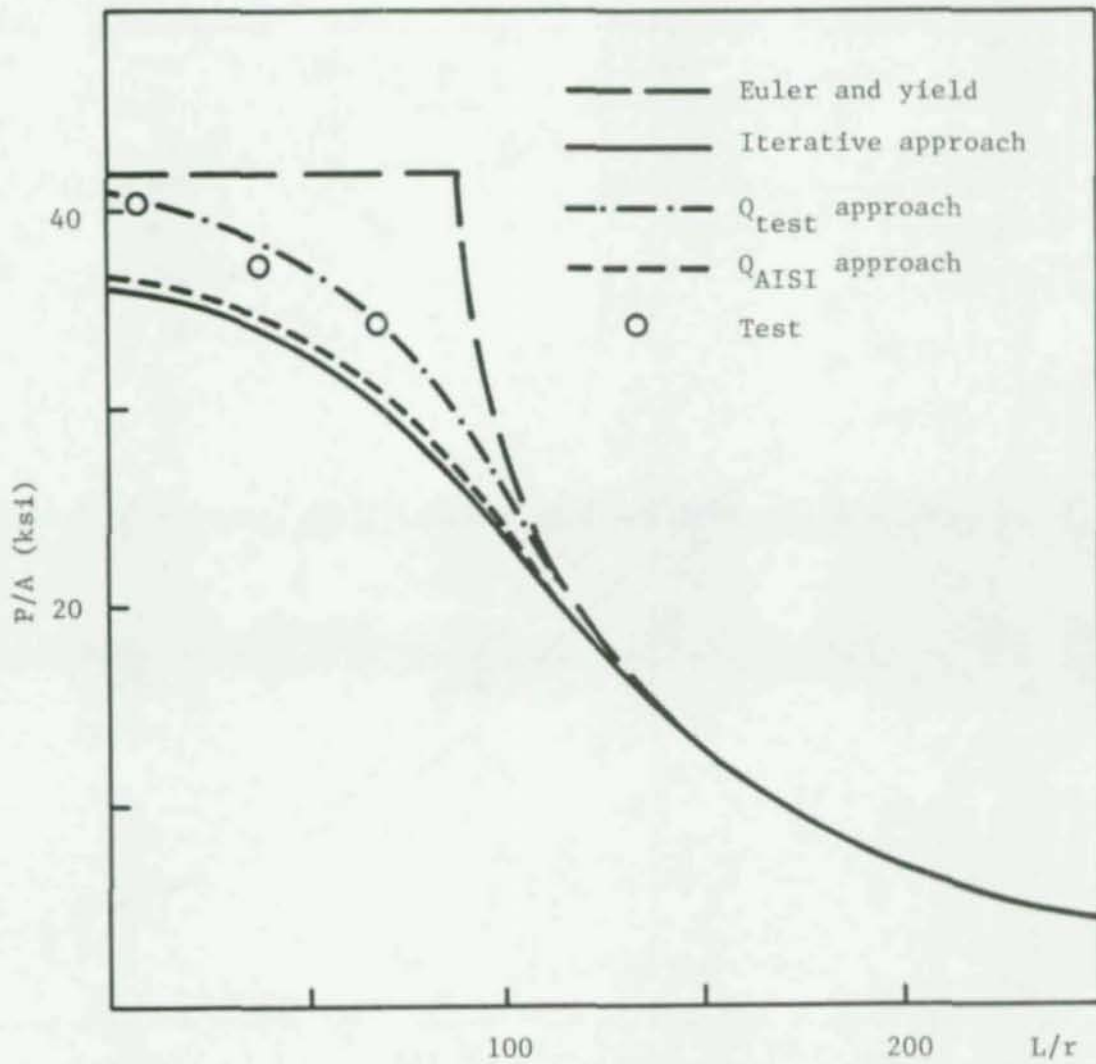
Fig. 4.2-1 Correlation of observed and calculated failure loads for
Section S-1 with w/t = 57.2
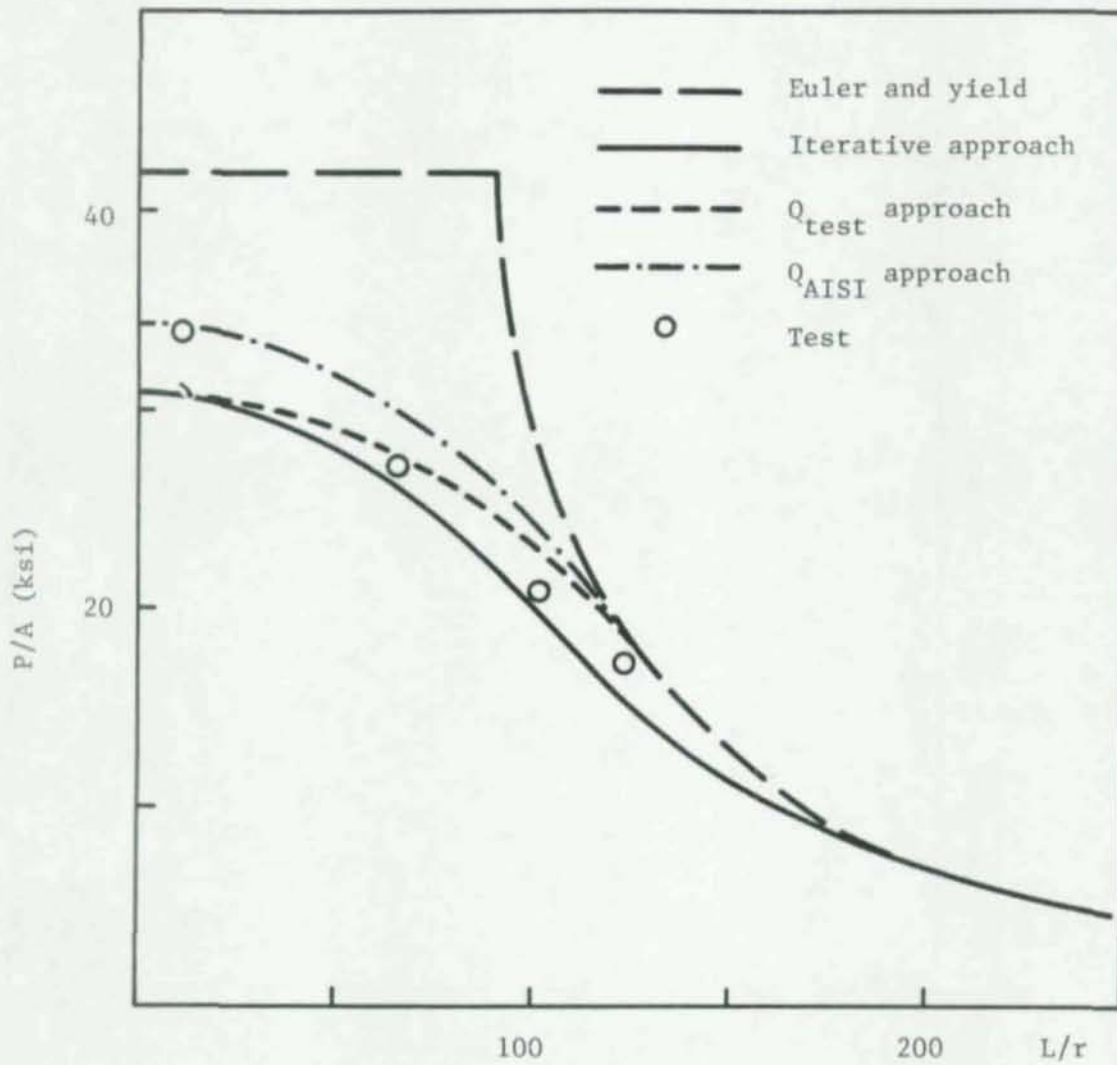
Fig. 4.2-2 Correlation of observed and calculated failure loads for
Section S-2 with w/t = 83.0
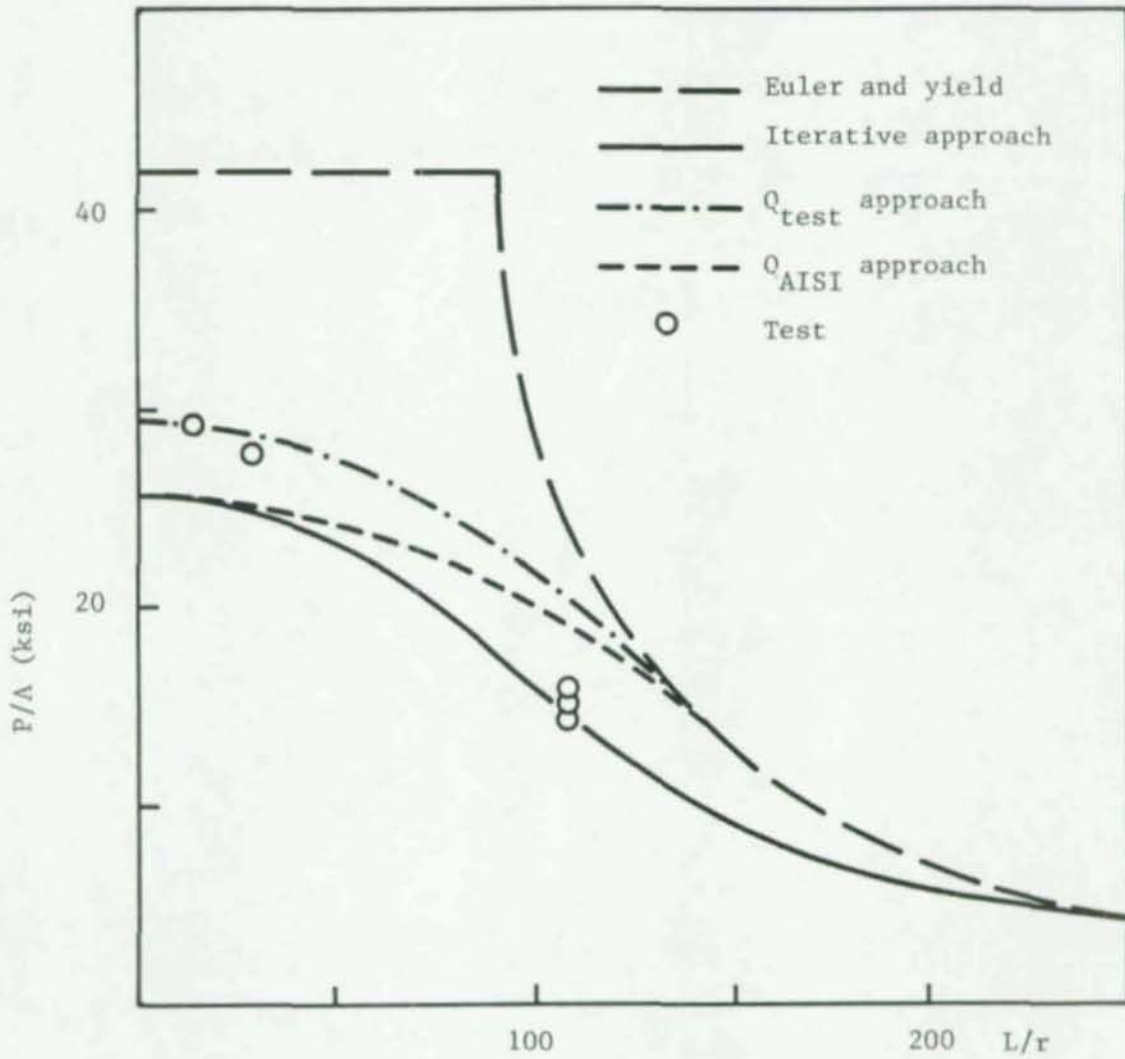
Fig. 4.2-3 Correlation of observed and calculated failure loads for
Section S-3 with w/t = 117.4
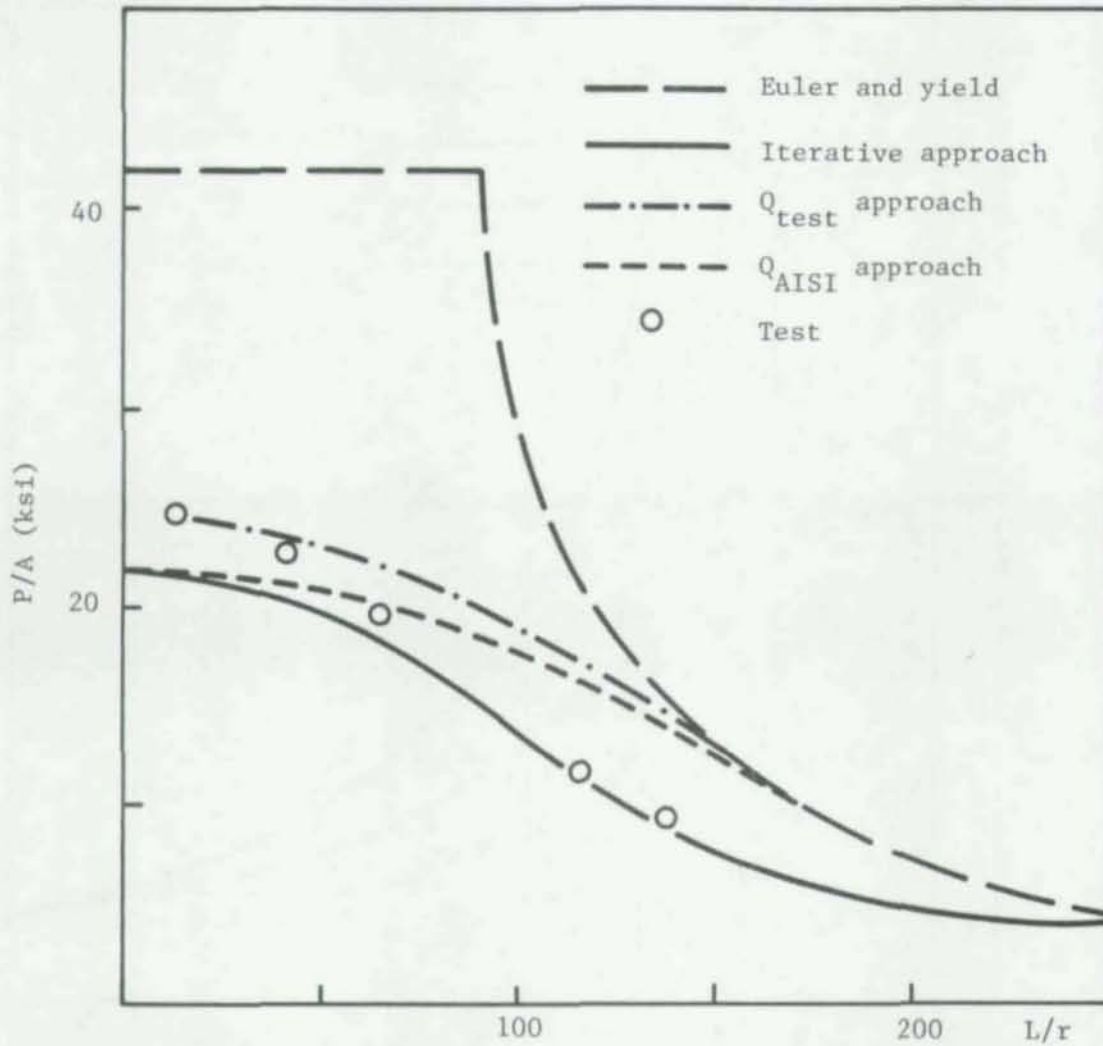
Fig. 4.2-4 Correlation of observed and calculated failure loads for
Section S-4 with w/t =151.8
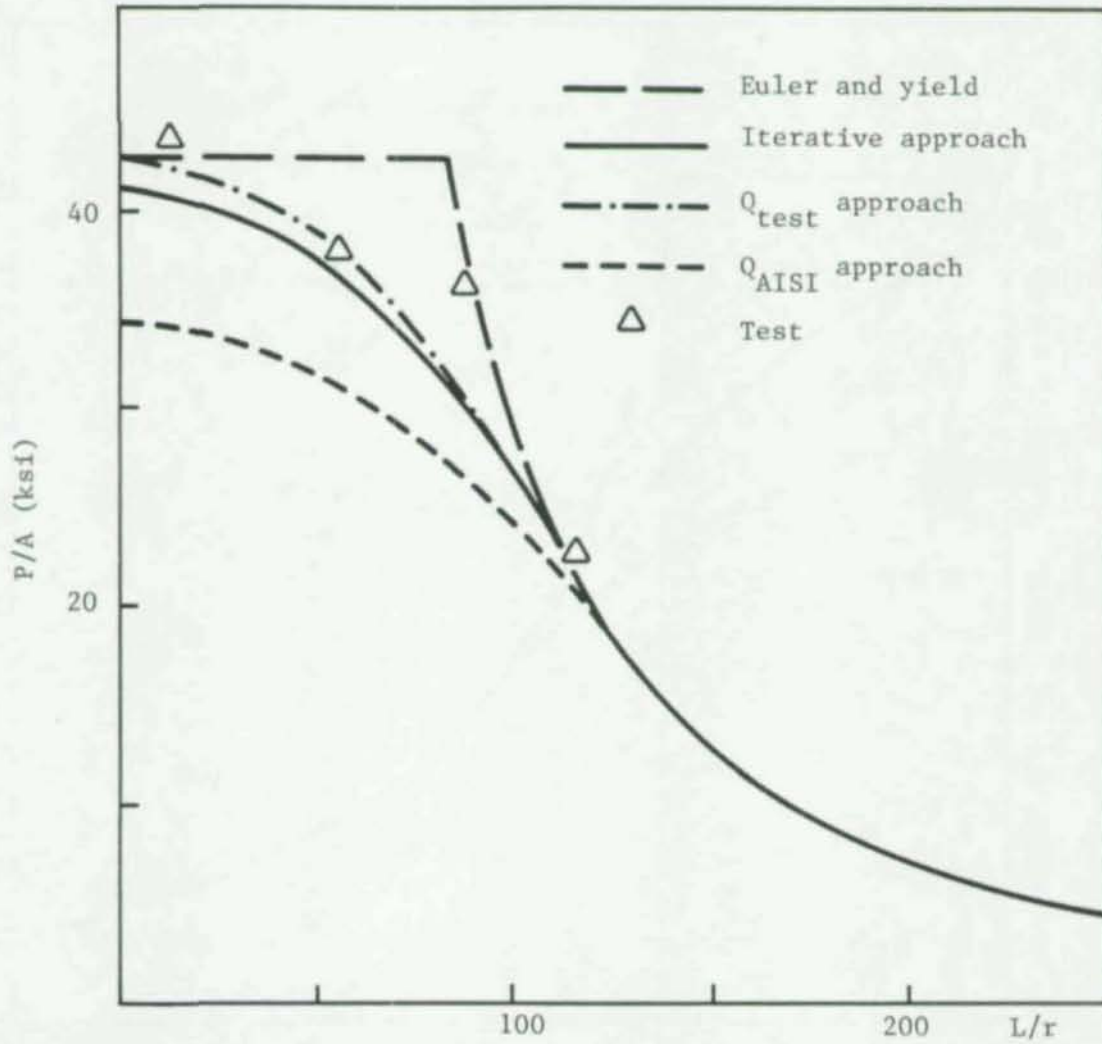
Fig. 4.2-5 Correlation of observed and calculated failure loads for
Section U-1 with w/t = 16.2
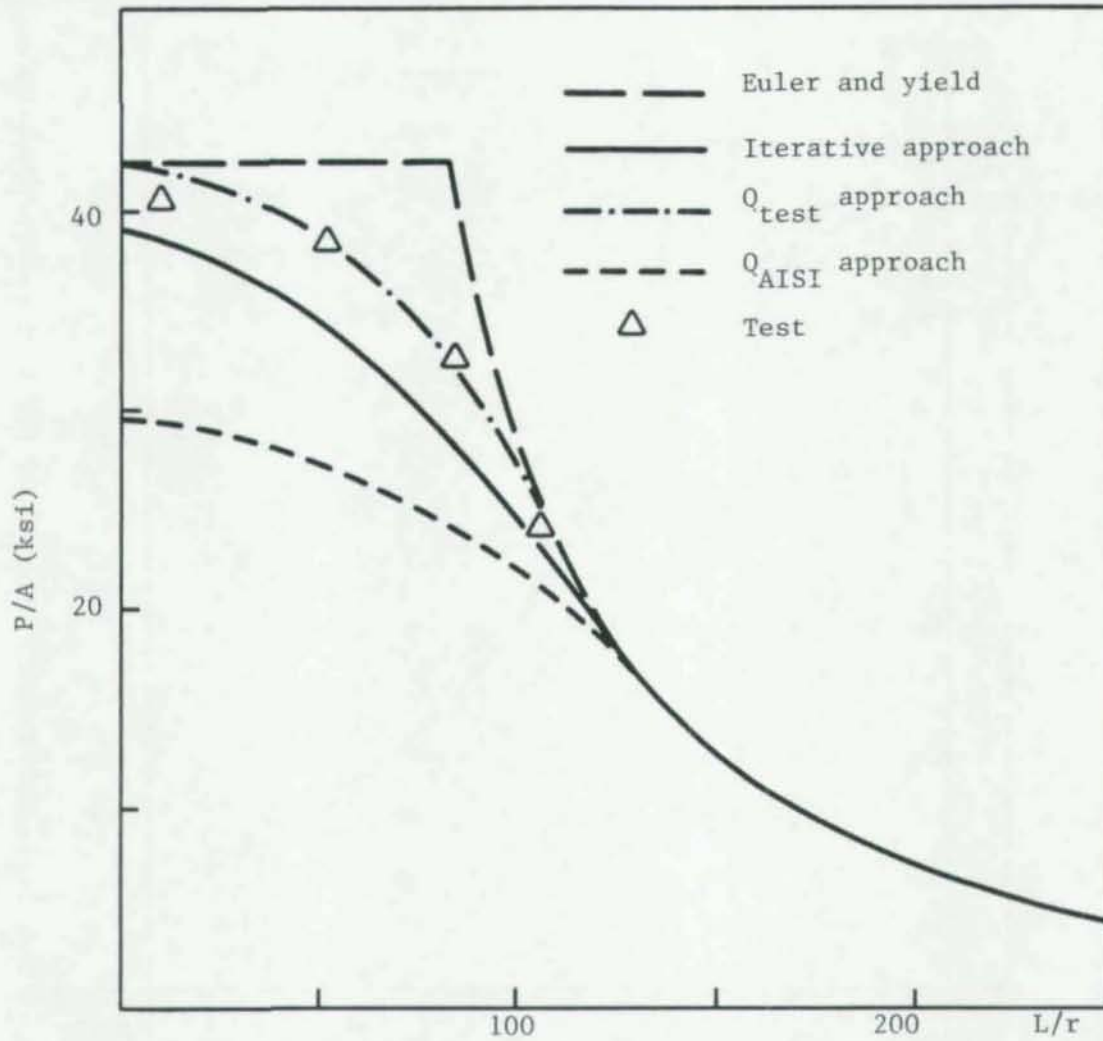
Fig. 4.2-6 Correlation of observed and calculated failure loads for
          Section U-2 with w/t = 20.5
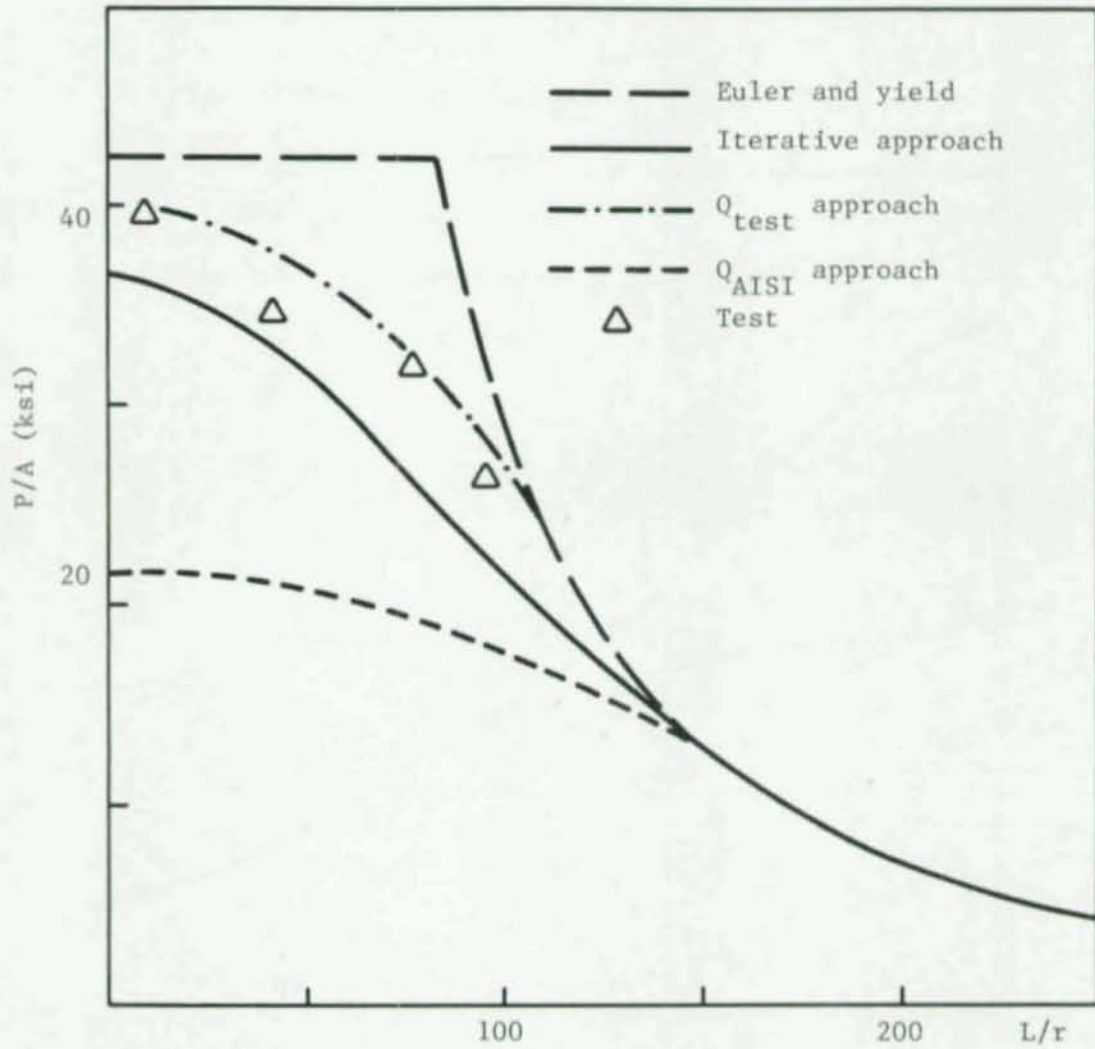
Fig. 4.2-7 Correlation of observed and calculated failure loads for
Section U-3 with w/t = 24.8
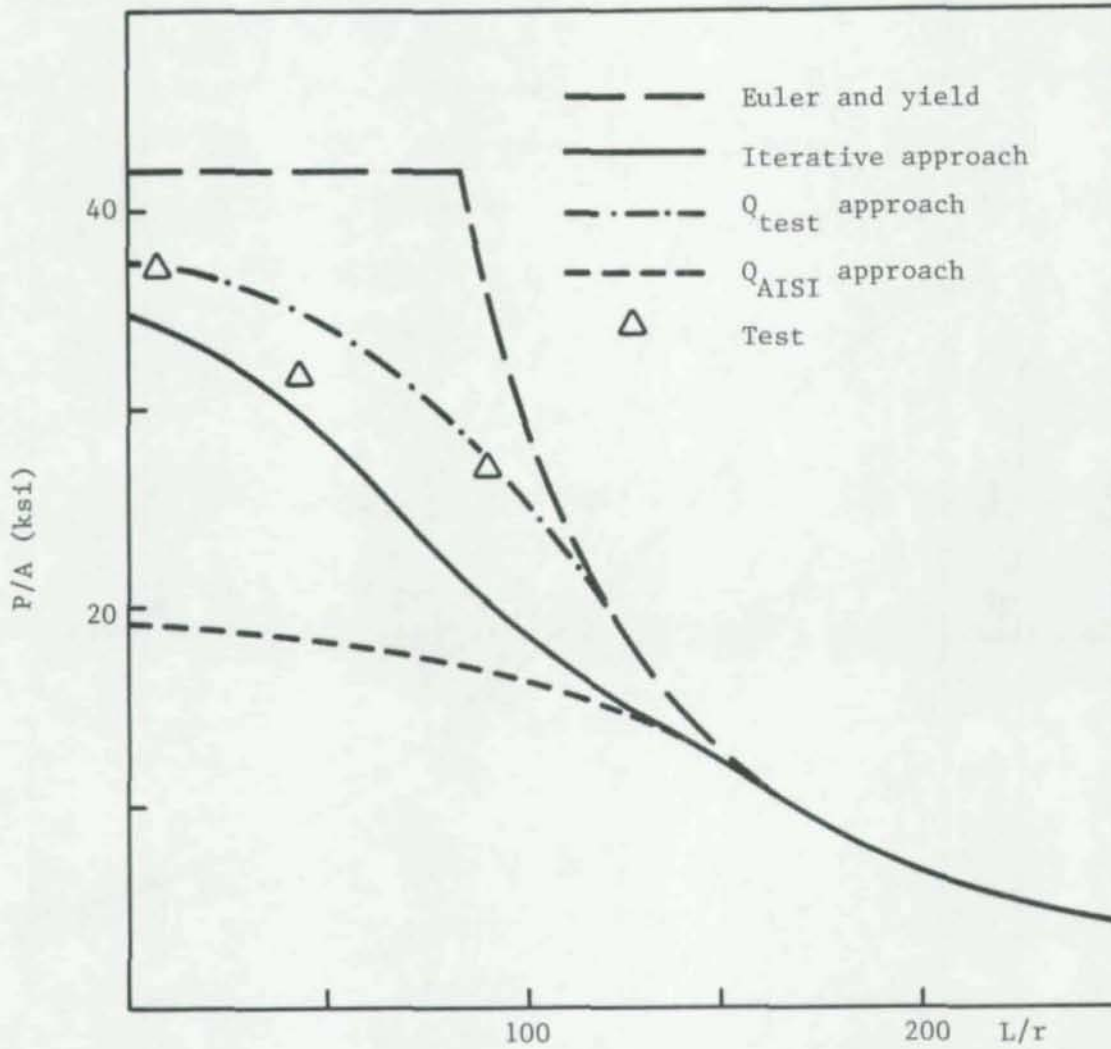
Fig. 4.2-8 Correlation of observed and calculated failure loads for
Section U-4 with w/t = 29.1
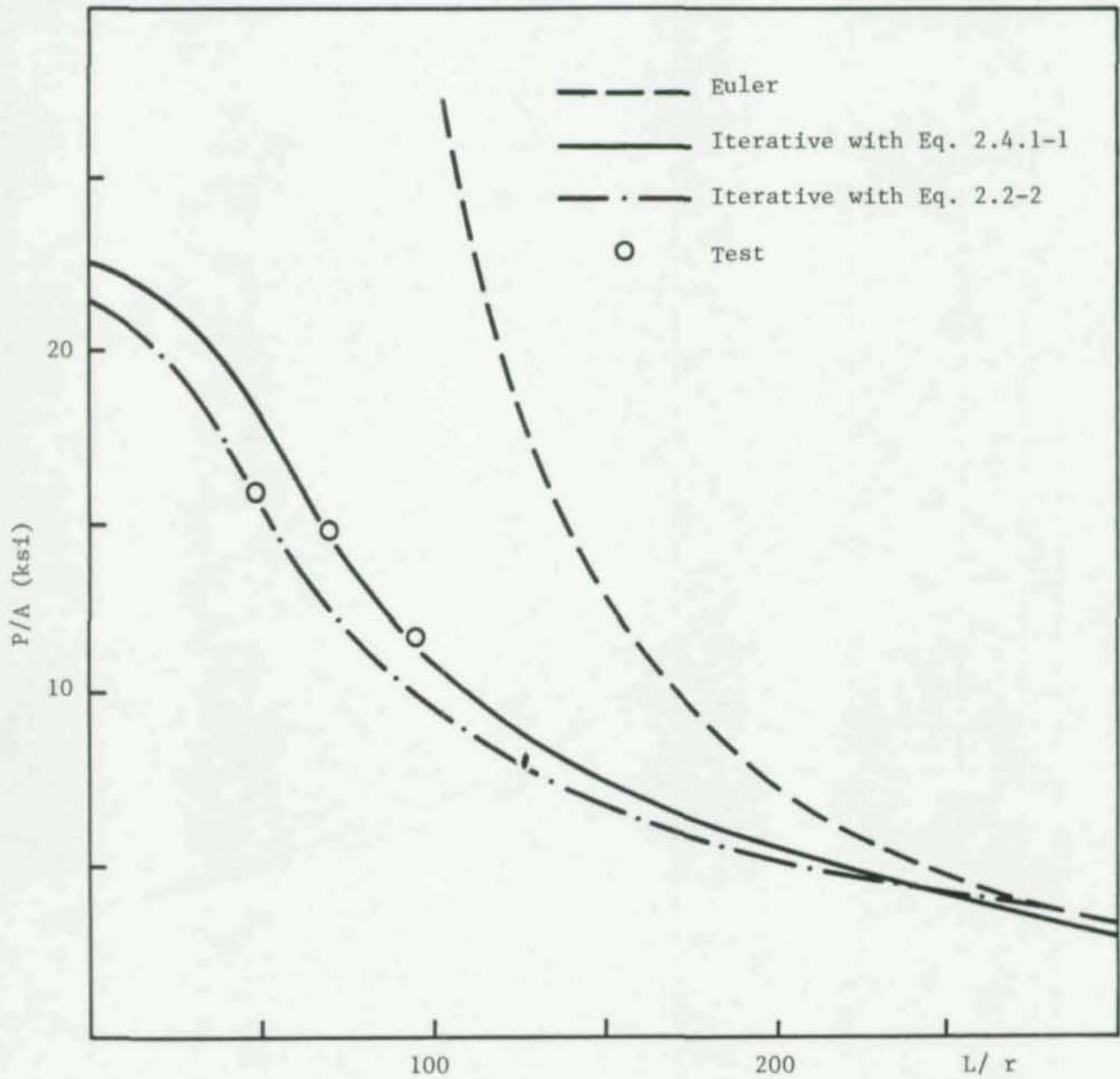
Fig. 4.2-9 Correlation of calculated and observed failure loads for Section LC-1
with w/t = 57.5
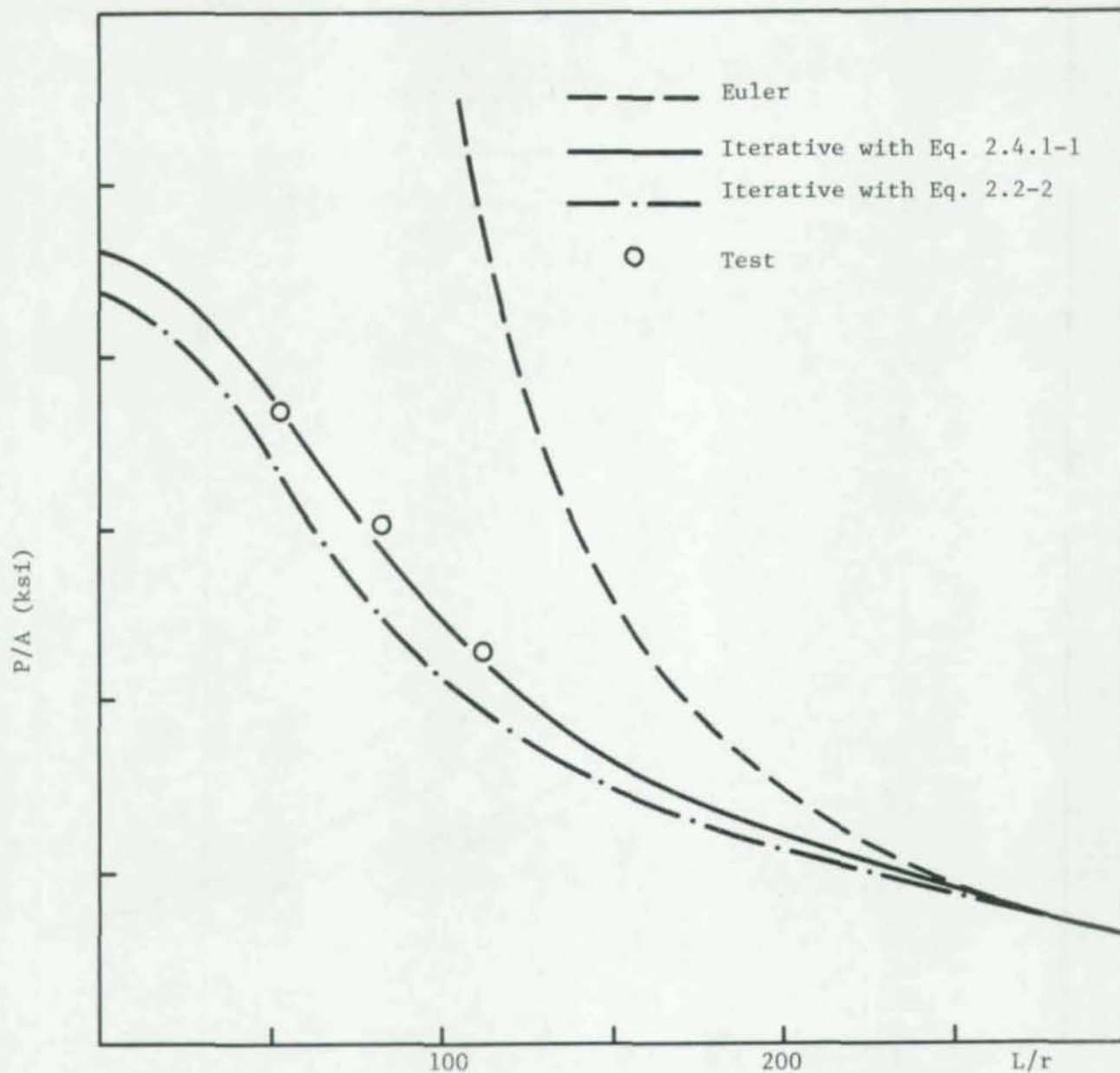
Fig. 4.2-10 Correlation of calculated and observed failure loads for Section LC-II
with w/t = 50.5
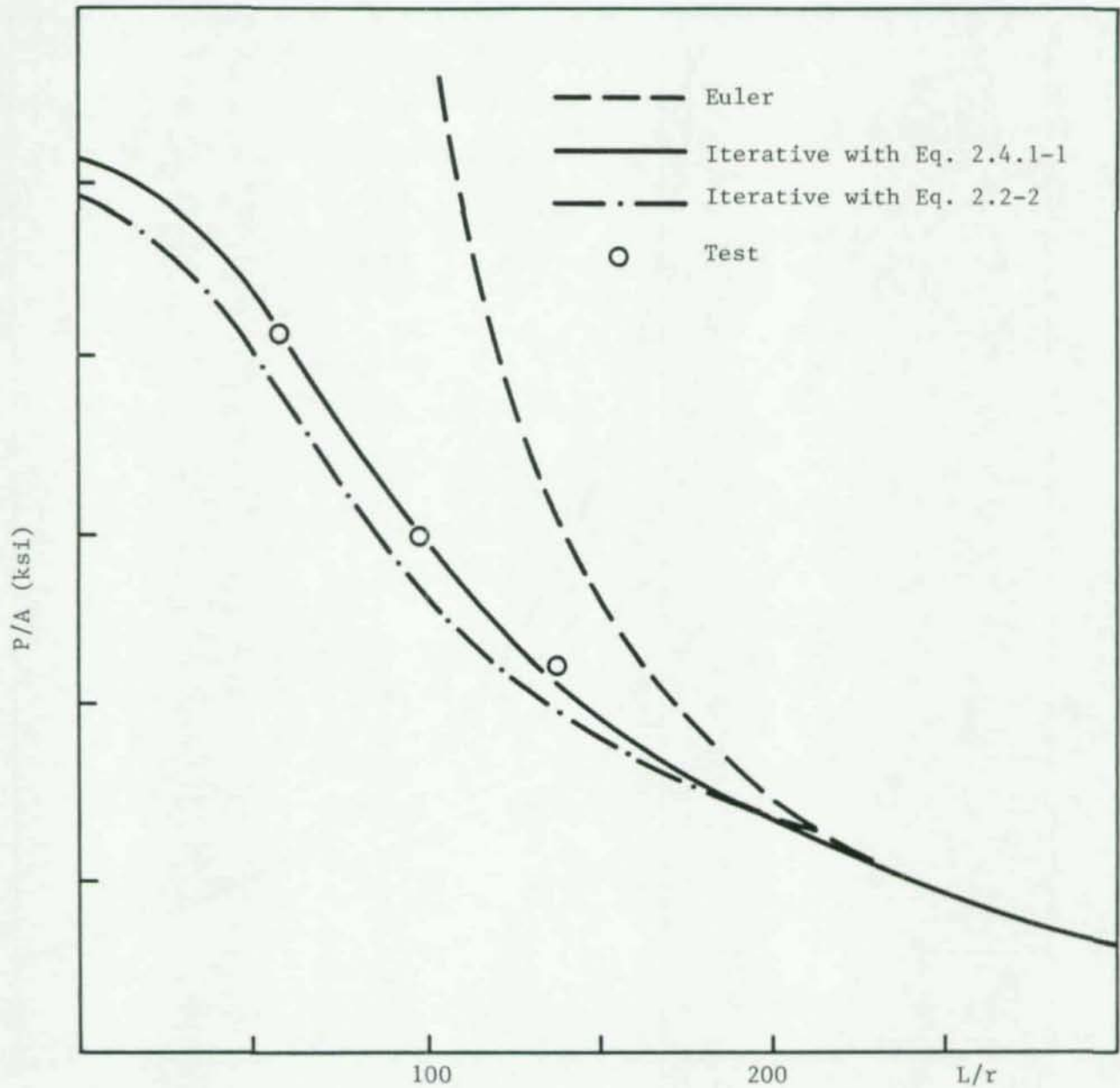
Fig. 4.2-11 Correlation of calculated and observed failure loads for Section LC-III
with w/t = 42.0
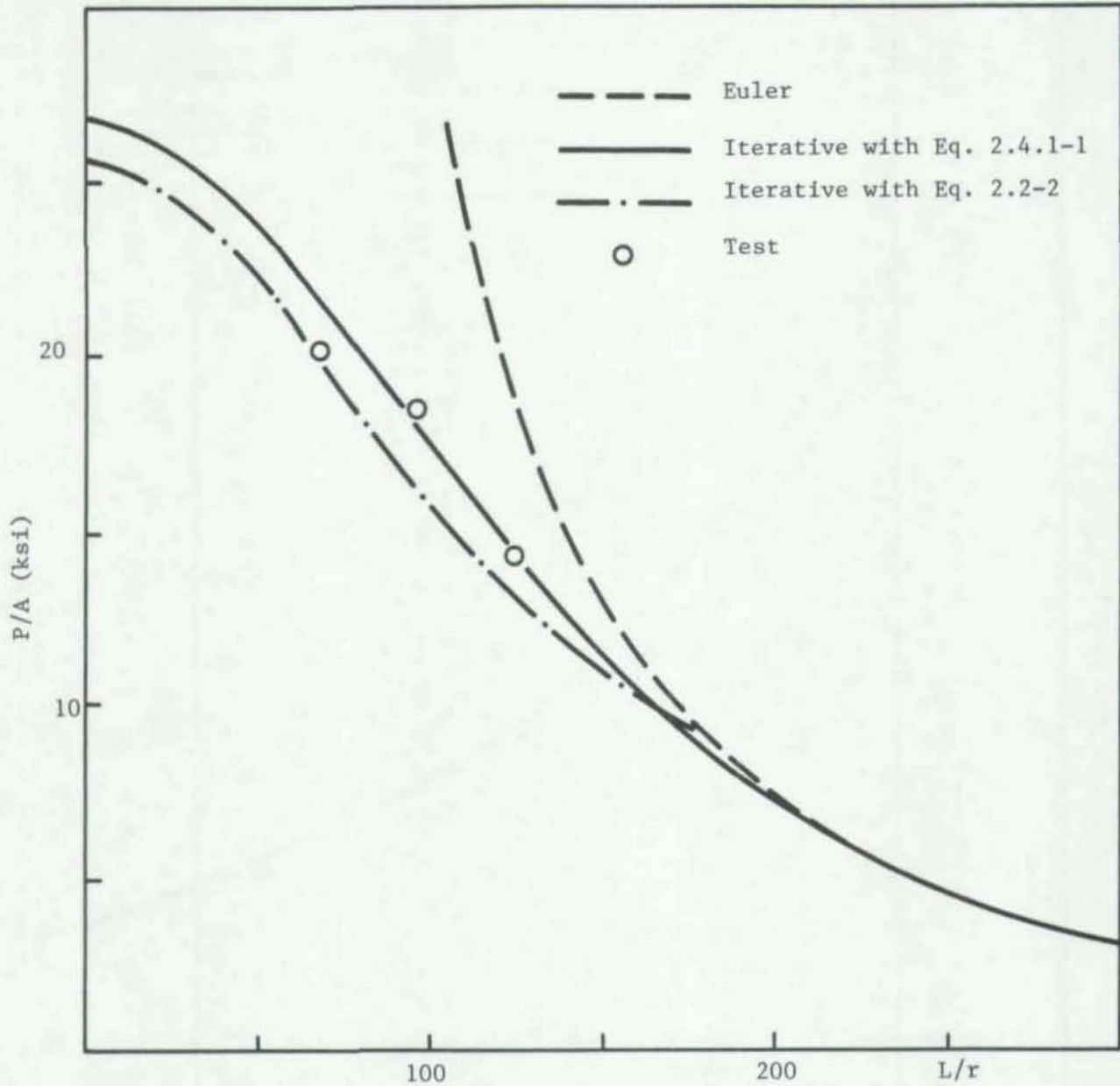
Fig. 4.2-12 Correlation of calculated and observed failure loads for Section LC-IV
with w/t = 35.0
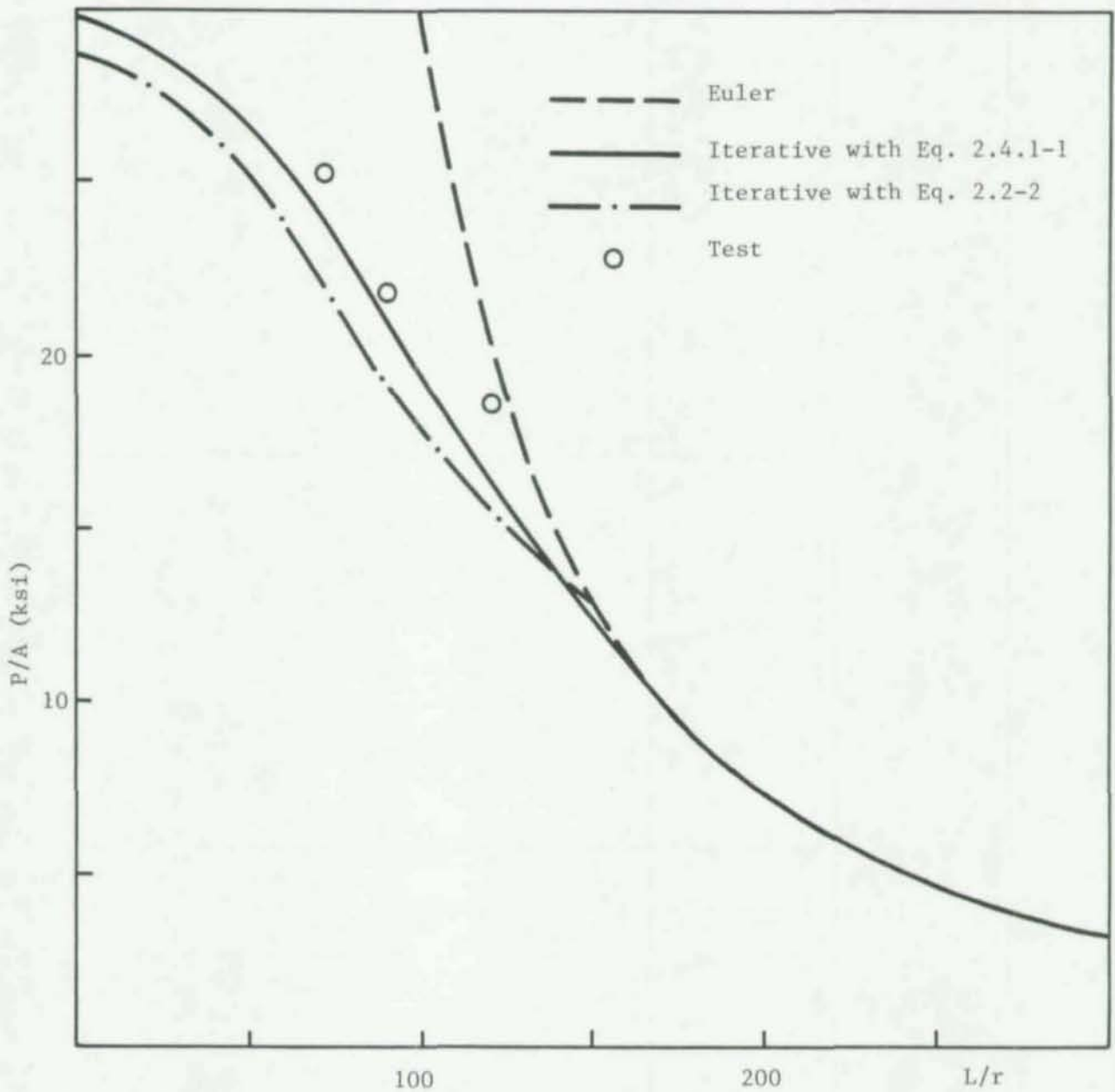
Fig. 4.2-13 Correlation of calculated and observed failure loads for Section LC-V
          with w/t = 29.5
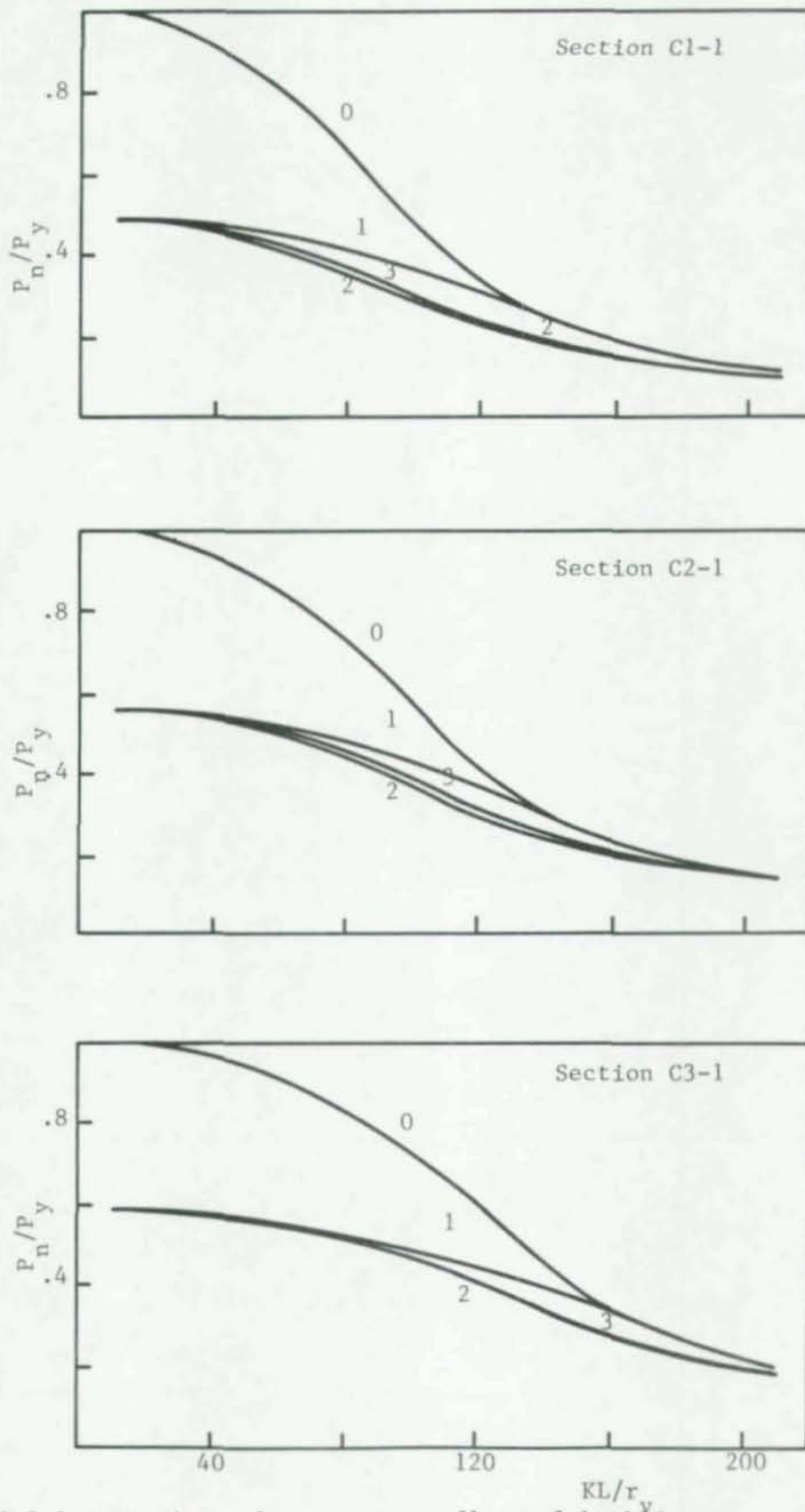
Fig. 4.3-1 C-Section column curves - flexural buckling
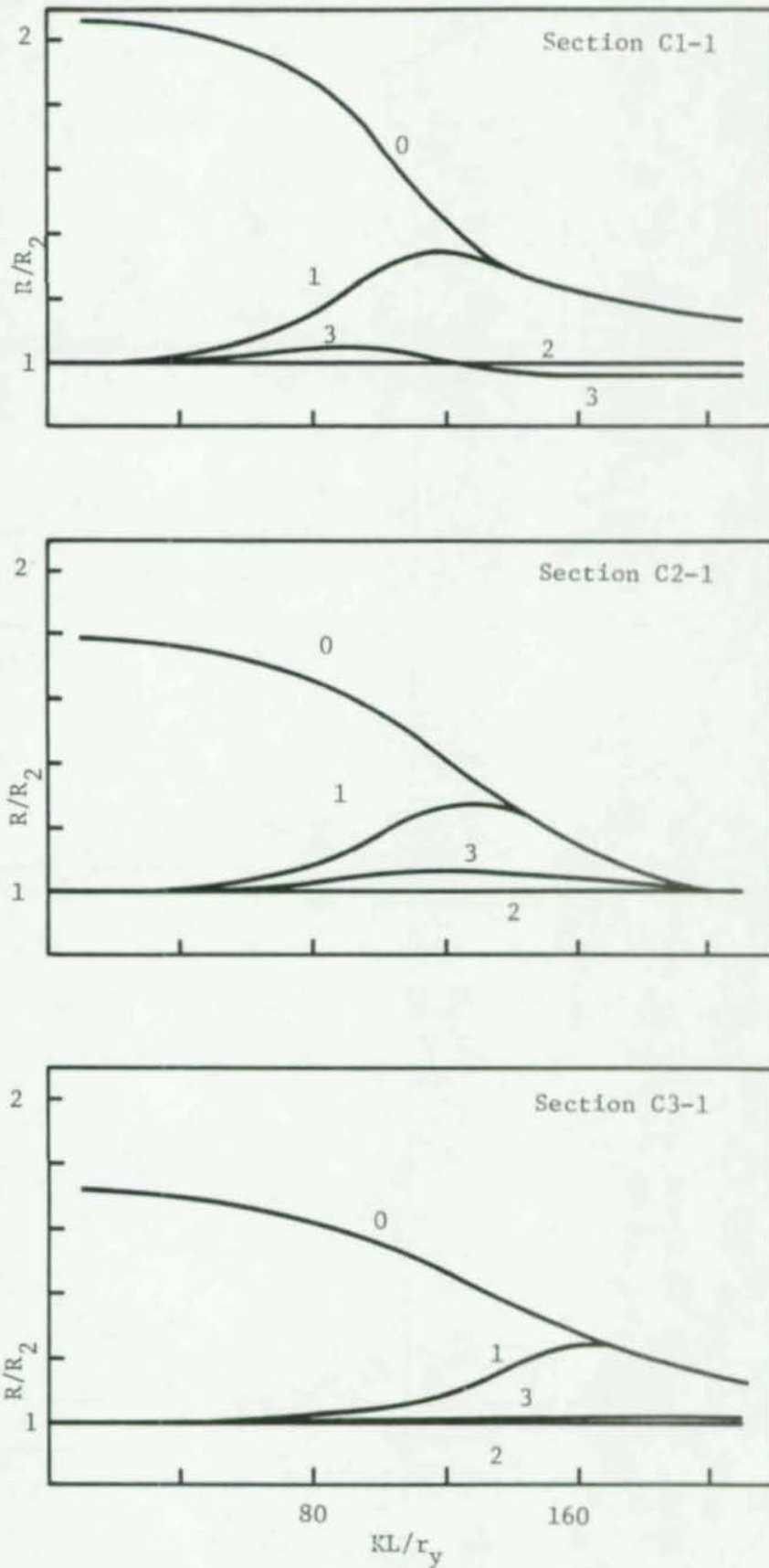
Fig. 4.3-2   C-section column curve comparisons - flexural buckling
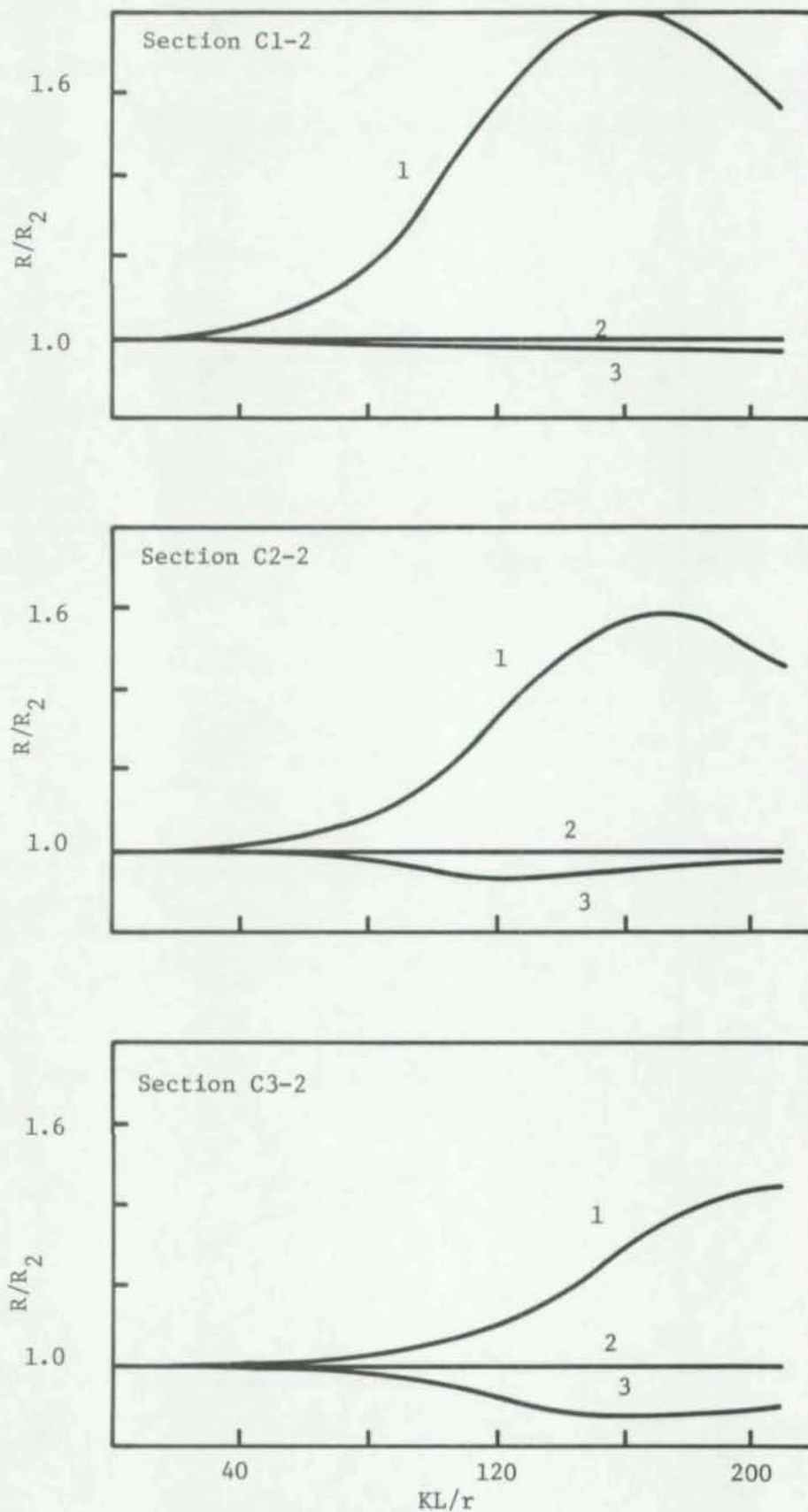
Fig. 4.3-3   C-section column curve comparisons - flexural buckling
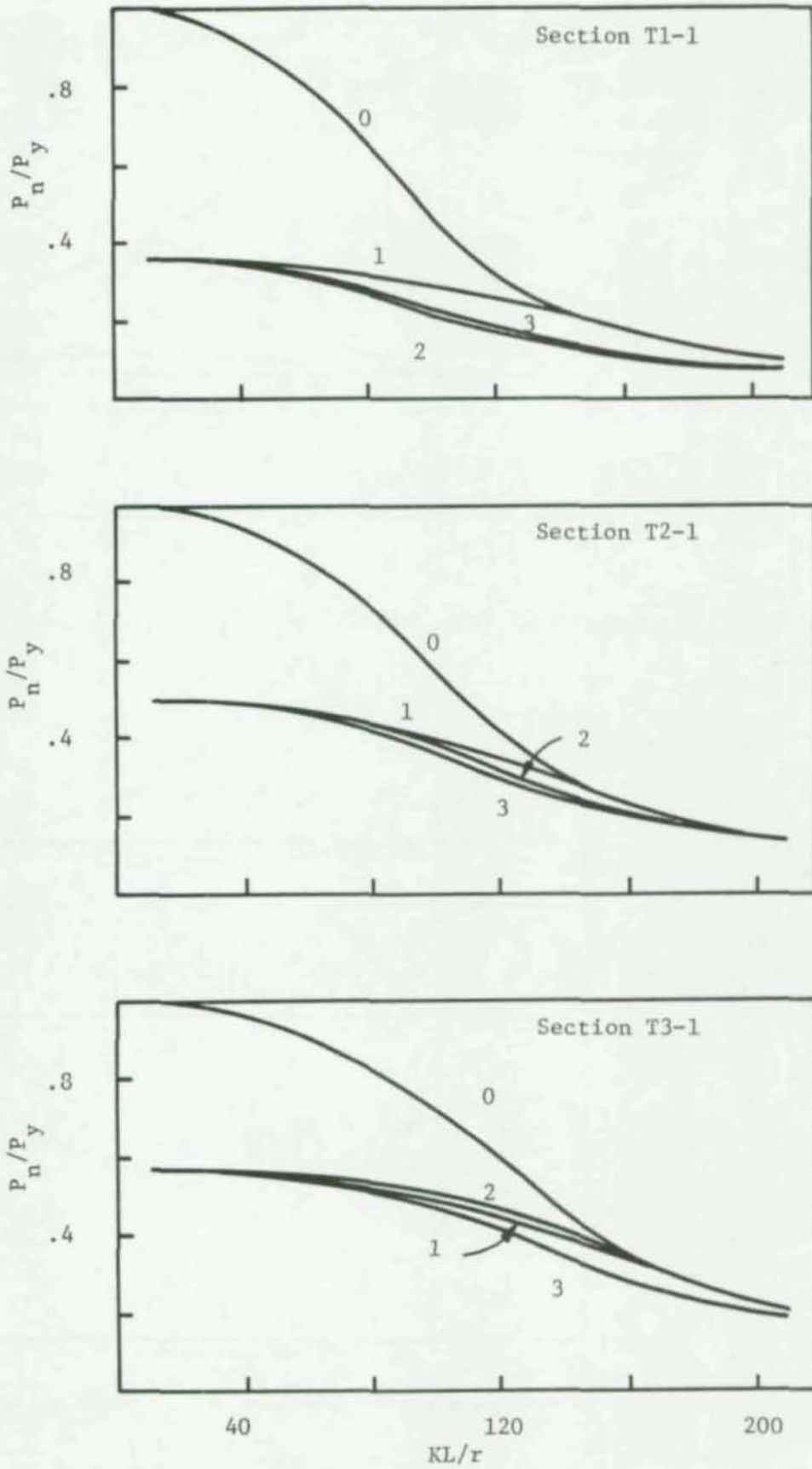
Fig. 4.3-4   Tube column curves - flexural buckling
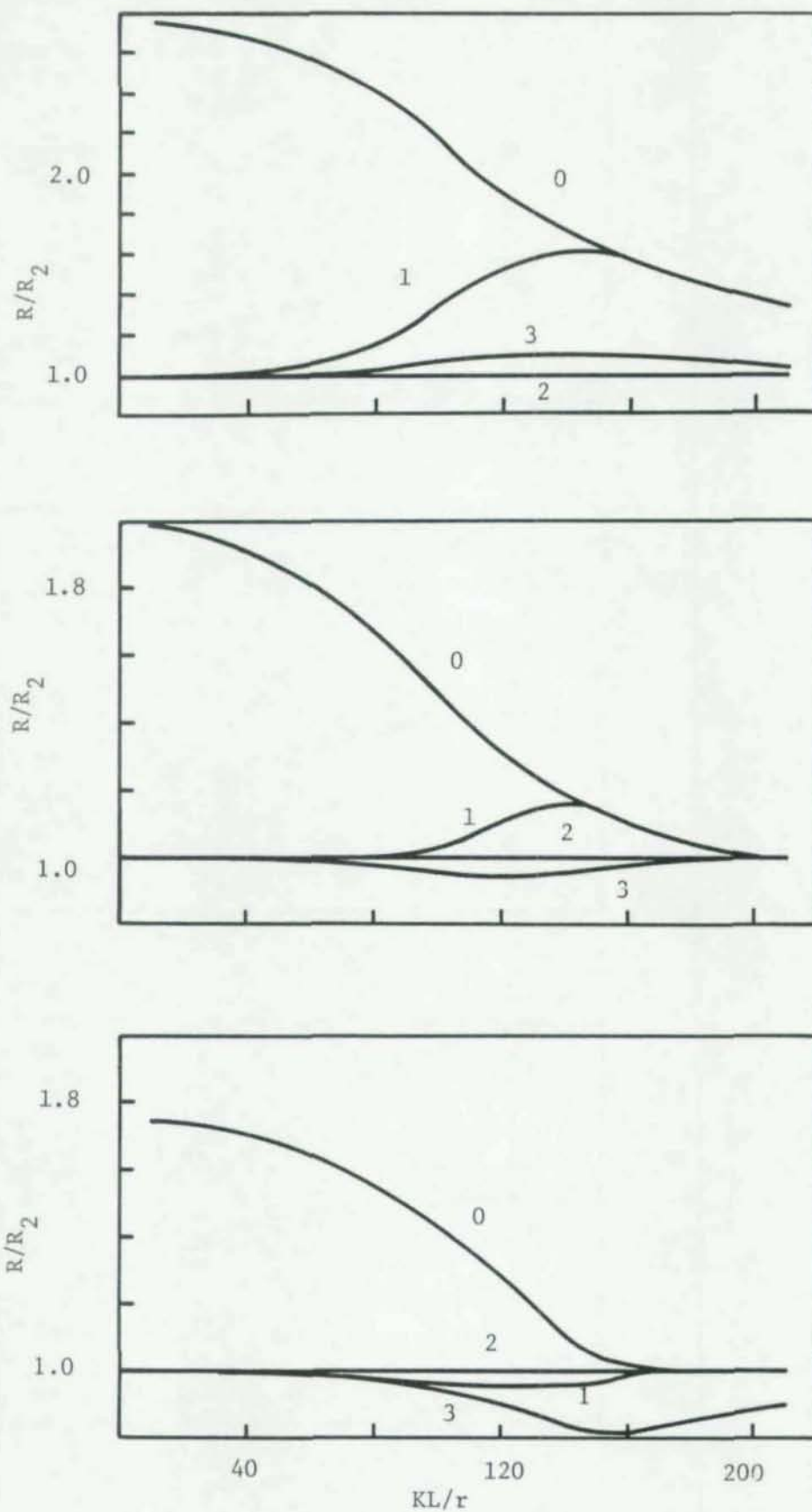
Fig. 4.3-5   Tube column curve comparisons
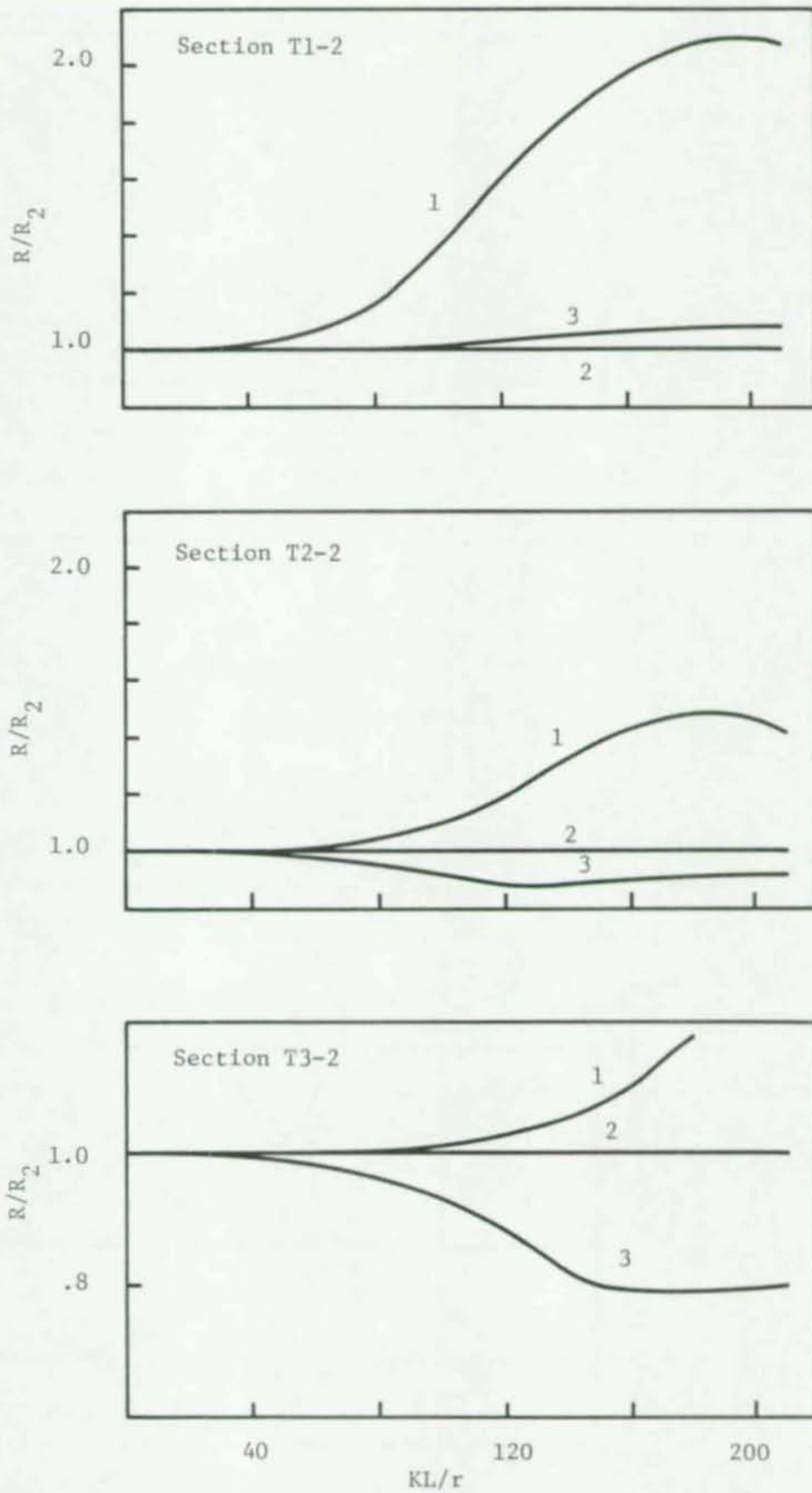
Fig. 4.3-6   Tube column curve comparisons
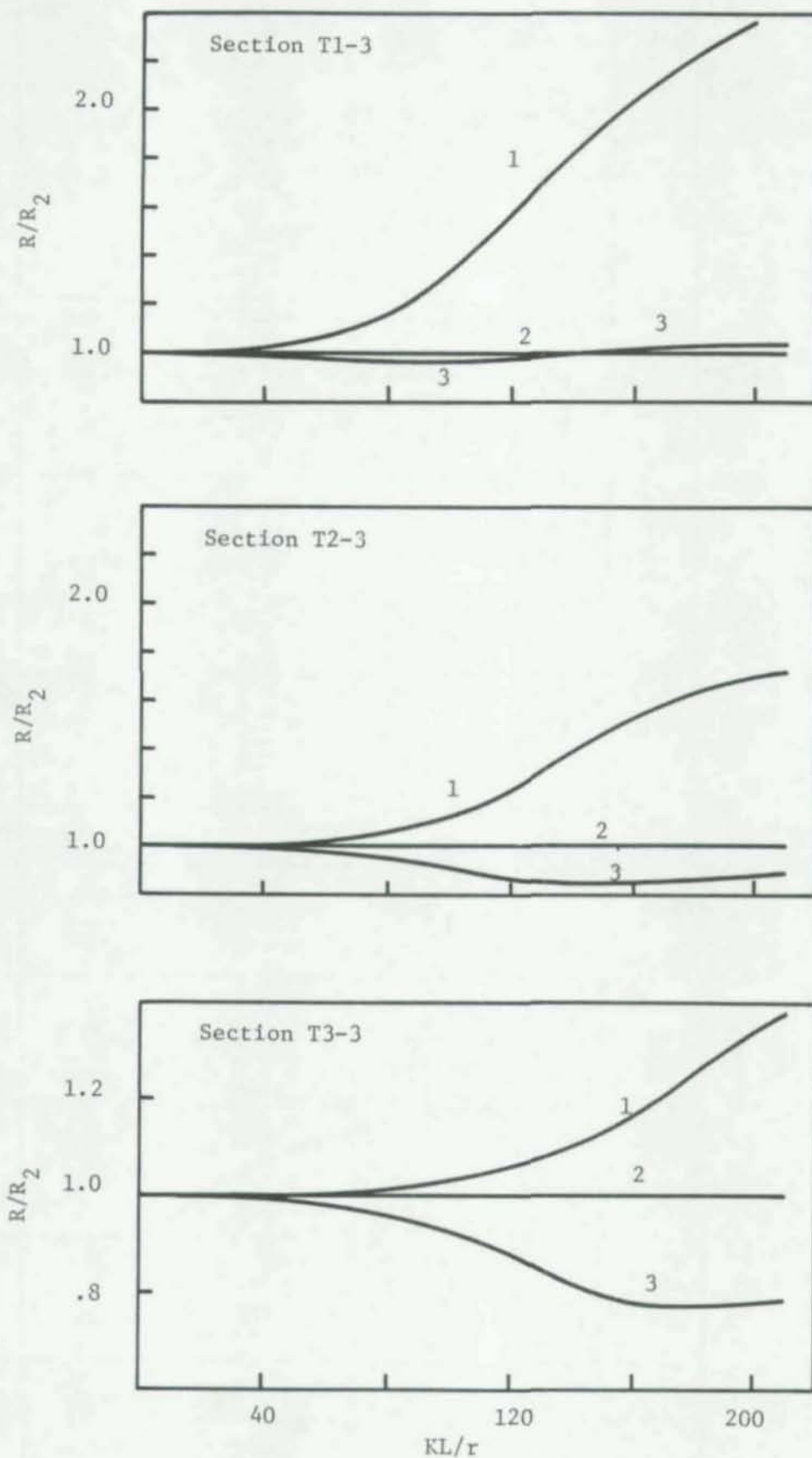
Fig. 4.3-7   Tube column curve comparisons
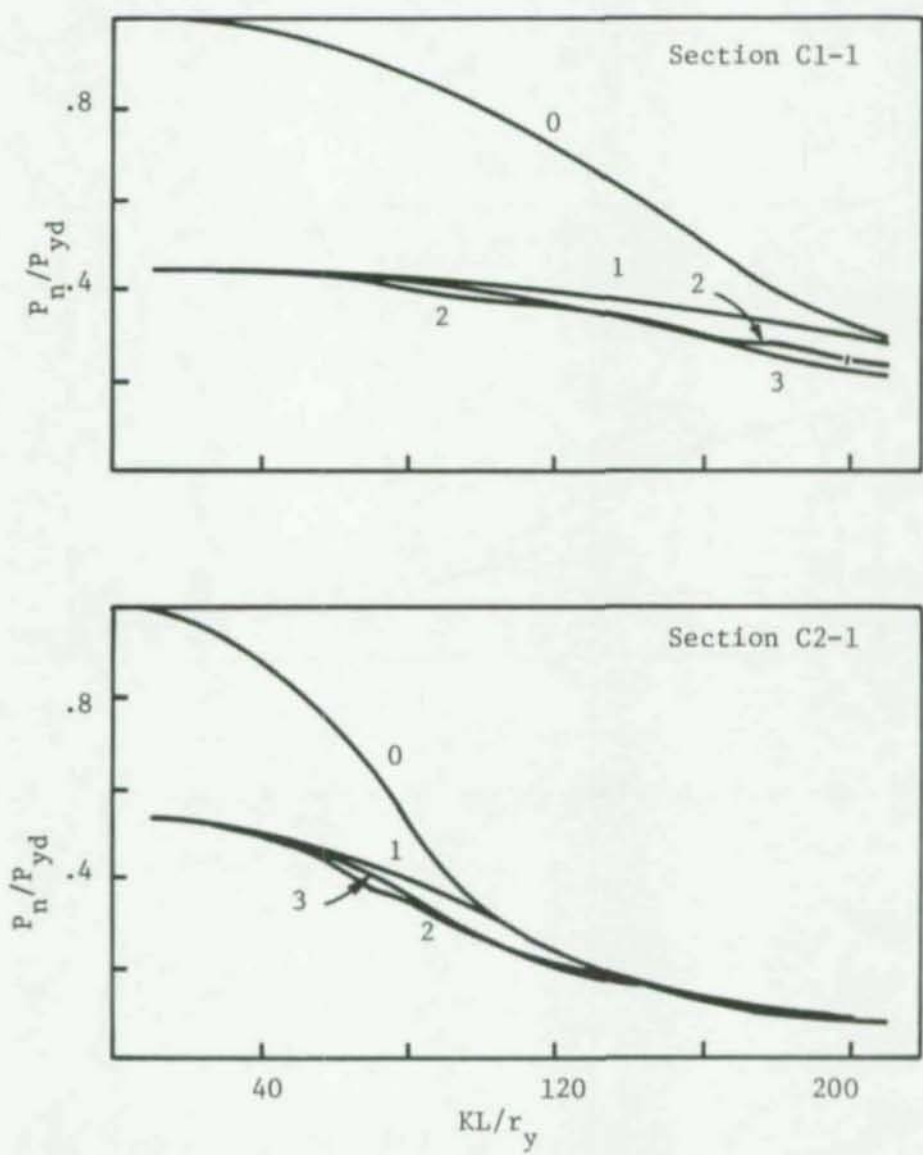
Fig. 5.2-1 a   C-section column curves - torsional-flexural buckling
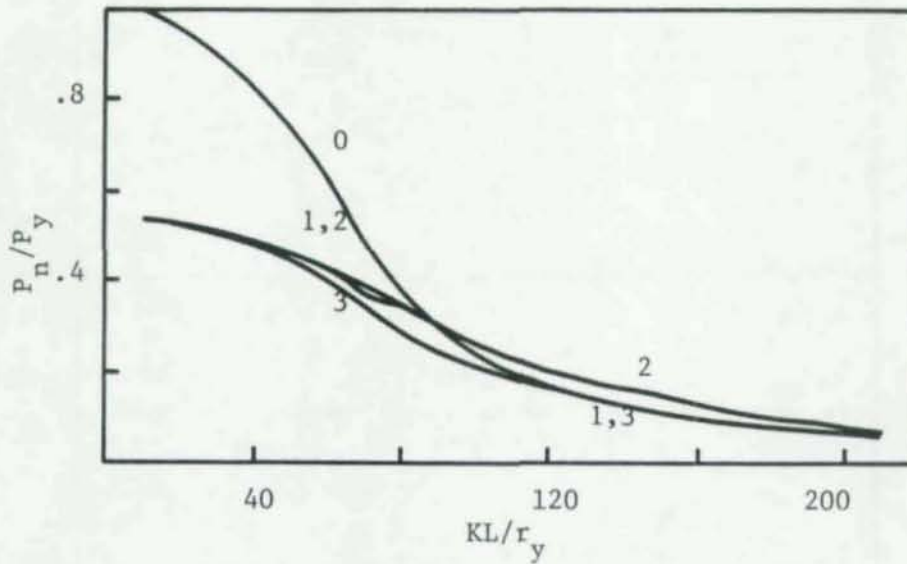
Fig. 5.2-1 b   Hat section column curves - torsional-flexural buckling
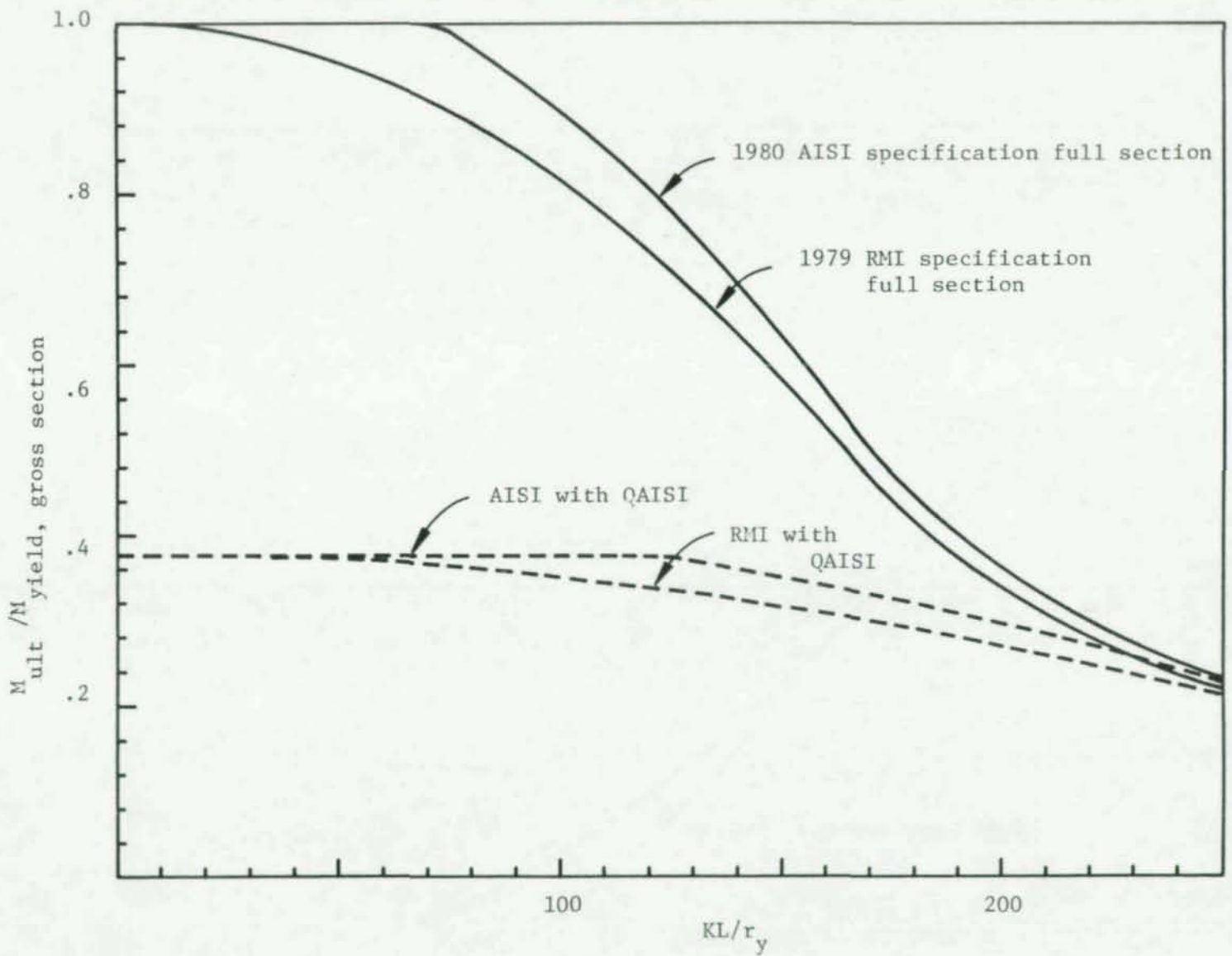
Fig. 6.2-1   Lateral buckling moment about the symmety axis - Section C1-1

Fig. 6.2-2   Lateral buckling moment about the symmetry axis - Section C2-1
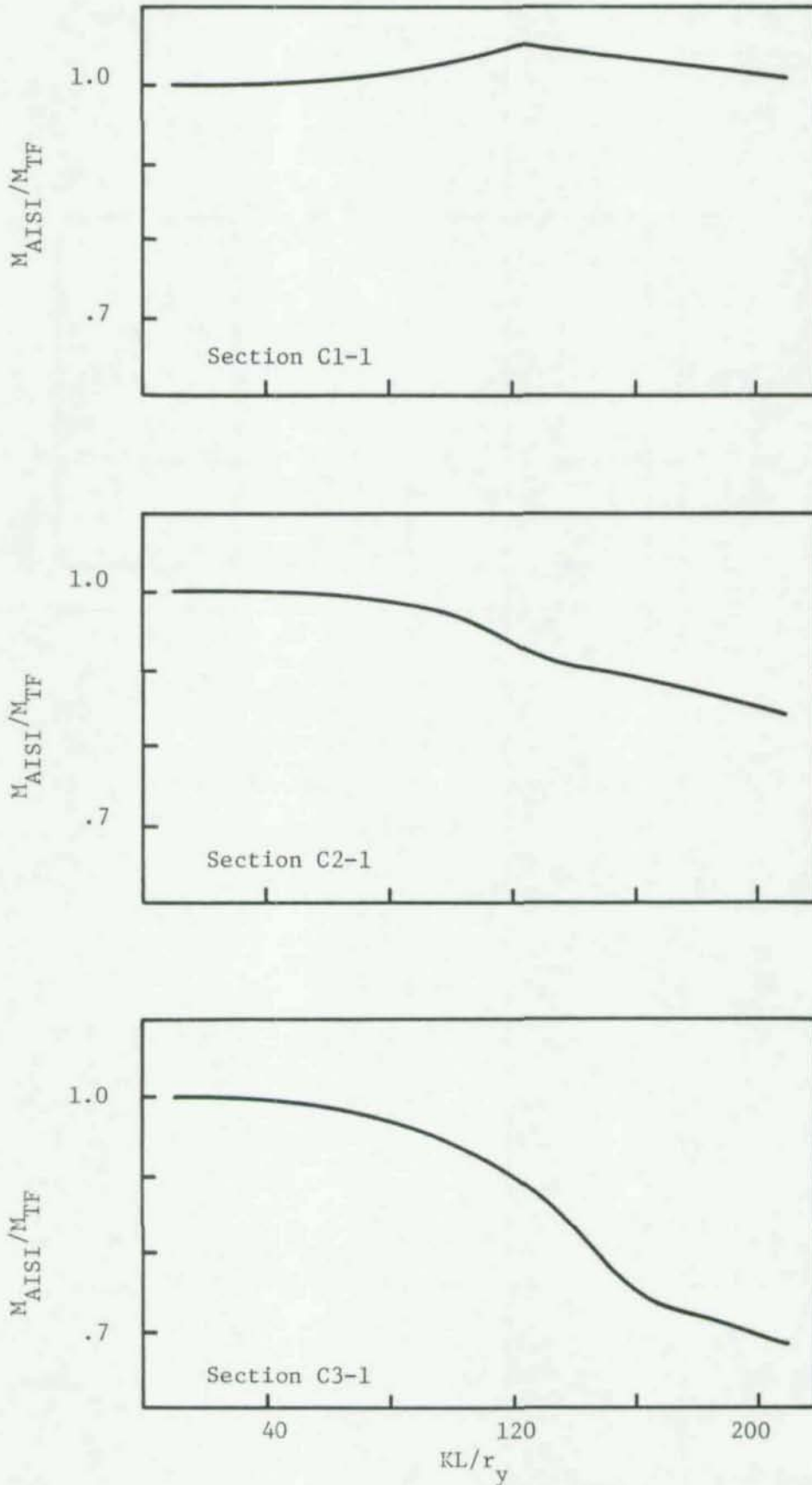
Fig. 6.2-3   Ratio of the lateral buckling moment according
             to the 1980 AISI specification to that according
             to the torsional-flexural buckling theory - C-Sections
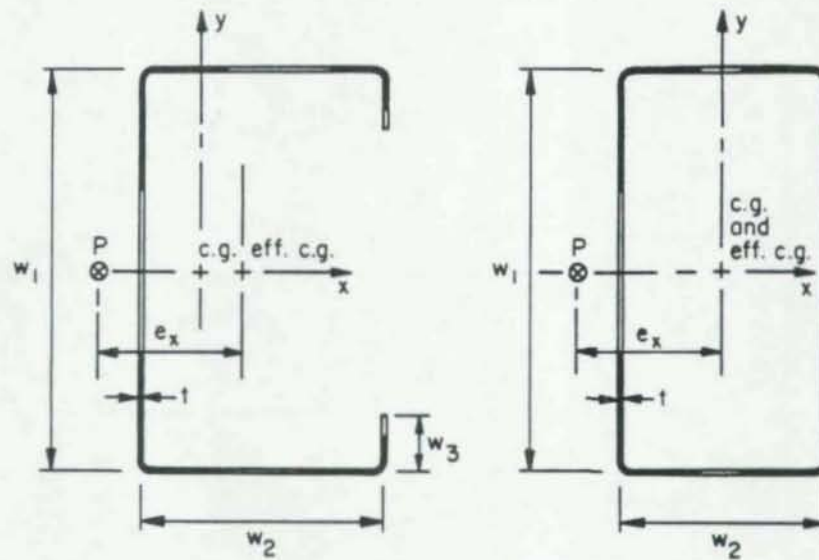
Fig. 7.1-1 Section geometry and generalized effective section
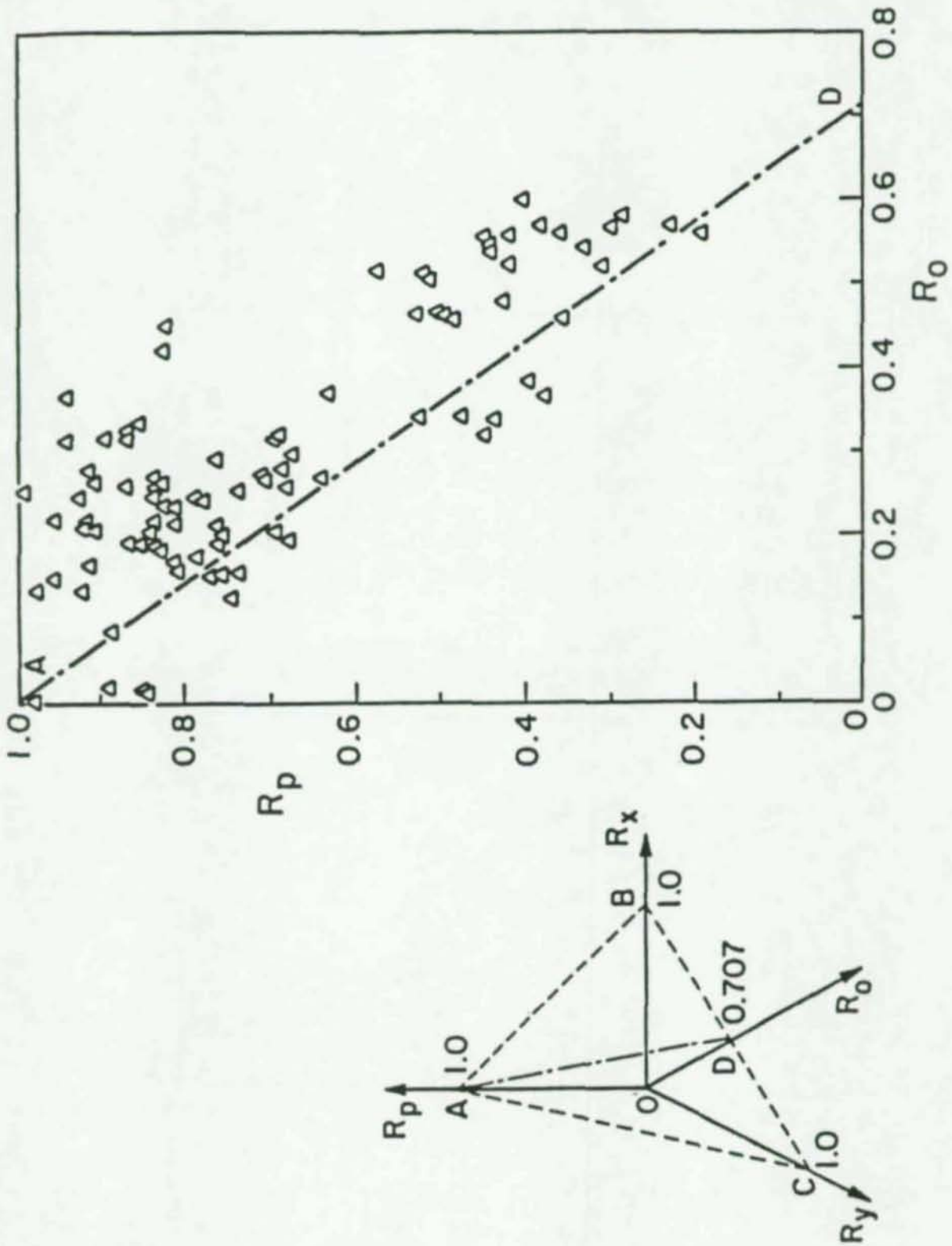
Fig. 7.3-1 Correlation of test results with the unified approach for beam columns
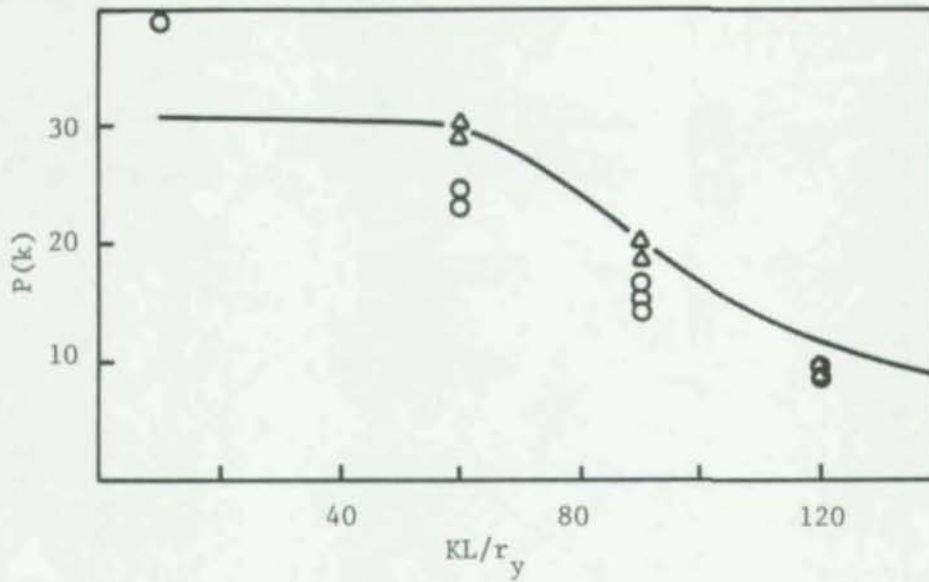
Fig. 8.3-1a Section 1 - Unified approach with $e_x = 0$
      O Columns deflecting towards the corner of
        the section
      △ Columns deflecting towards the tips of
        flanges
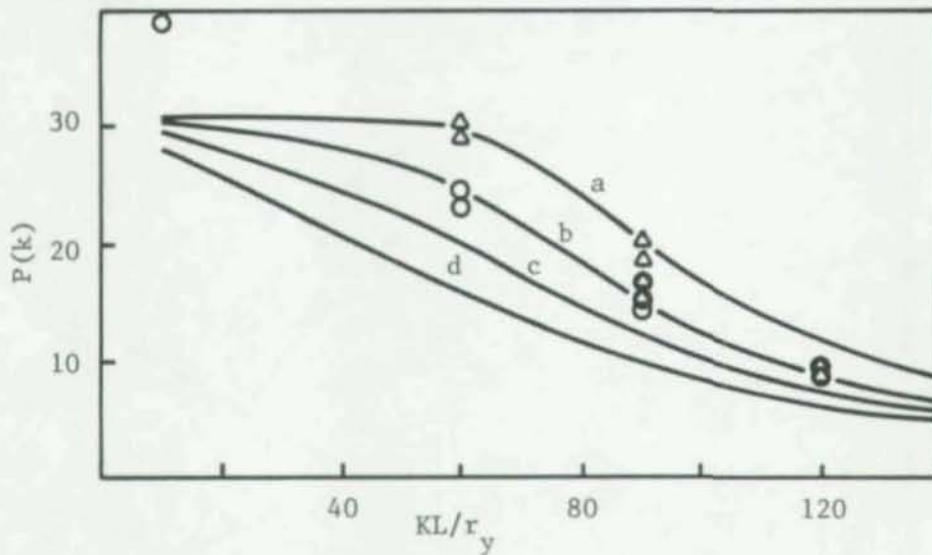
Fig. 8.3-1b Section 1 - Unified approach
        Curve a: $e_x = 0$
        Curve b: $e_x = L/1000$
        Curve c: $e_x = L/500$
        Curve d: $e_x = 3L/1000$
        O Columns deflecting towards the corner of the
          section
        △ Columns deflecting towards the tips of flanges
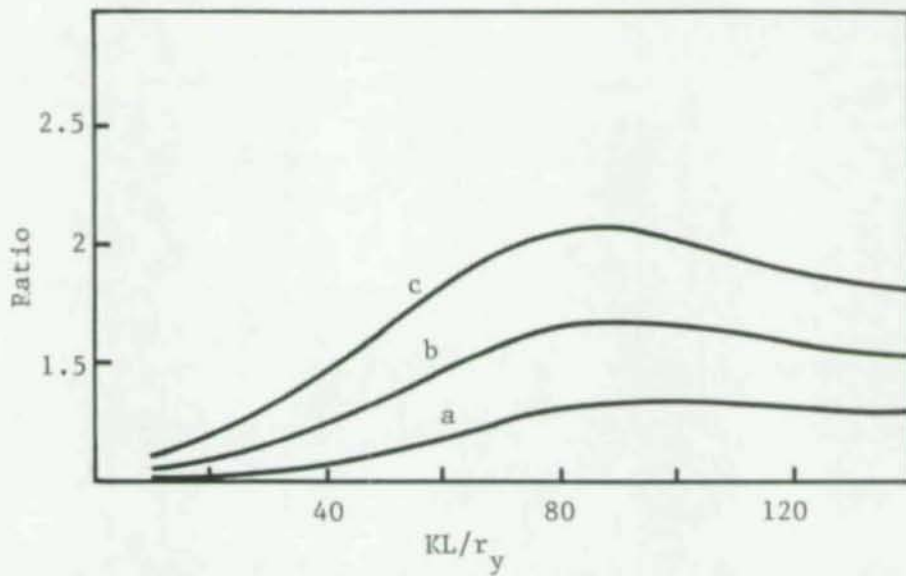
Fig. 8.3-1c Section 1 - Unified approach
Curve a: (P_{ult} for $e_x = 0$)/(P_{ult} for $e_x = L/1000$)
Curve b: (P_{ult} for $e_x = 0$)/(P_{ult} for $e_x = L/500$)
Curve c: (P_{ult} for $e_x = 0$)/(P_{ult} for $e_x = 2L/1000$)
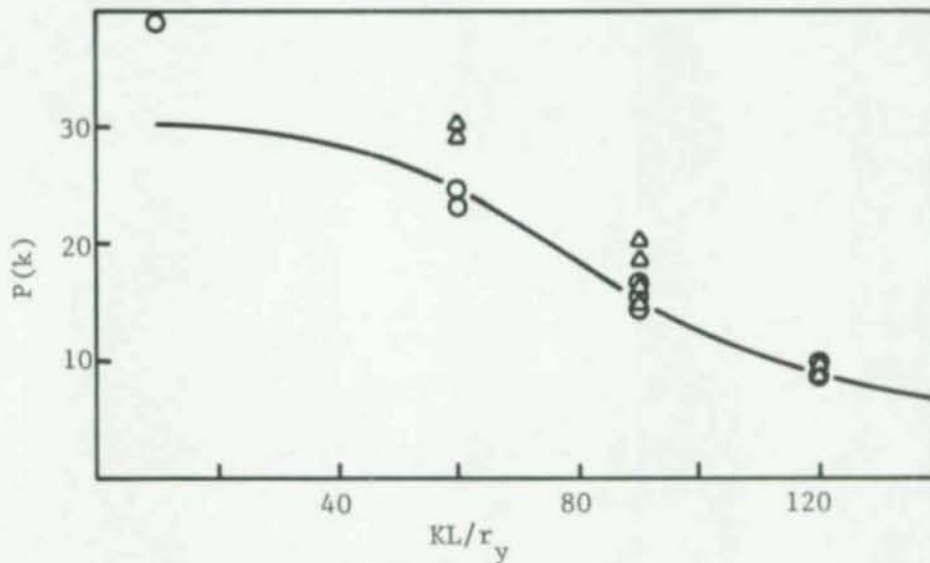
Fig. 8.3-1d Section 1 - Unified approach with $e_x = L/1000$
     O Columns deflecting towards the corner of the
        section
     Δ Columns deflecting towards the tips of
        flanges
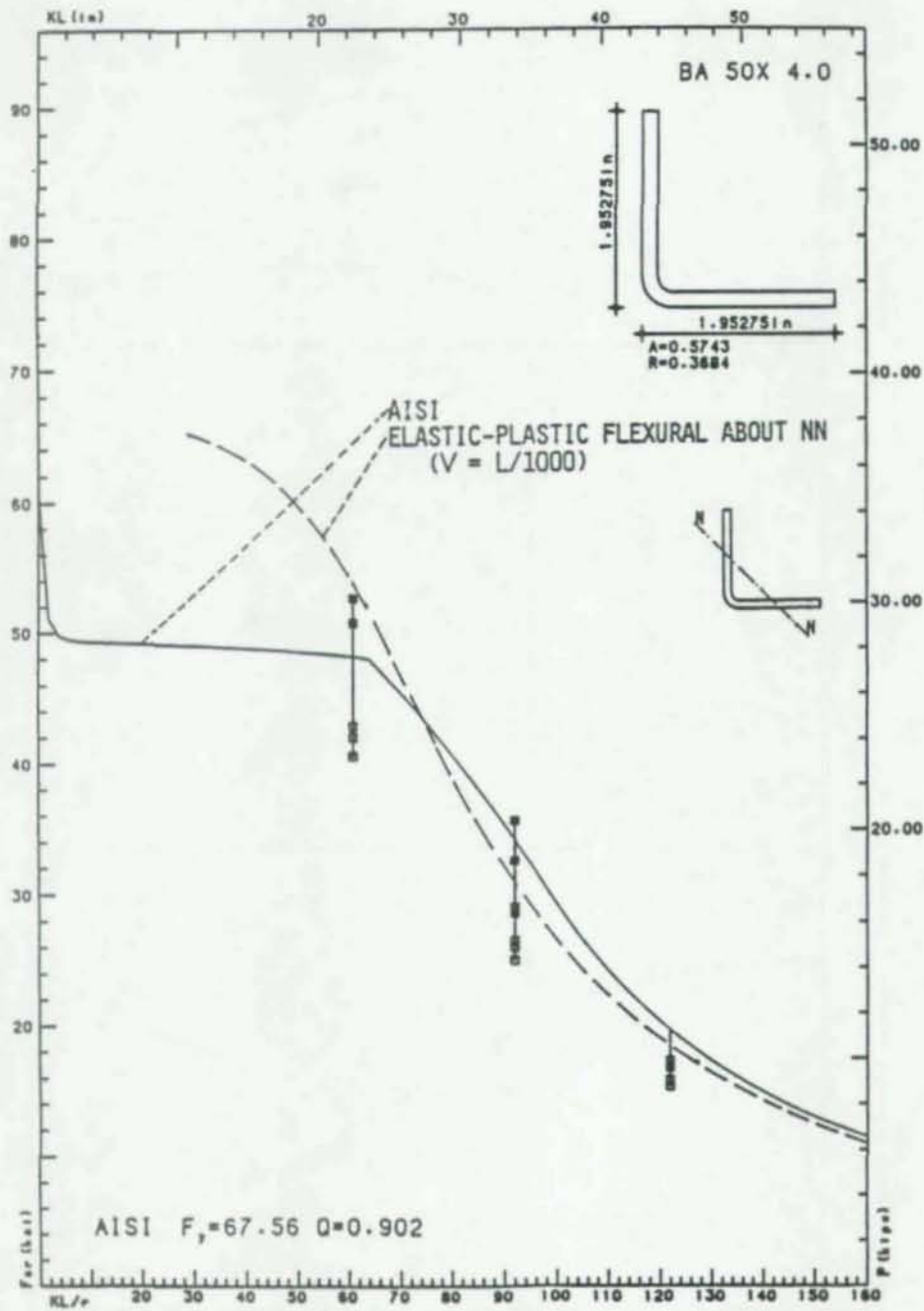
Fig. 8.3-1e   Section 1 - Correlation with the 1980 AISI approach
and other approaches
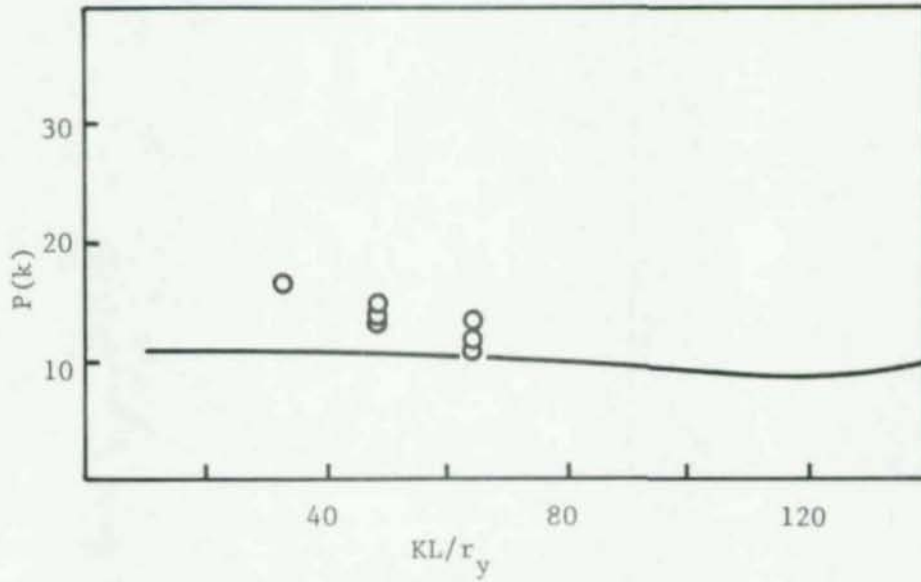
Fig. 8.3-2a Section 2 - Unified approach with $e_x = 0$
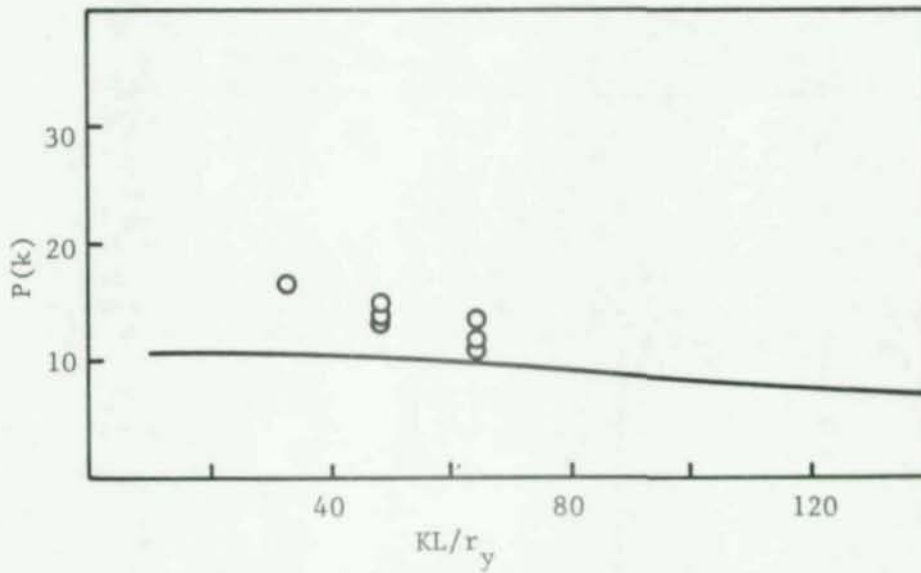
Fig. 8.3-2b Section 2 - Unified approach with $e_x = L/1000$
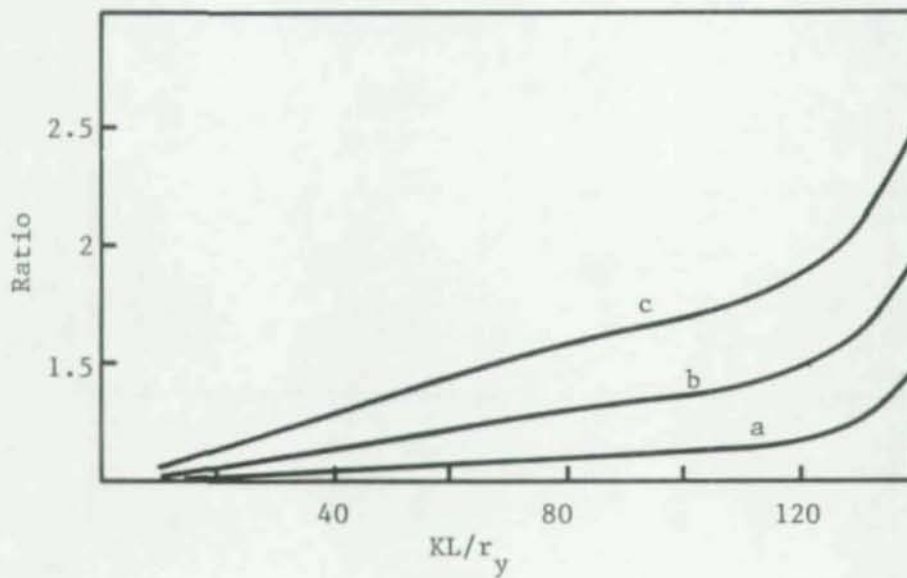
Fig. 8.3-2c Section 2 - Unified approach
    Curve a: $(P_{ult}$ for $e_x = 0)/(P_{ult}$ for $e_x = L/1000)$
    Curve b: $(P_{ult}$ for $e_x = 0)/(P_{ult}$ for $e_x = L/500)$
    Curve c: $(P_{ult}$ for $e_x = 0)/(P_{ult}$ for $e_x = 2L/1000)$
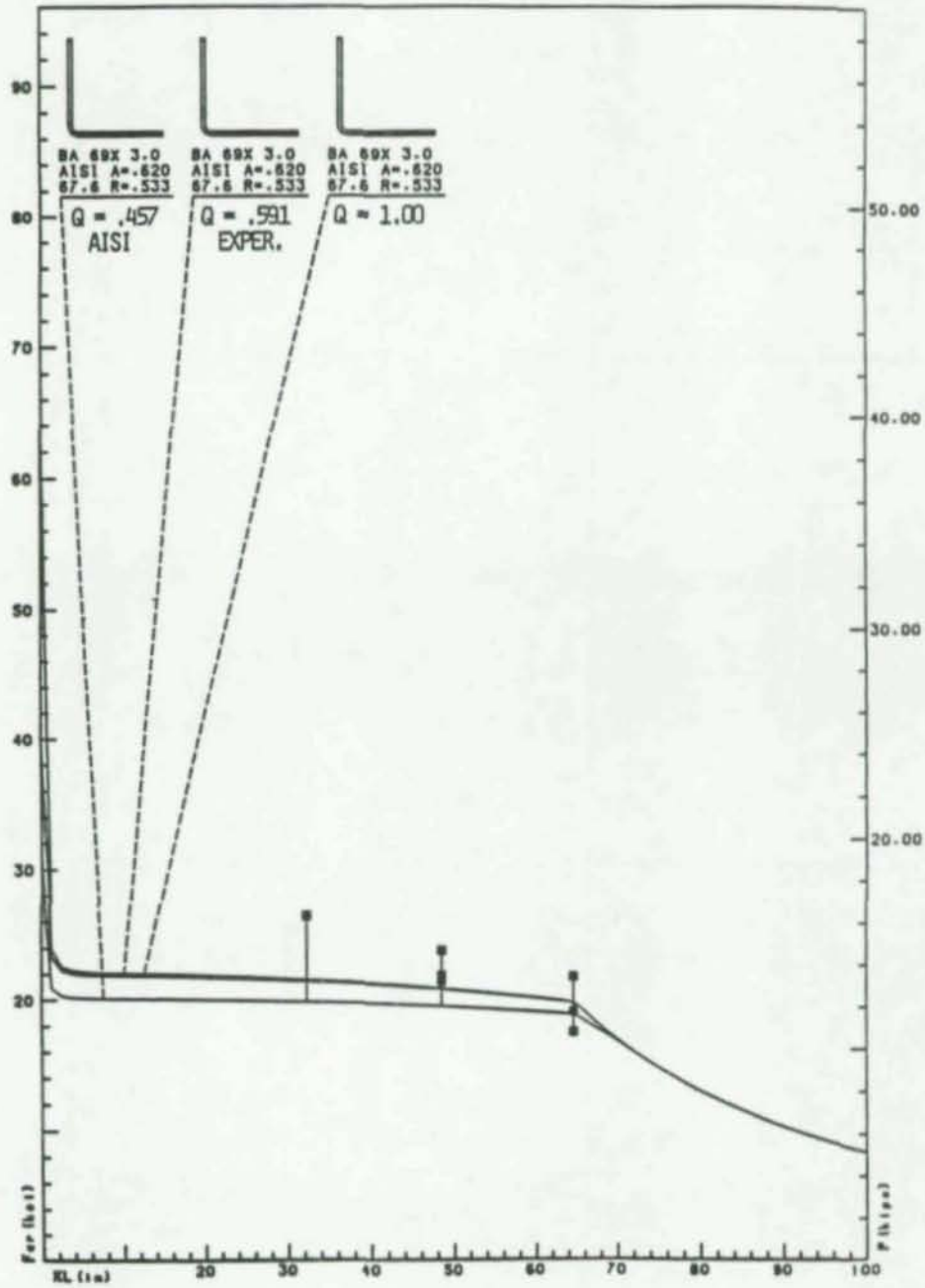
Fig. 8.3-2d Section 2 - Correlation with the 1980 AISI approach
and other approaches
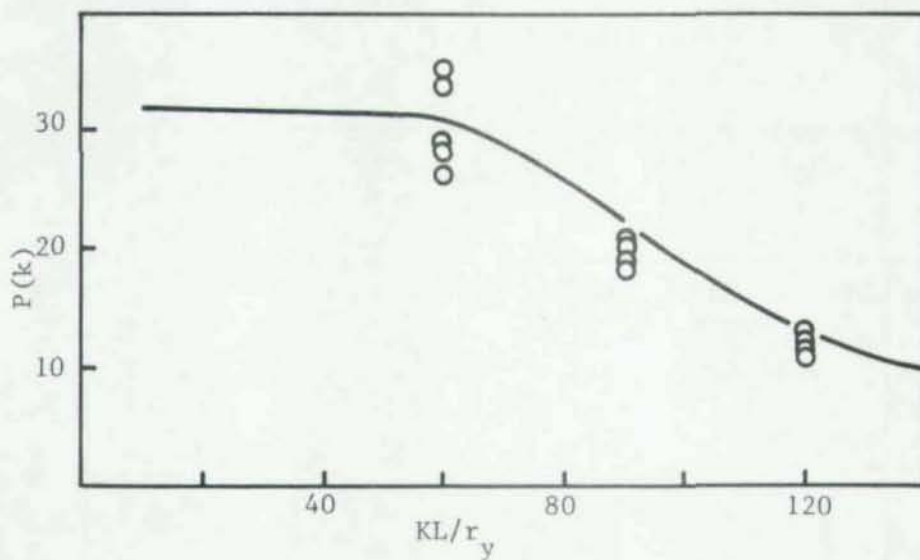
Fig. 8.3-3a Section 3 - Unified approach with $e_x = 0$
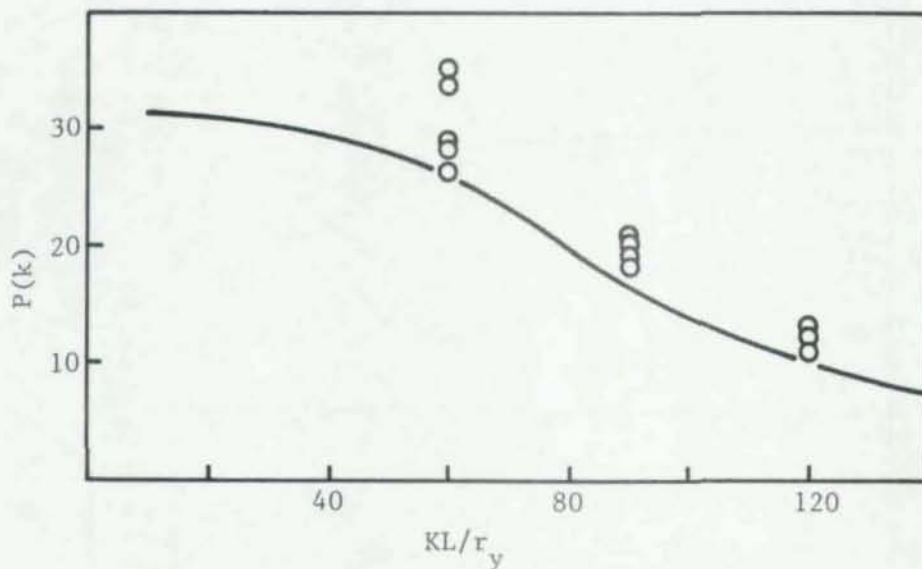
Fig. 8.3-3b Section 3 - Unified approach with $e_x = L/1000$
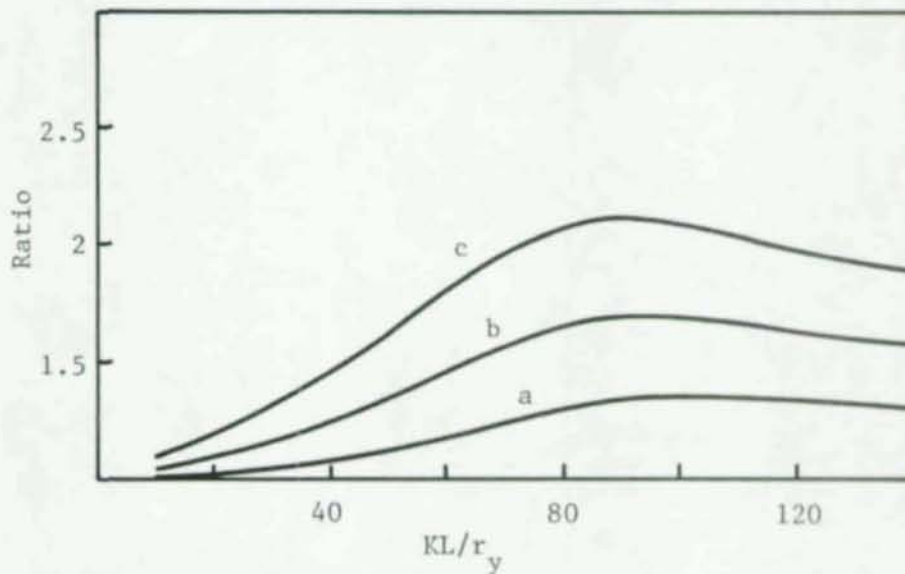
Fig. 8.3-3c Section 3 - Unified approach
Curve a: $(P_{ult}$ for $e_x = 0)/(P_{ult}$ for $e_x = L/1000)$
Curve b: $(P_{ult}$ for $e_x = 0)/(P_{ult}$ for $e_x = L/500)$
Curve c: $(P_{ult}$ for $e_x = 0)/(P_{ult}$ for $e_x = 2L/1000)$
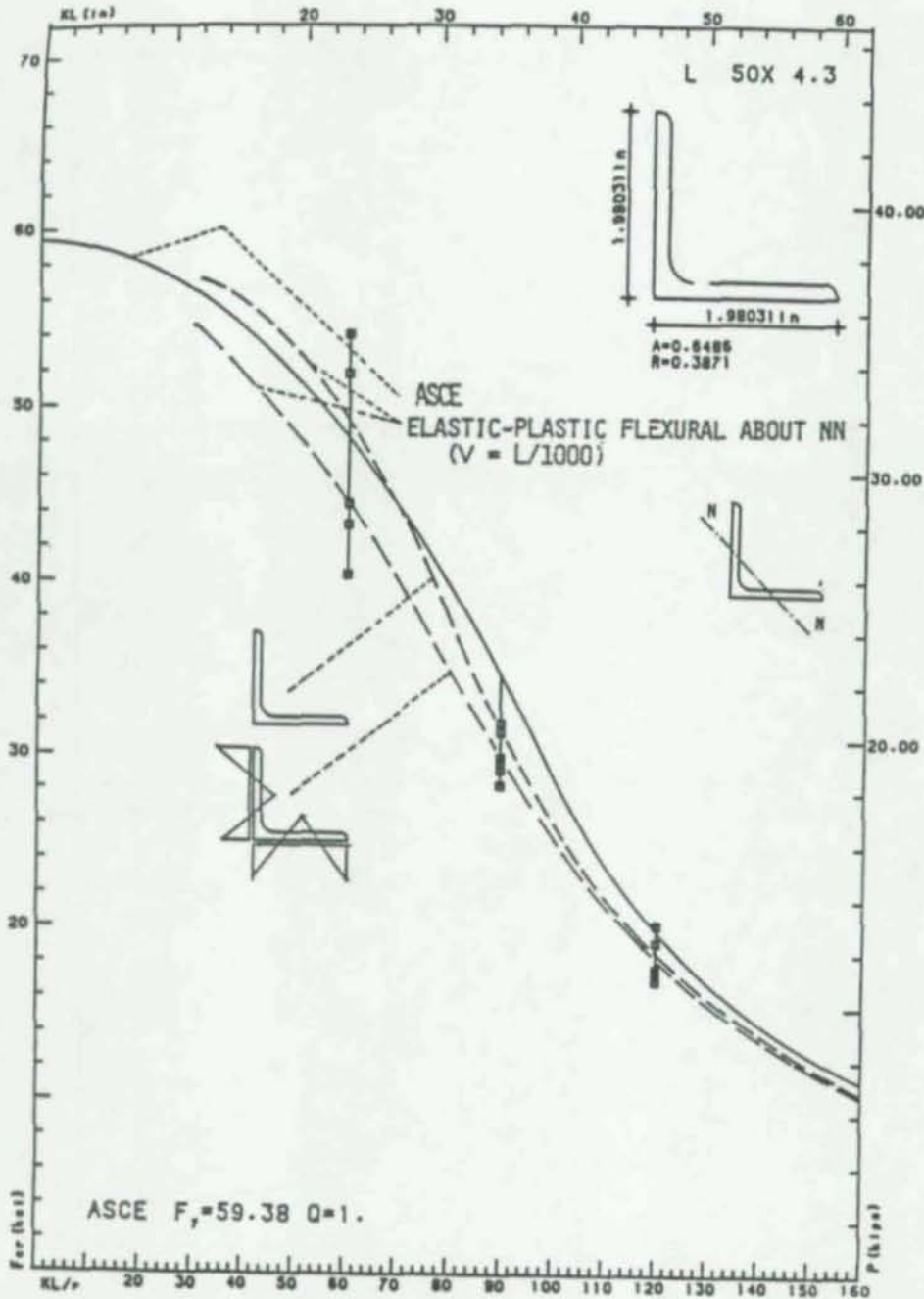
Fig. 8.2-3d Section 3 - Correlation with the 1980 AISI approach
and other approaches
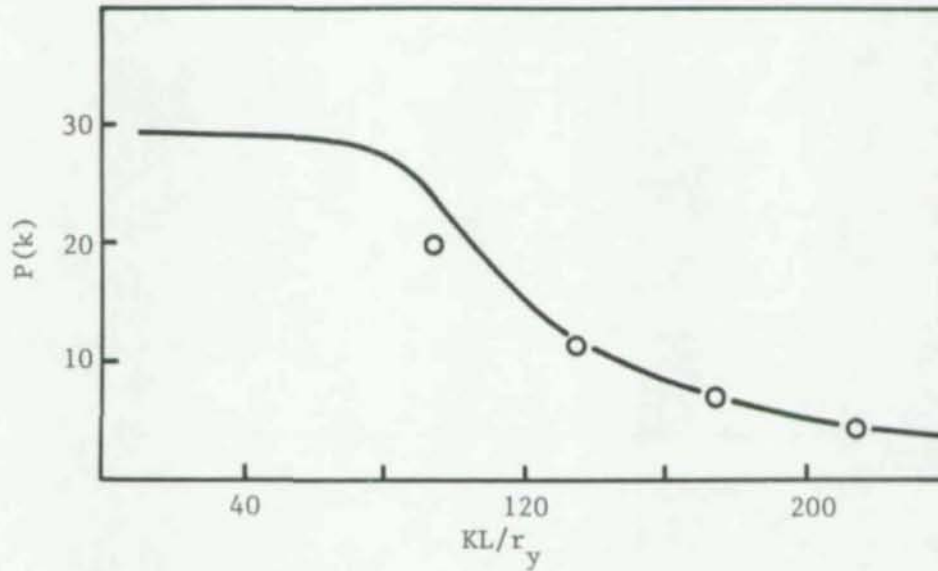
Fig. 8.3-4a Section 4 - Unified approach with $e_x = 0$
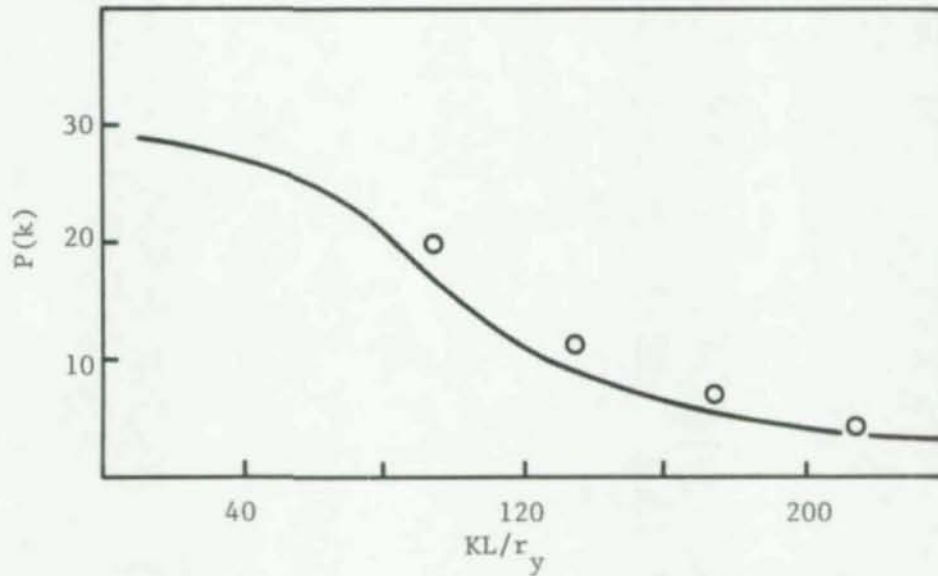
Fig. 8.3-4b Section 4 - Unified approach with $e_x = L/1000$
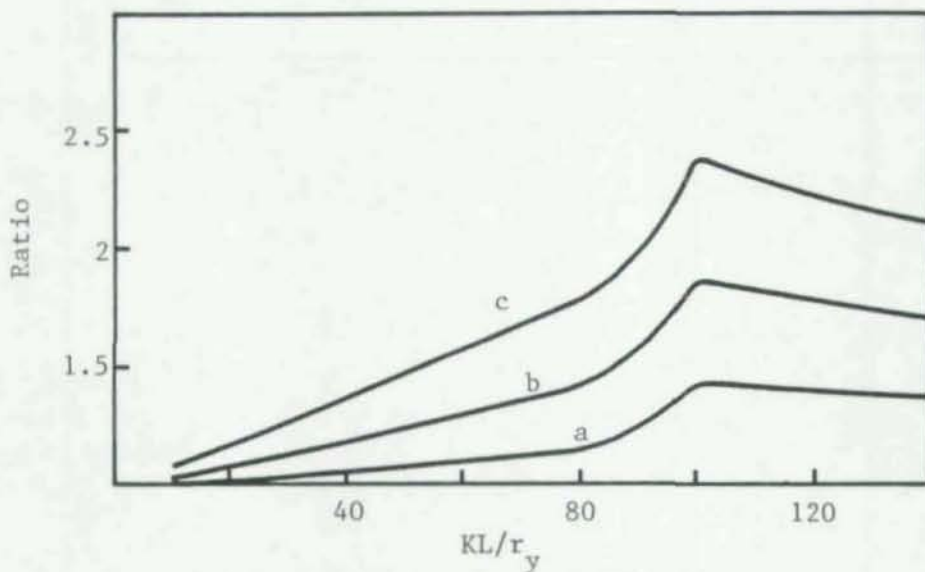
Fig. 8.3-4c Section 4 - Unified approach
        Curve a: (P_{ult} for $e_x = 0$)/(P_{ult} for $e_x = L/1000$)
        Curve b: (P_{ult} for $e_x = 0$)/(P_{ult} for $e_x = L/500$)
        Curve c: (P_{ult} for $e_x = 0$)/(P_{ult} for $e_x = 2L/1000$)
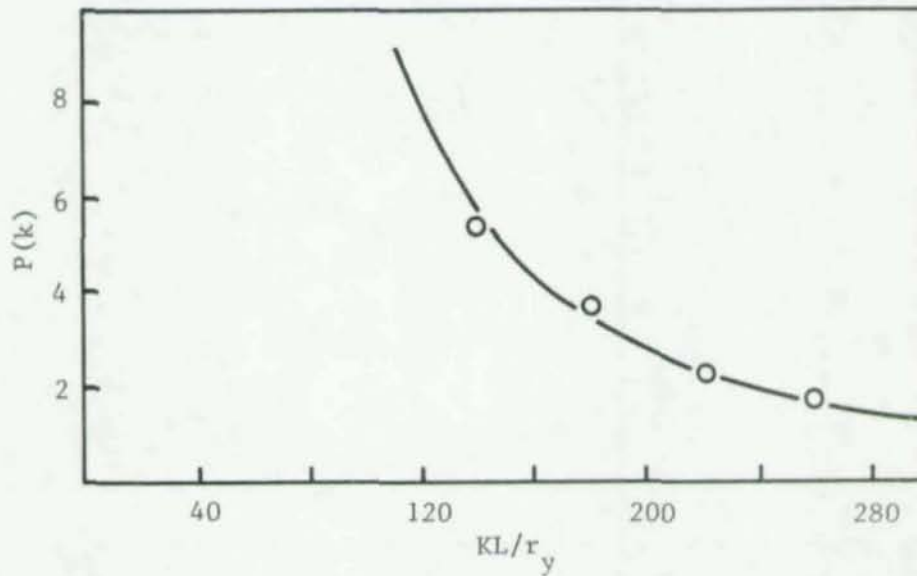
Fig. 8.3-5a Section 5 - Unified approach with $e_x = 0$
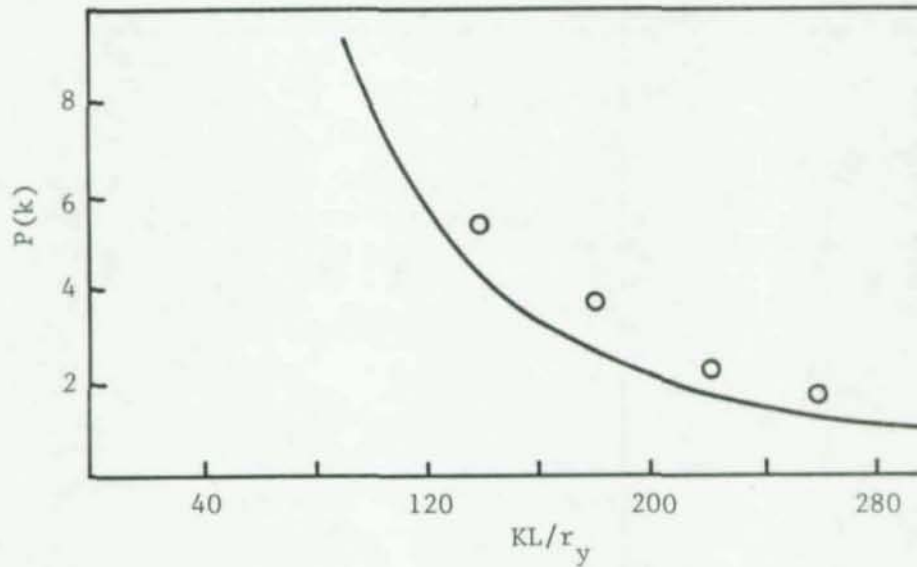
Fig. 8.3-5b Section 5 - Unified approach with $e_x = L/1000$
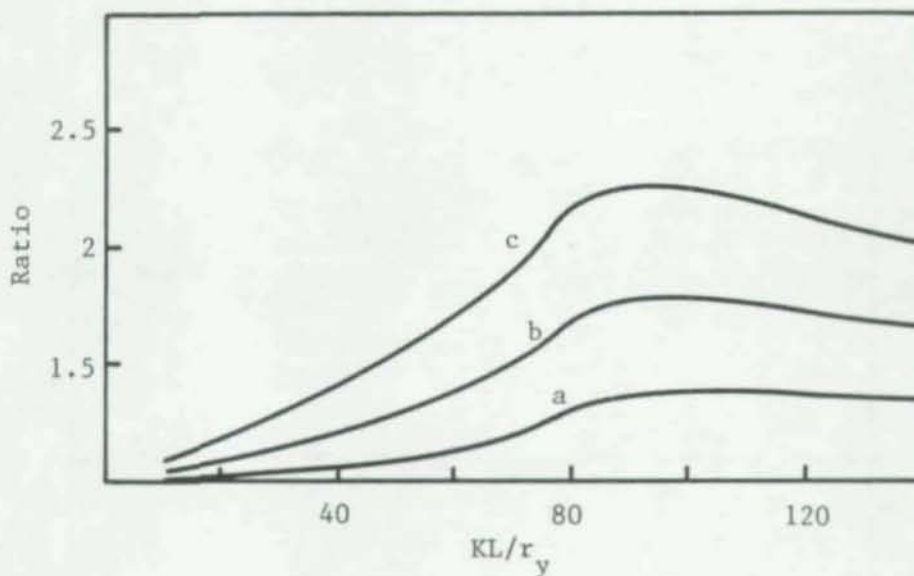
Fig. 8.3-5c Section 5 – Unified approach
 Curve a: $(P_{ult}$ for $e_x = 0)/(P_{ult}$ for $e_x = L/1000)$
 Curve b: $(P_{ult}$ for $e_x = 0)/(P_{ult}$ for $e_x = L/500)$
 Curve c: $(P_{ult}$ for $e_x = 0)/(P_{ult}$ for $e_x = 2L/1000)$
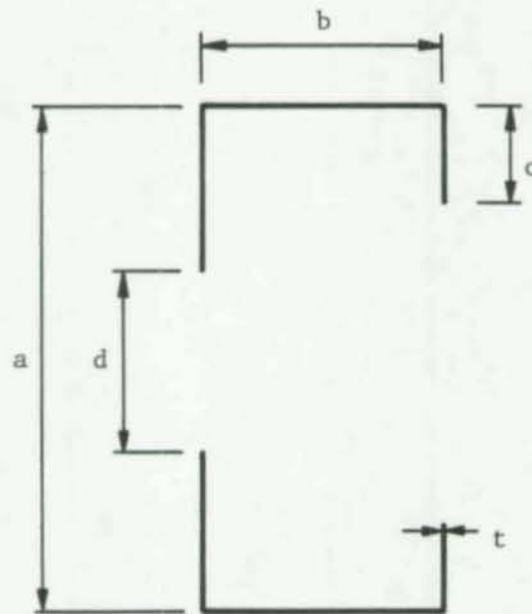
Fig. 9.1-1 Dimensions of the lipped channels tested

a=3.5 in   b=1.555 in   c=0.512 in

Assumed corner radius = 0.15 in
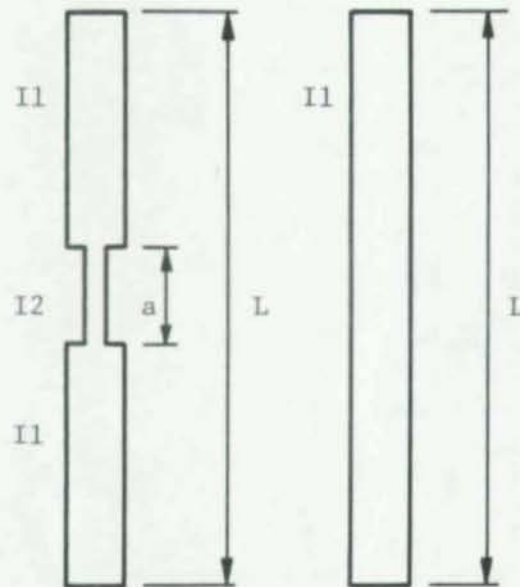
Fig. 9.4-1   Dimensions of columns used in the parametric study
on nonprismatic columns
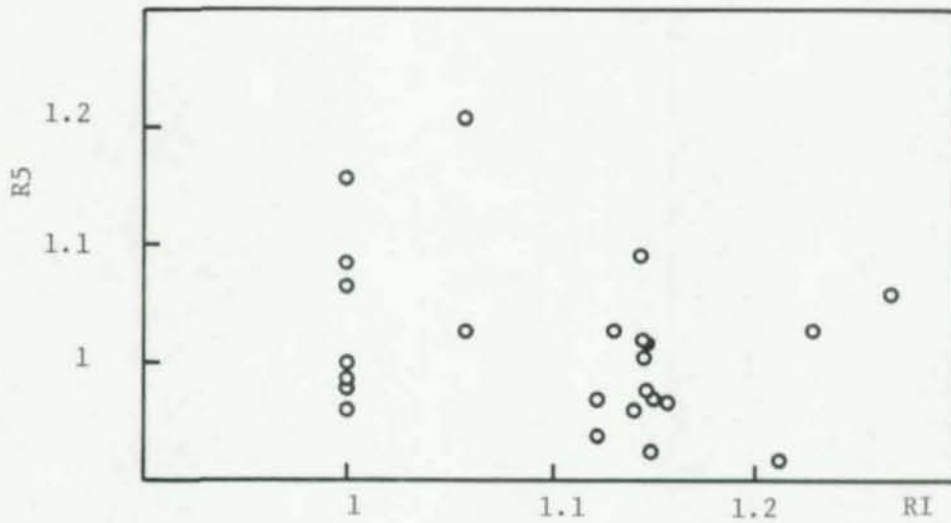
Fig. 9.4-2 Ratios of observed test results to calculated test results
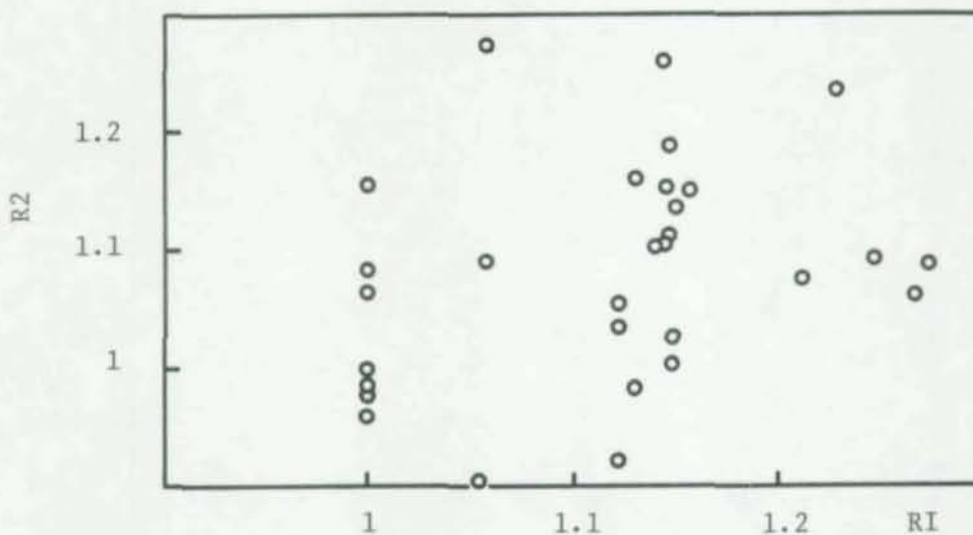
Fig. 9.4-3   Ratios of test results to calculated results
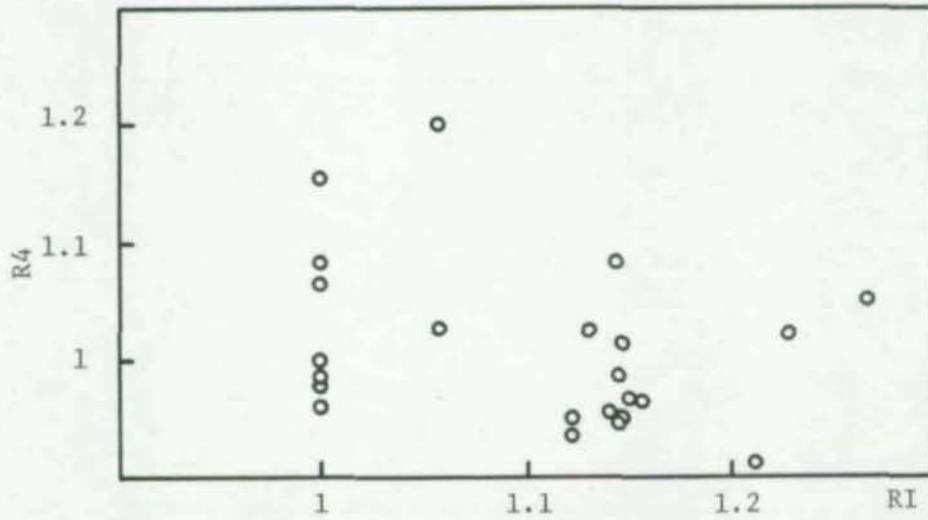
Fig. 9.4-4 Ratios of test results to calculated results
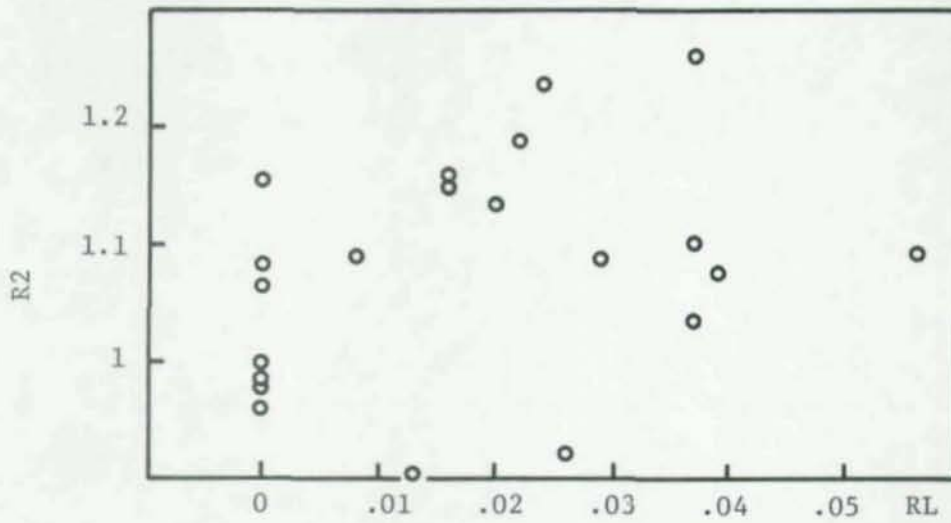
Fig. 9.4-5a Ratios of test results to calculated results
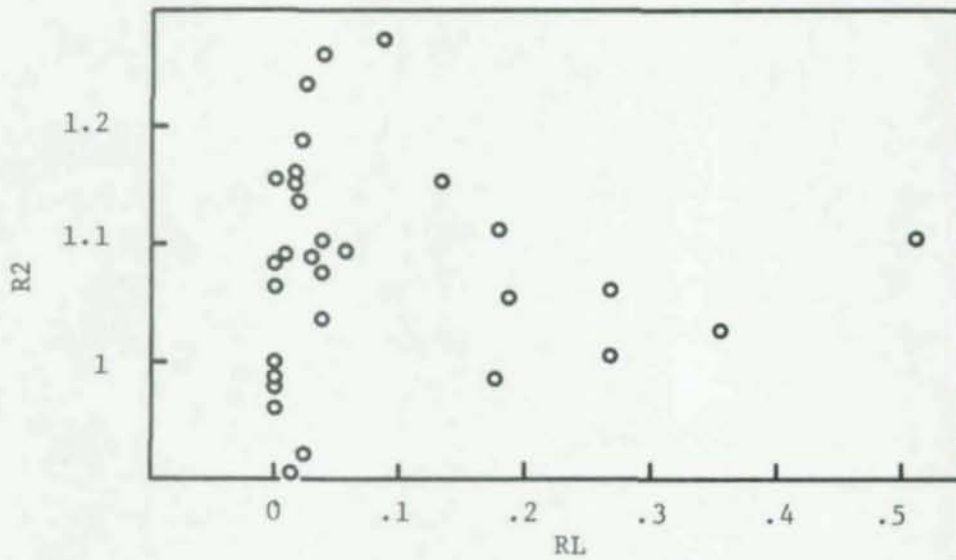
Fig. 9.4-5b Ratios of test results to calculated results
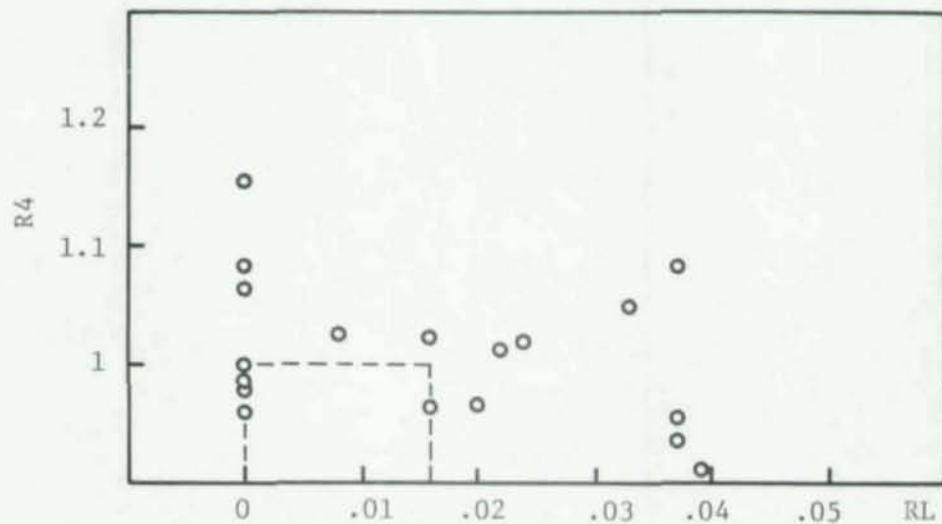
Fig. 9.4-6a   Ratios of test results to calculated results
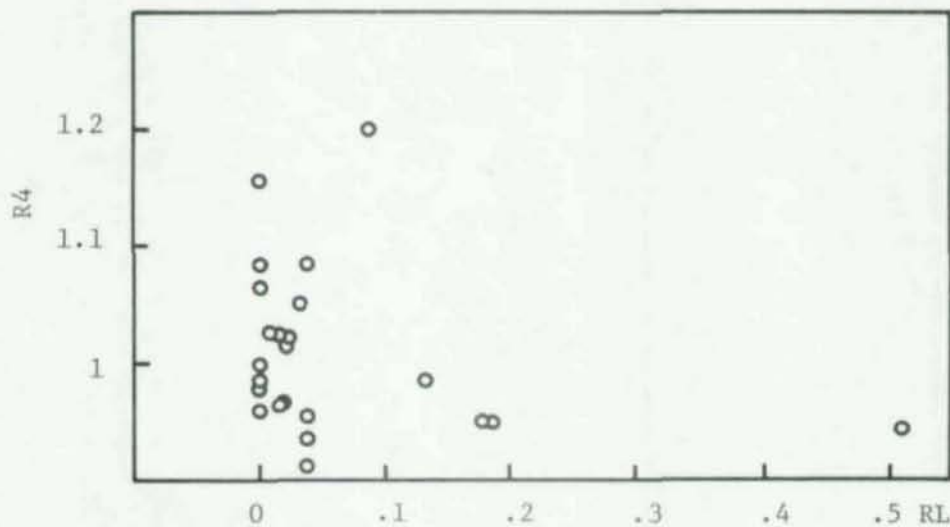
Fig. 9.4-6b   Ratios of test results to calculated results
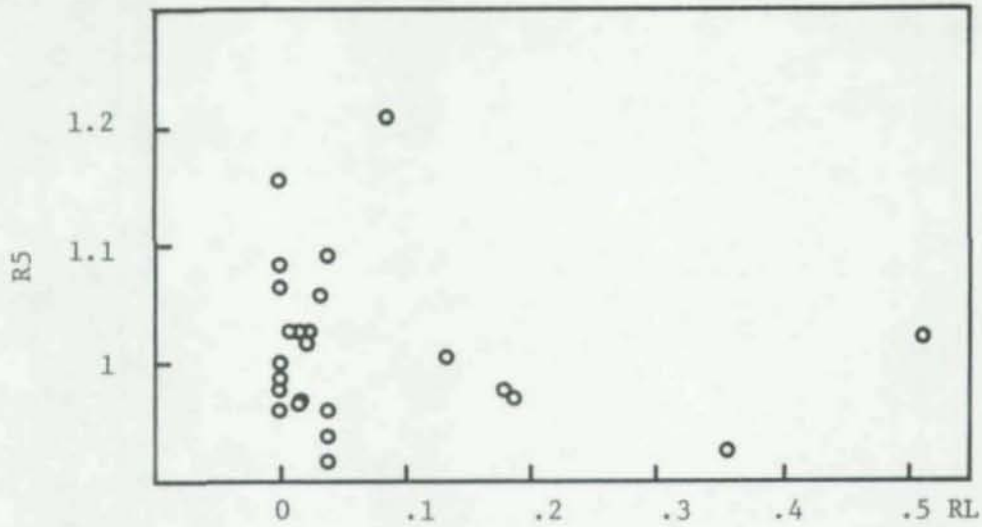
Fig. 9.4-7a Ratios test results to calculated results
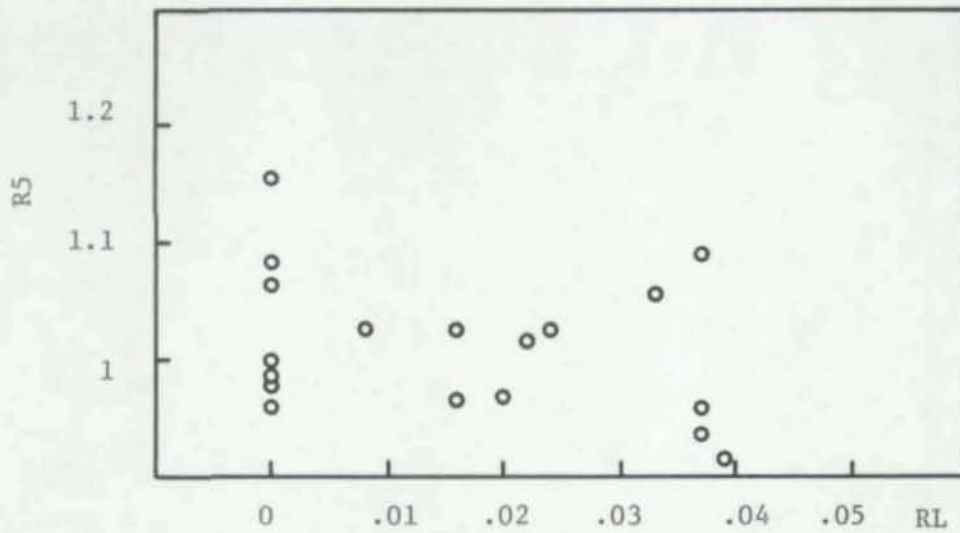
Fig. 9.4-7b Ratios of test results to calculated results
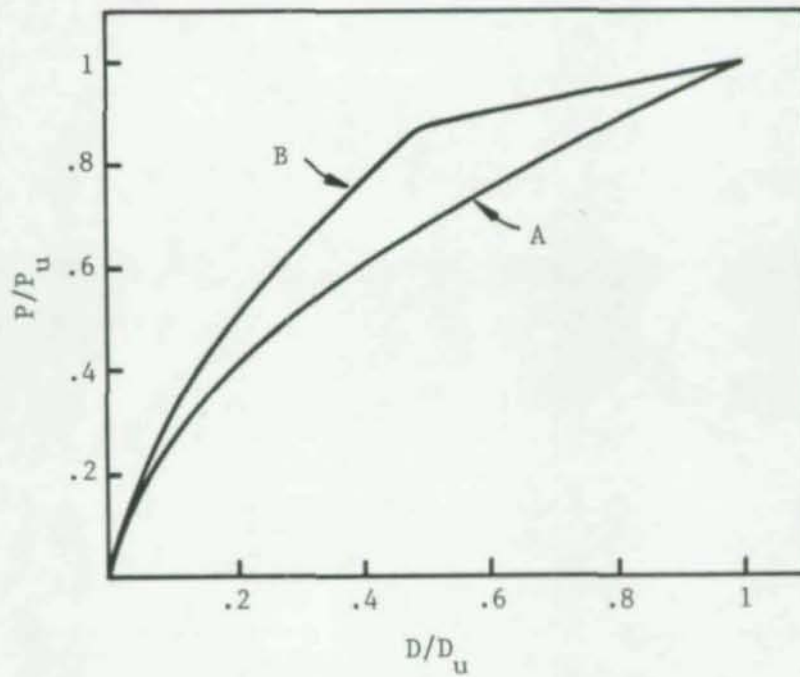
Fig. 10-1 Simulated stub column test results
8"x8" square tube of .05" thickness
Curve A – using Procedure (1)
Curve B – using Procedure (2)
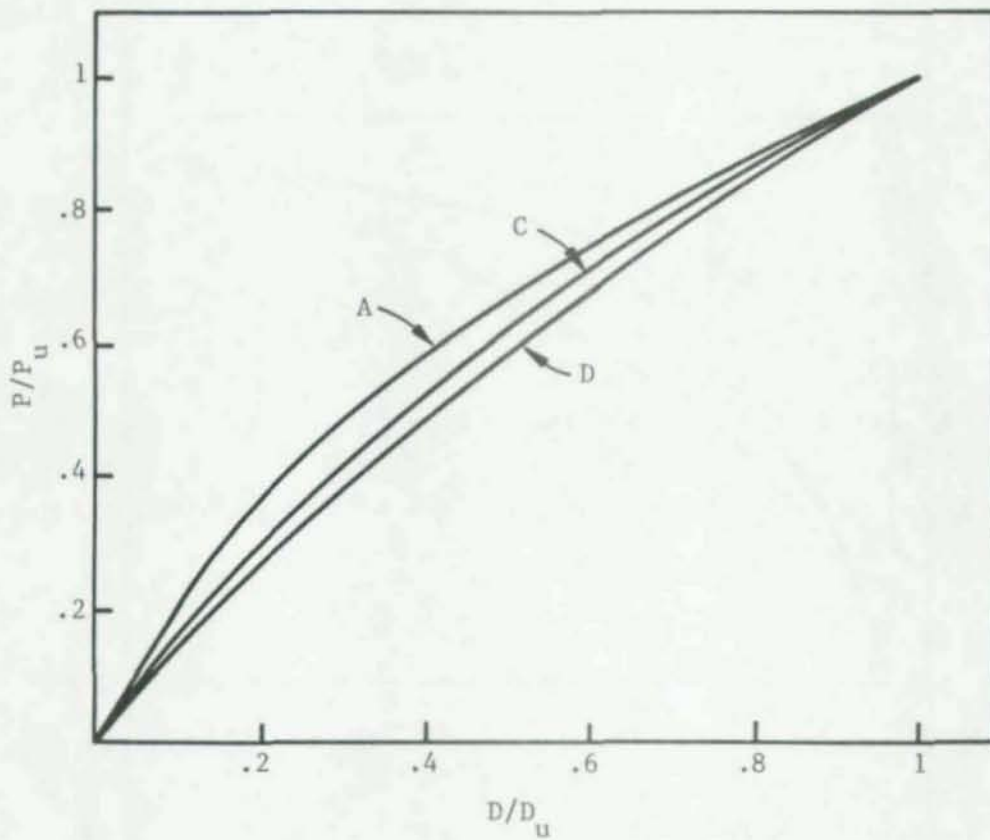
Fig. 10-2 Simulated stub column test results 4"x4" square tube
of .05" thickness
Curve A - using Procedure (1)
Curve C - Eq. 10-8 with n = 1/3
Curve D - Eq. 10-8 with n = 1/5
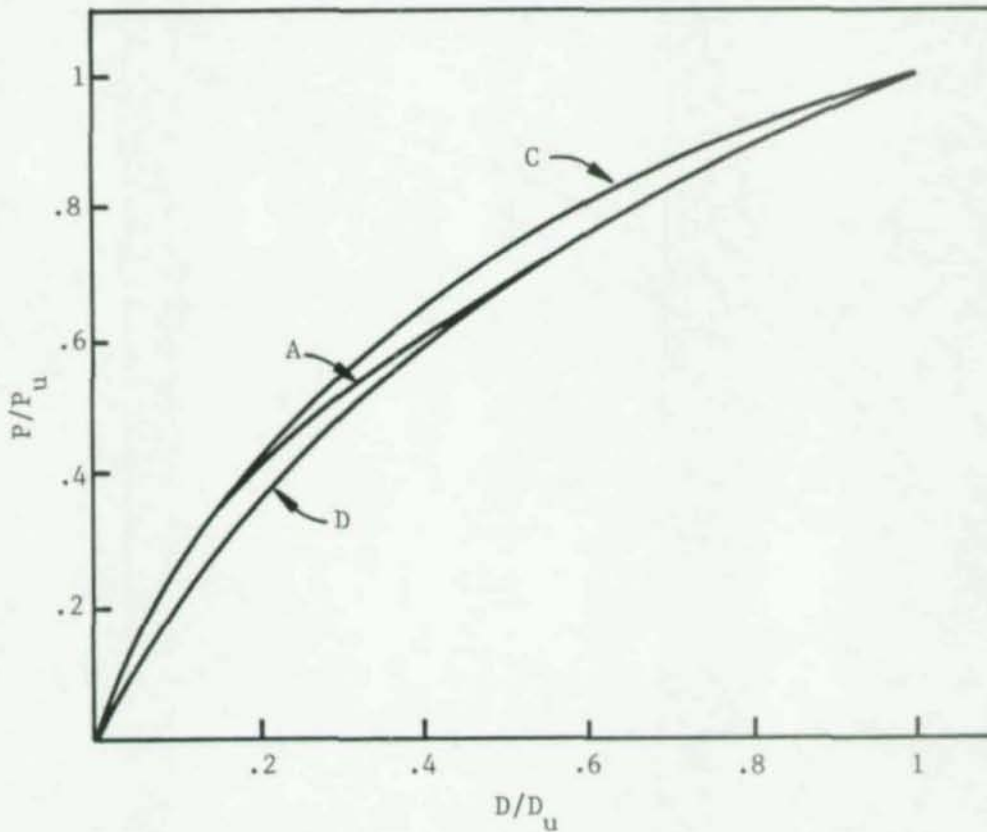
Fig. 10-3 Simulated stub column test results 8"x8" square tube
of .05" thickness
Curve A - using Procedure (1)
Curve C - Eq. 10-8 with n = 1/3
Curve D - Eq. 10-8 with n = 1/5
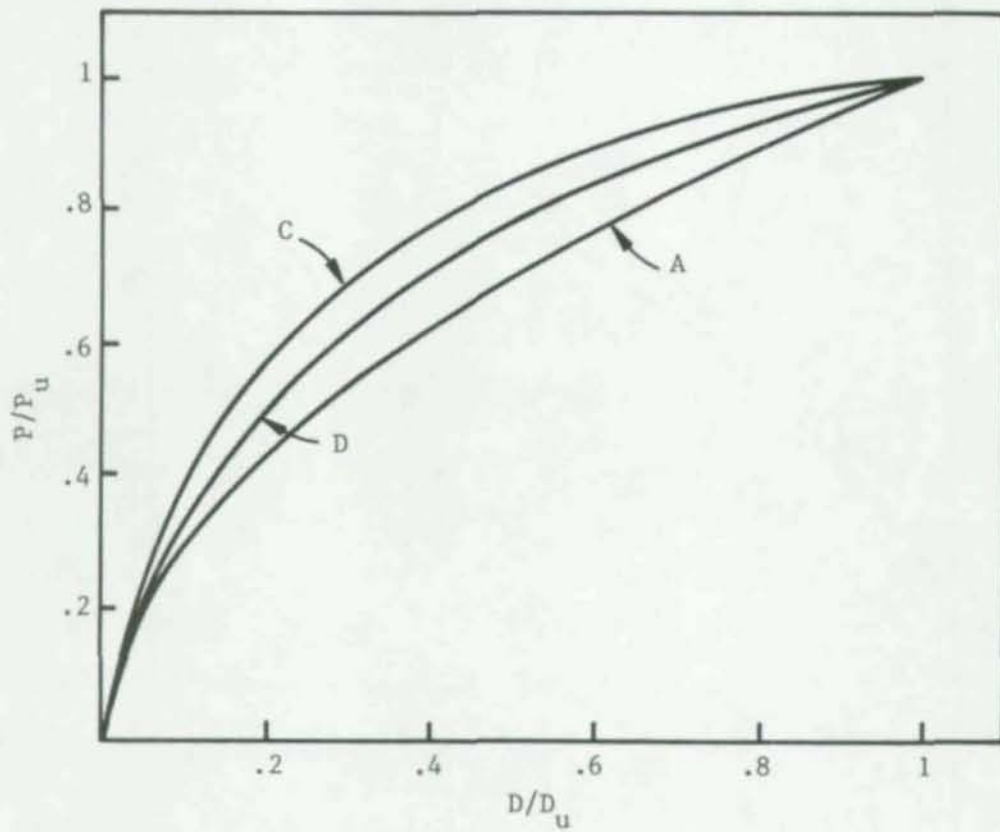
Fig. 10-4 Simulated stub column test results 16"x16" square
        tube of .05" thickness
        Curve A - using Procedure (1)
        Curve C - Eq. 10-8 with n = 1/3
        Curve D - Eq. 10-8 with n = 1/5
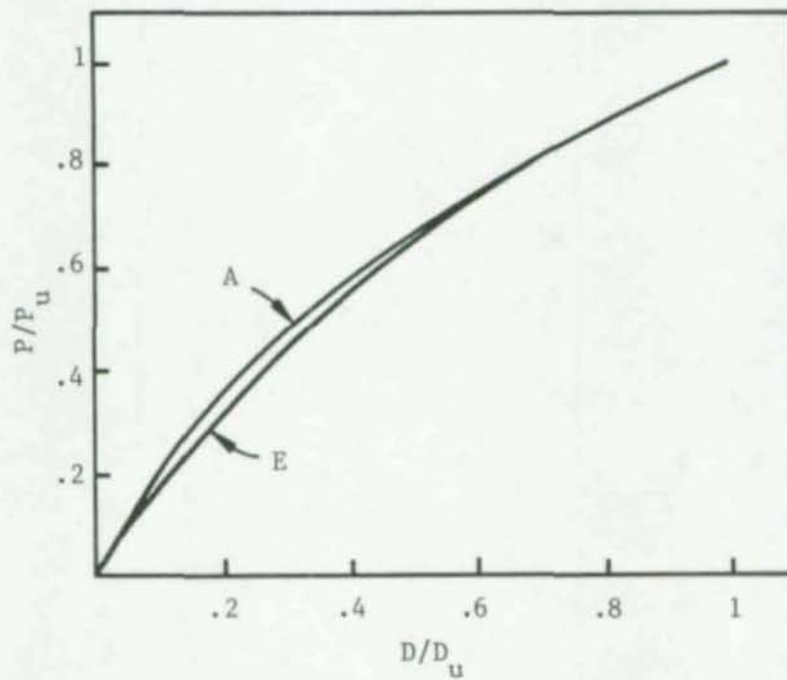
Fig. 10-5 Simulated stub column test results 4"x4"
          square tube of .05" thickness
          Curve A - using Procedure (1)
          Curve E - Eq. 10-8 with $n = A_{eu} / A$ (Eq. 10-9)
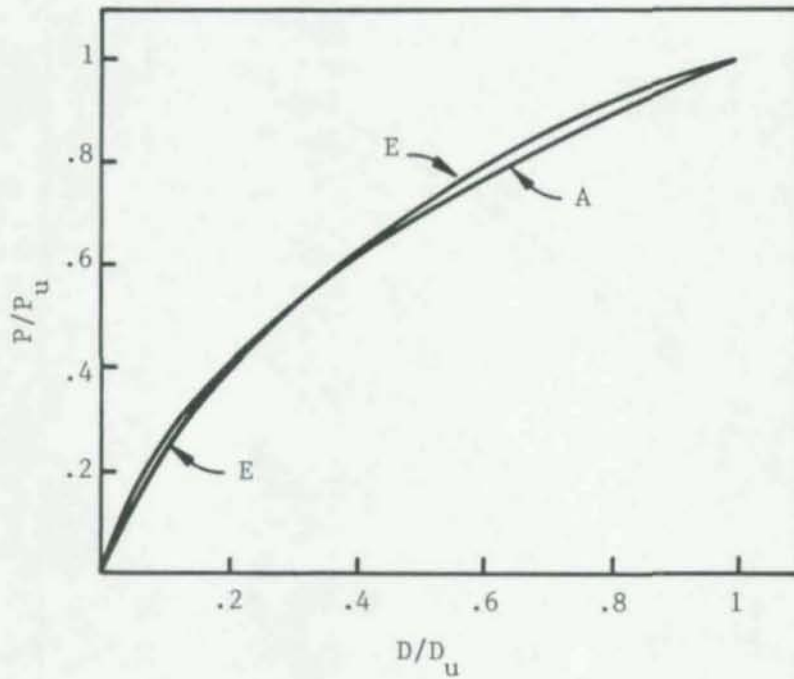
Fig. 10-6 Simulated stub column test results 8"x8"
            square tube of .05" thickness
            Curve A - using Procedure (1)
            Curve E - Eq. 10-8 with n = A_{eu} / A (Eq. 10-9)
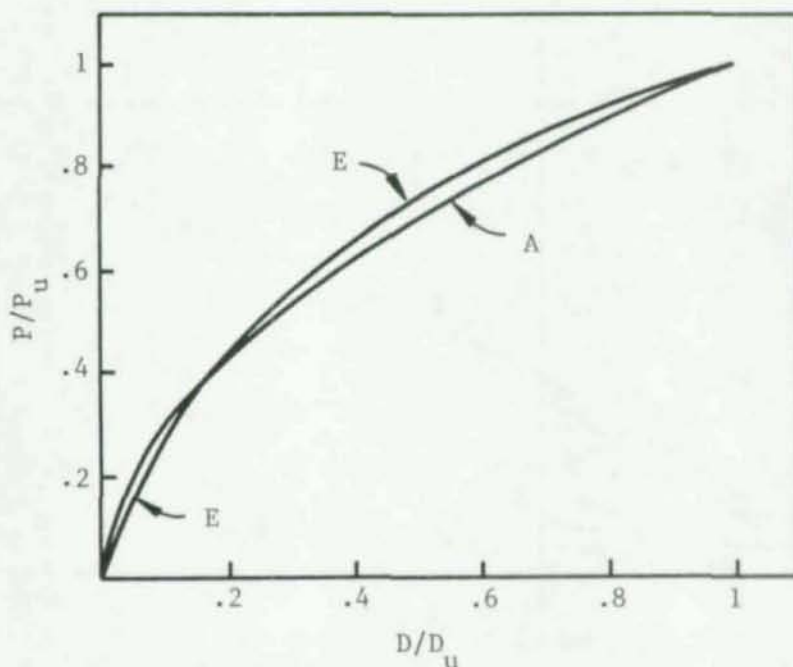
Fig. 10-7 Simulated stub column test results 16"x16"
          square tube of .05" thickness
          Curve A – using Procedure (1)
          Curve E – Eq. 10-8 with $n = A_{eu} / A$ (Eq. 10-9)
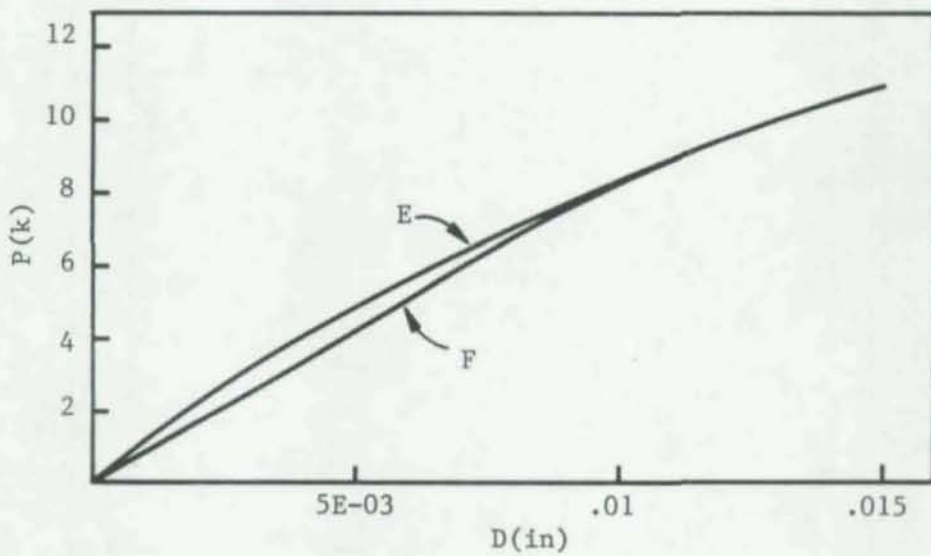
Fig. 10-8 Actual stub column test results specimen
          slc/1 60x30
          Curve E - Eq. 10-8 with n = A$_{eu}$ / A (Eq. 10-9)
          Curve F - Actual test result
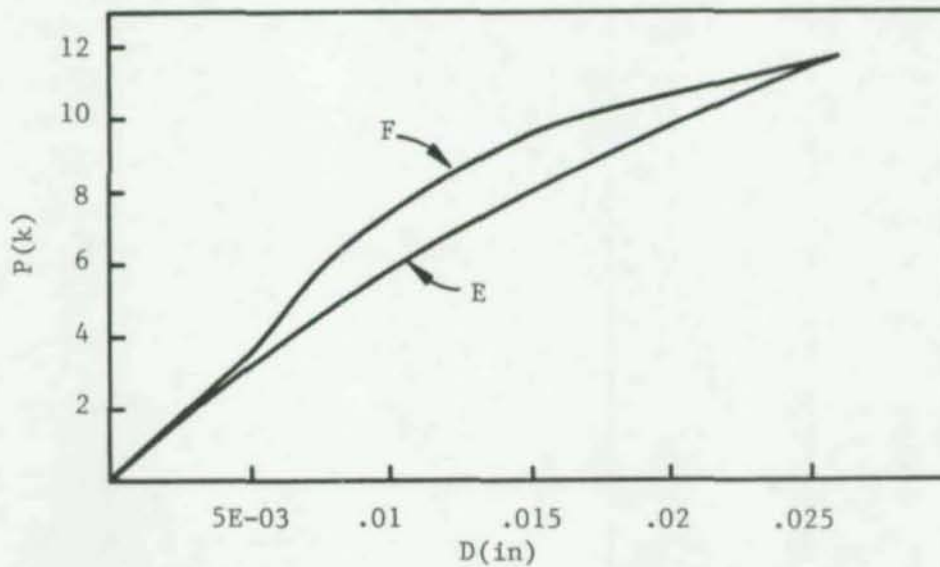
Fig. 10-9 Actual stub column test results specimen slc/2 60/90
Curve E - Eq. 10-8 with n = A_{eu} / A (Eq. 10-9)
Curve F - Actual test result
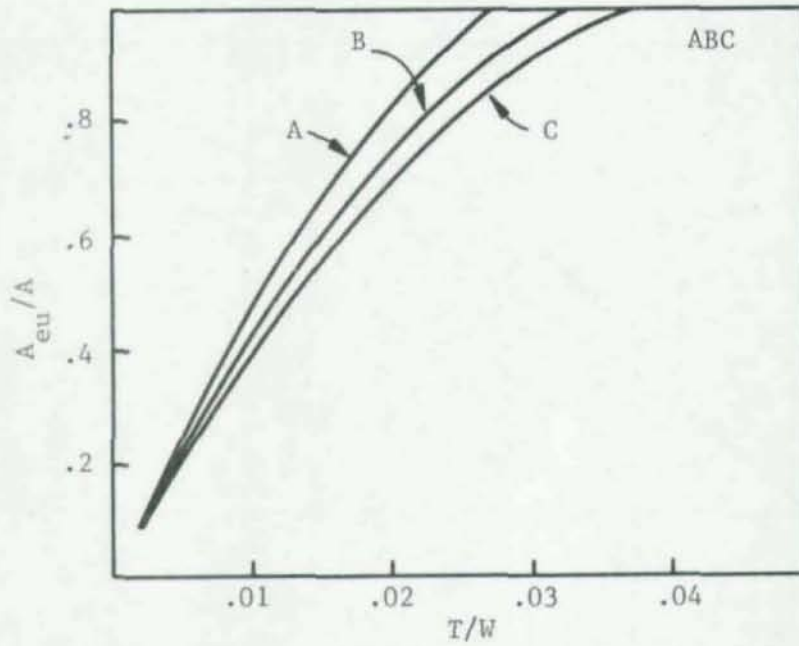
Fig. 10-10 Simulated stub column test results
4"x4" square tube
Curve A – F_y = 35 ksi
Curve B – F_y = 48 ksi
Curve C – F_y = 60 ksi
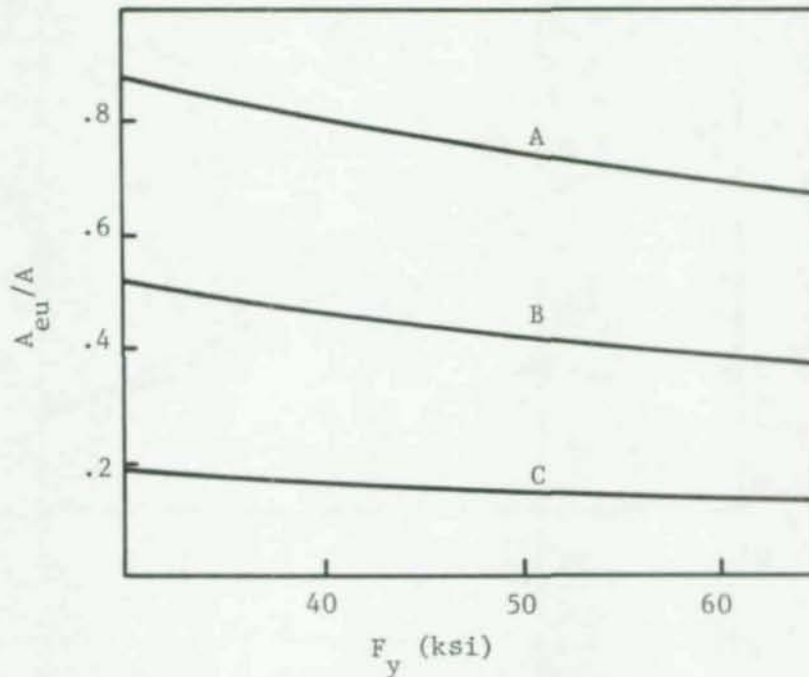
Fig. 10-11 Simulated stub column test results
4"x4" square tube
Curve A - w/t = 50
Curve B - w/t = 100
Curve C - w/t = 300
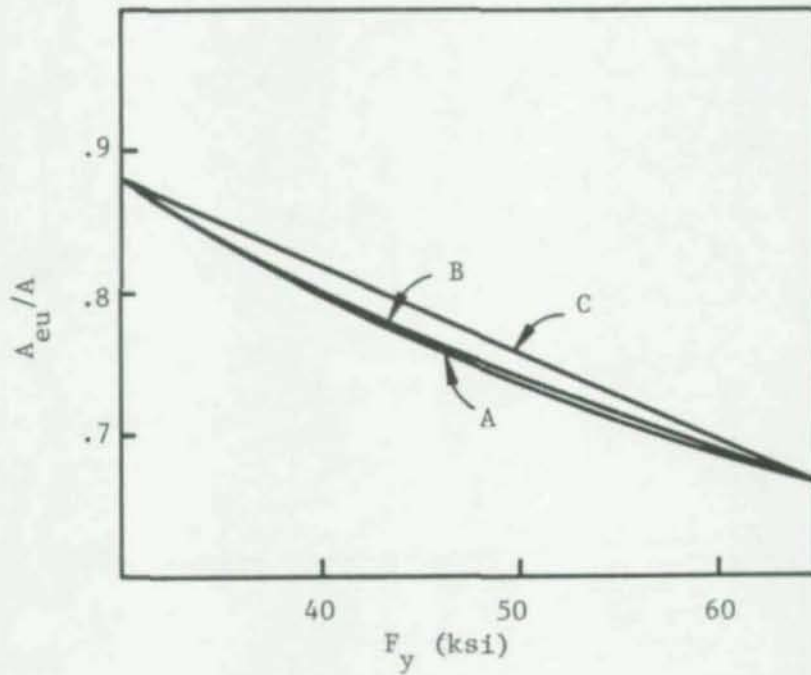
Fig. 10-12 Simulated stub column test results
         Curve A - Eq. 14 with m = 0.8
         Curve B - Simulated stub column test results
         Curve C - Eq. 14 with m = 1
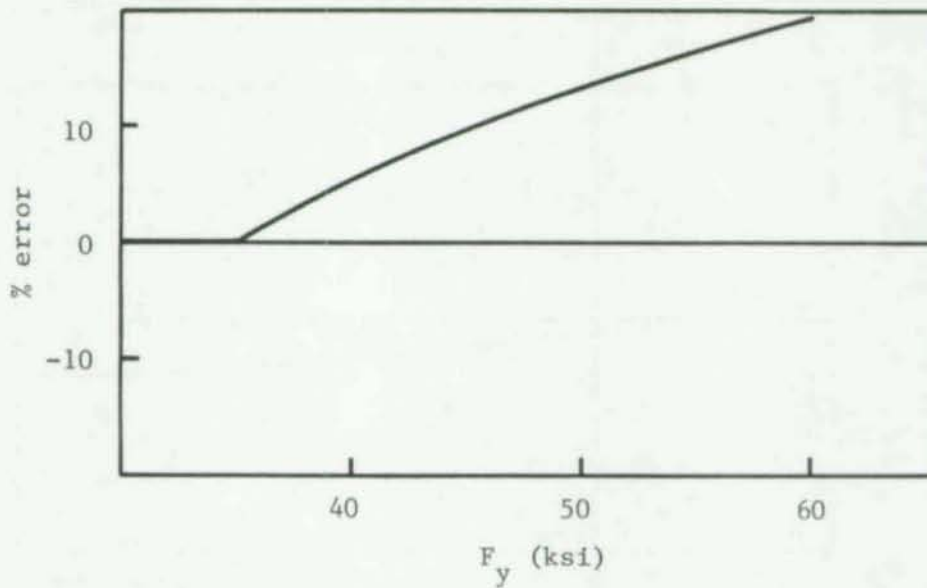
Fig. 10-13 Extrapolation for yield stress from F_y = 35 ksi,
          w/t = 20
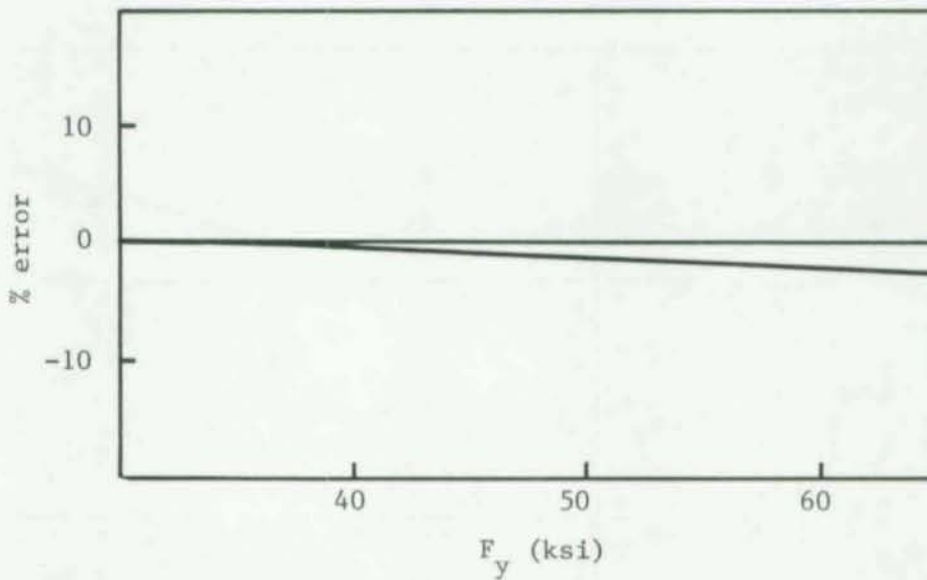
Fig. 10-14 Extrapolation for yield stress from F_y = 35 ksi,
          w/t = 100
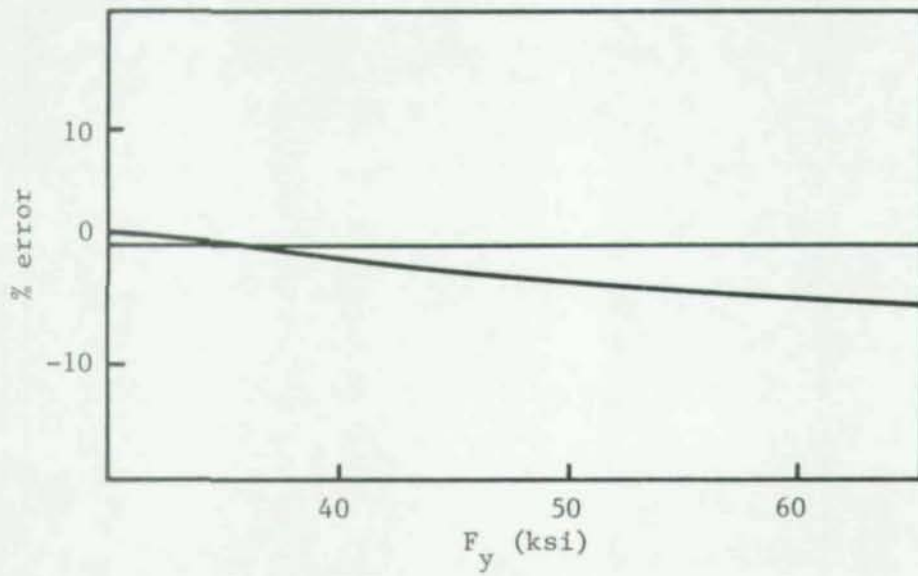
Fig. 10-15 Extrapolation for yield stress from F_y = 35 ksi,
         w/t = 500
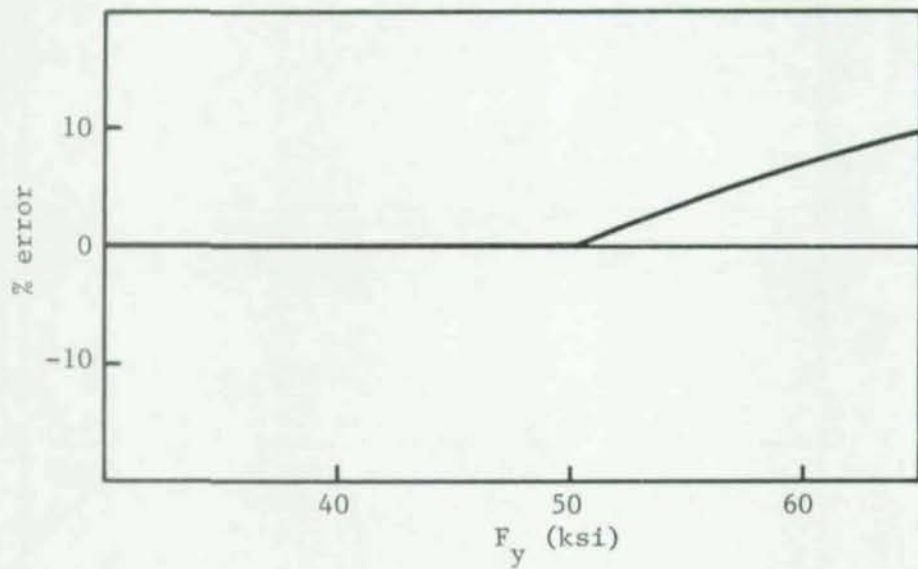
Fig. 10-16 Extrapolation for yield stress from F_y = 50 ksi,
         w/t = 20
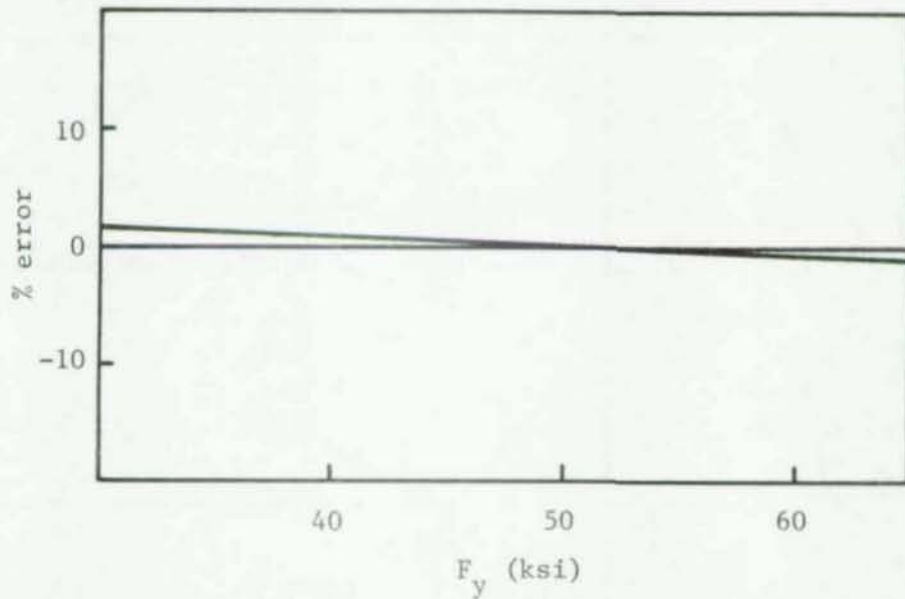
Fig. 10-17 Extrapolation for yield stress from F_y = 50 ksi,
w/t = 100
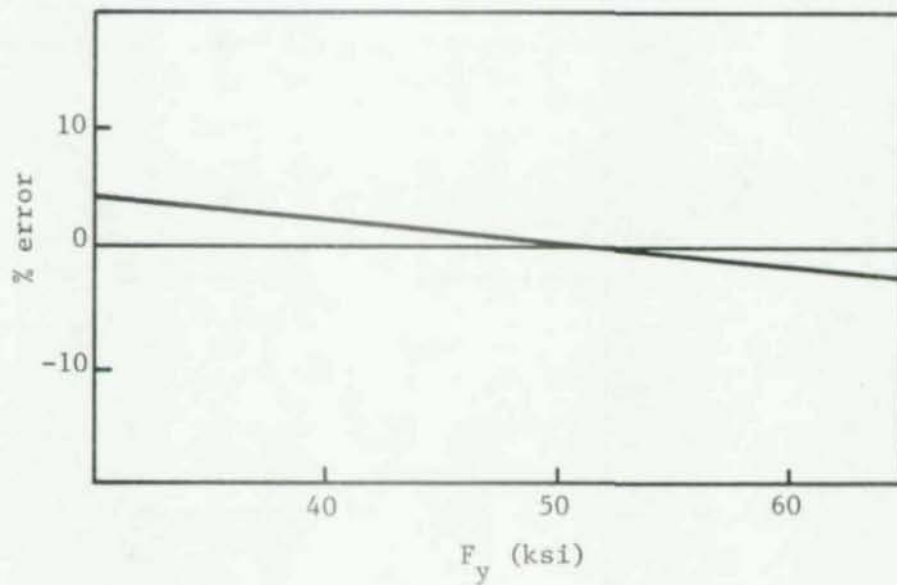
Fig. 10-18 Extrapolation for yield stress from F_y = 50 ksi,
w/t = 500
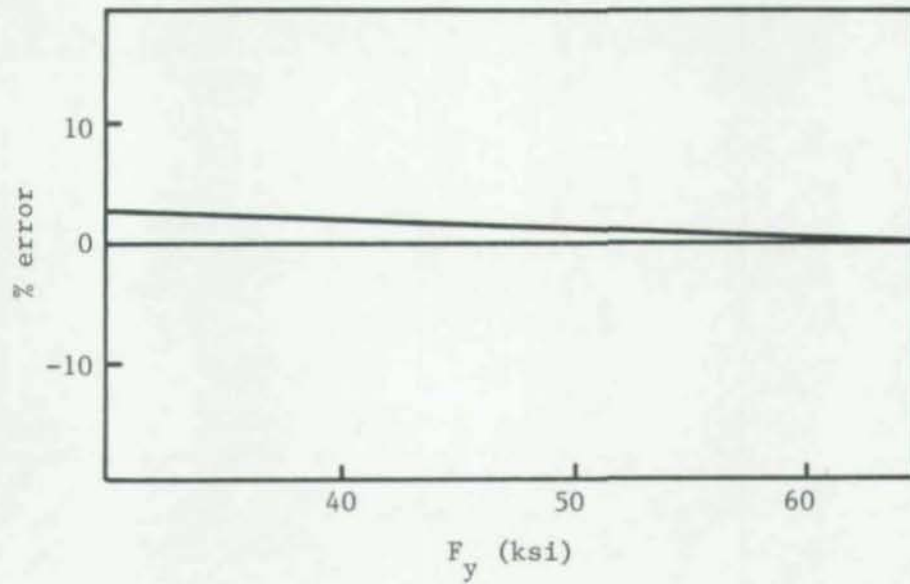
Fig. 10-19 Extrapolation for yield stress from F_y = 65 ksi,
             w/t = 100
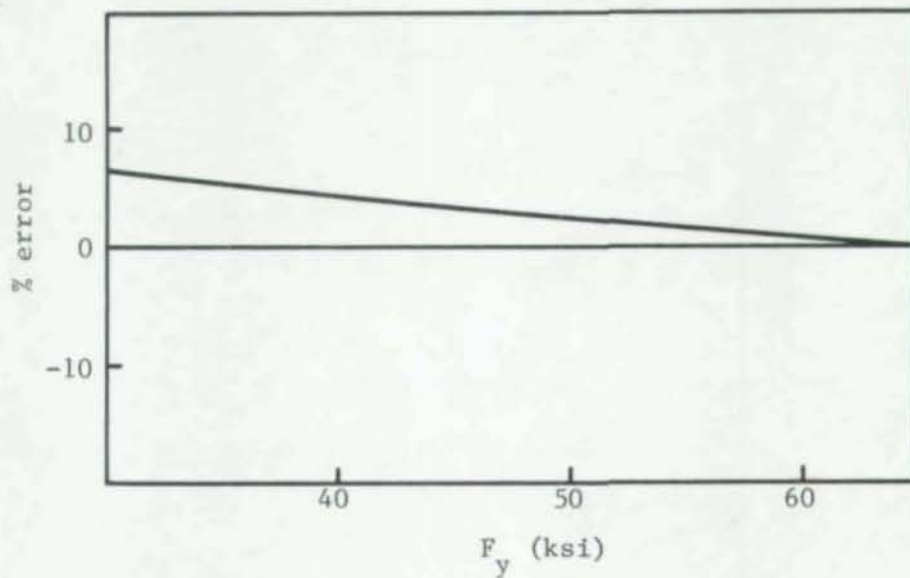
Fig. 10-20 Extrapolation for yield stress from F_y = 65 ksi,
             w/t = 500
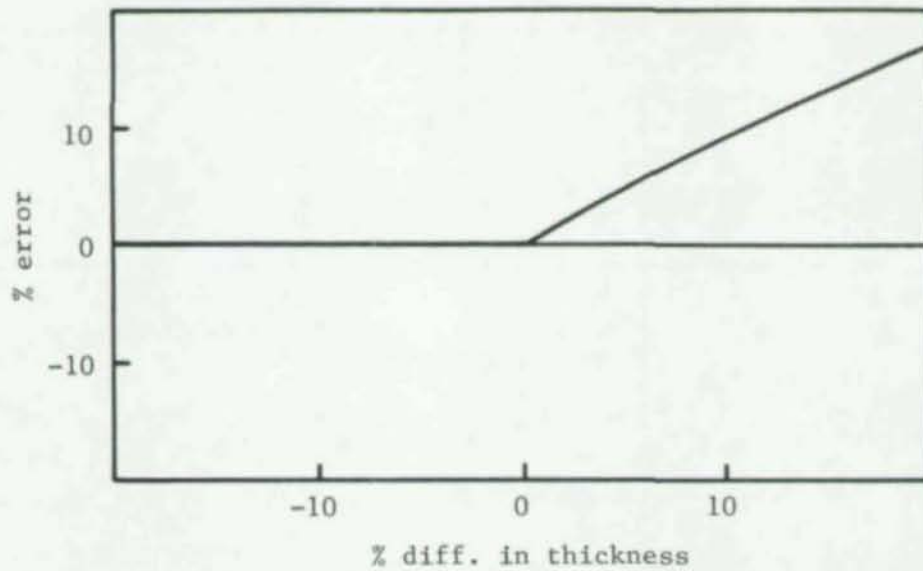
Fig. 10-21 Extrapolation for thickness from F_y = 55 ksi,
    w/t = 20
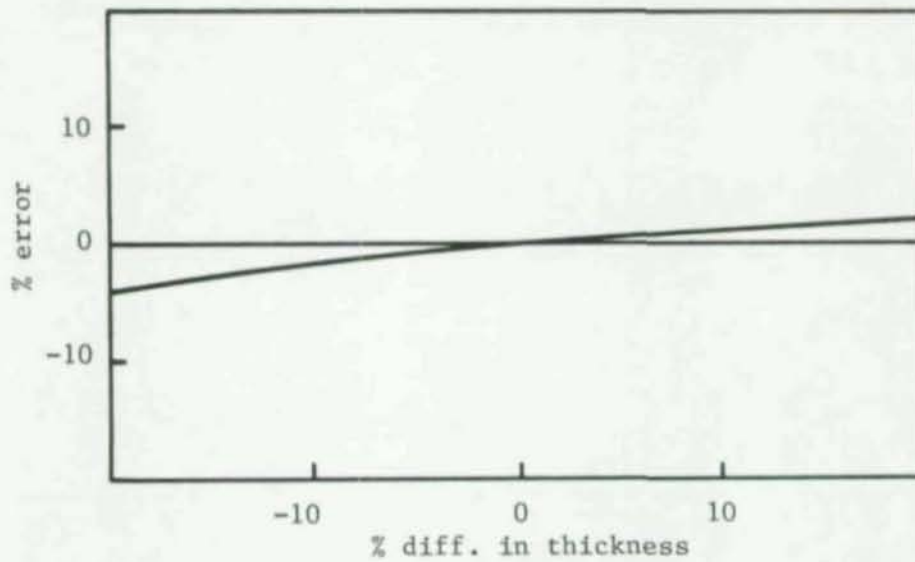
Fig. 10-22 Extrapolation for thickness from F_y = 35 ksi,
    w/t = 100
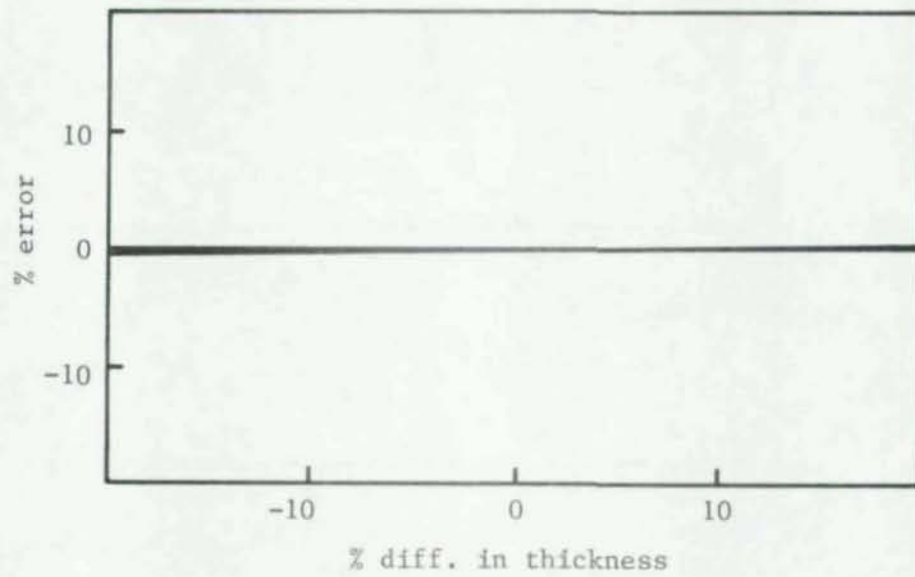
Fig. 10-23 Extrapolation for thickness from F_y = 35 ksi,
w/t = 500
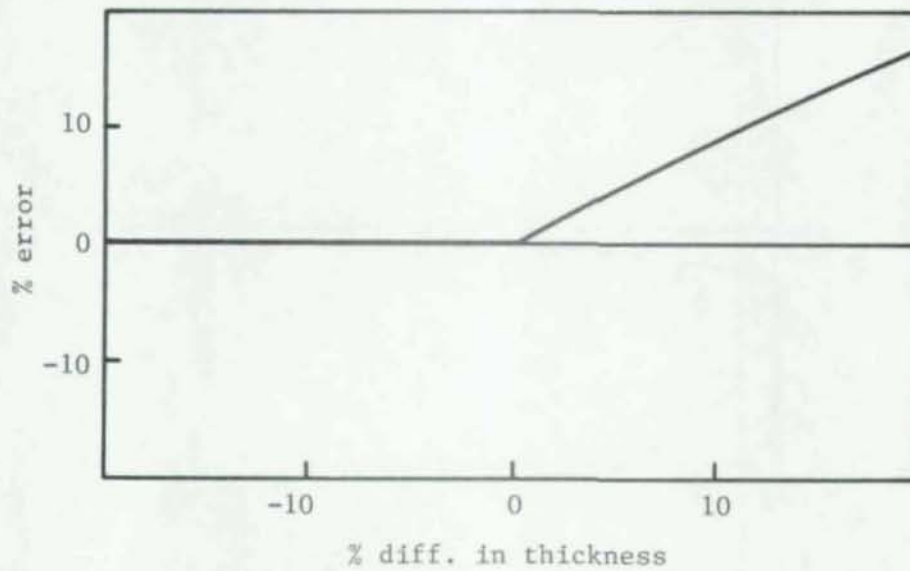
Fig. 10-24 Extrapolation for thickness from F_y = 55 ksi,
w/t = 20
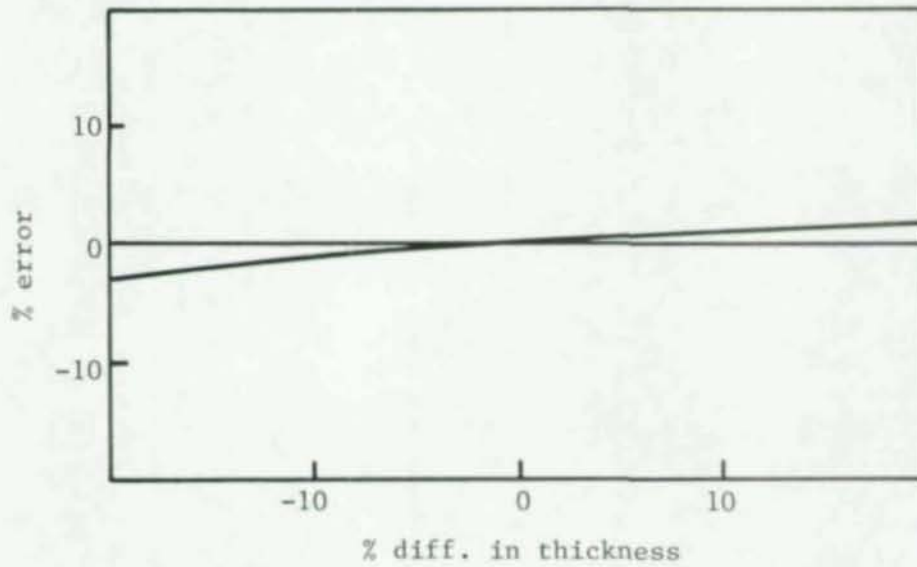
Fig. 10-25 Extrapolation for thickness from F_y = 55 ksi,
          w/t = 100
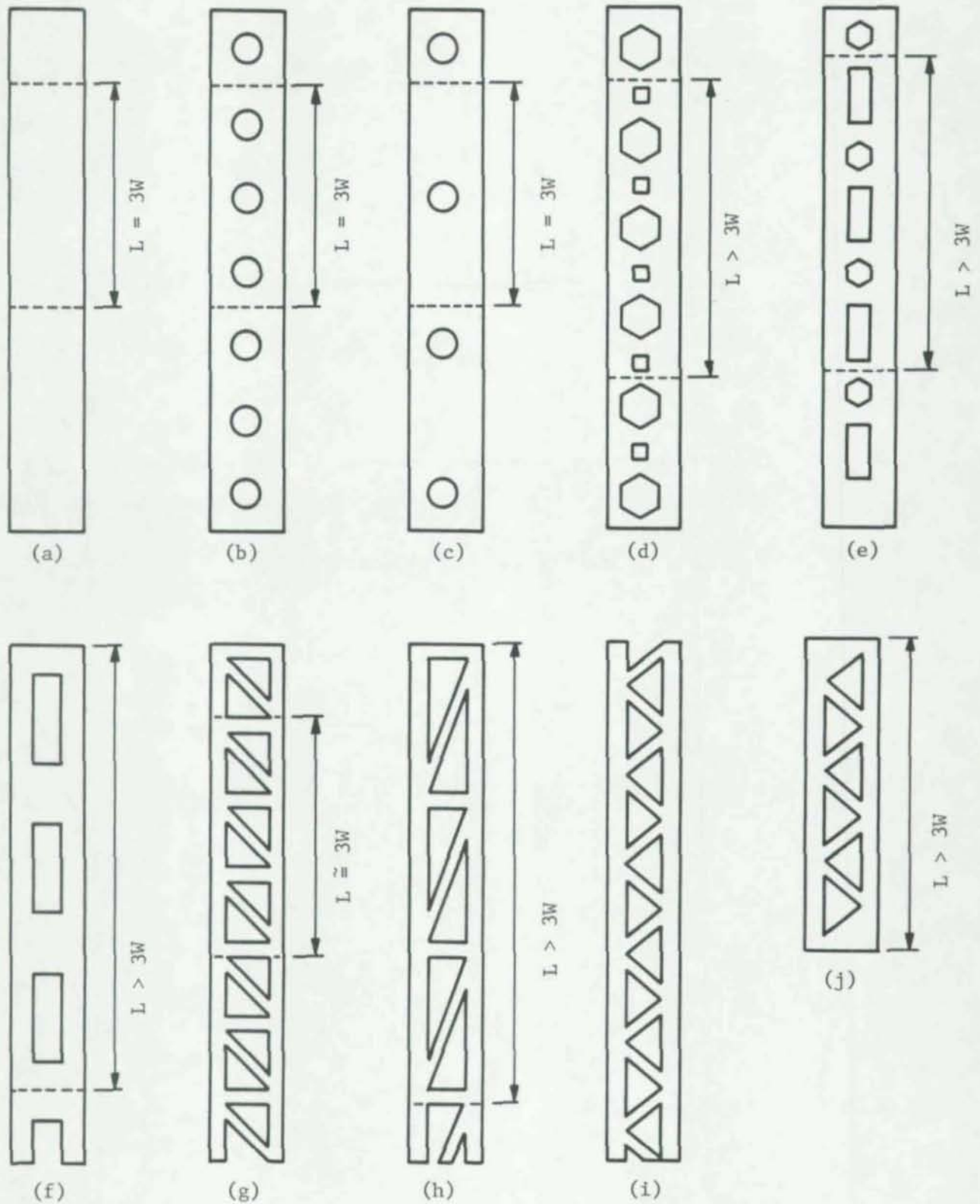
Fig. 10-26   Hypothetical perforation patterns and stub column length.
It is assumed that the perforations shown are in the web
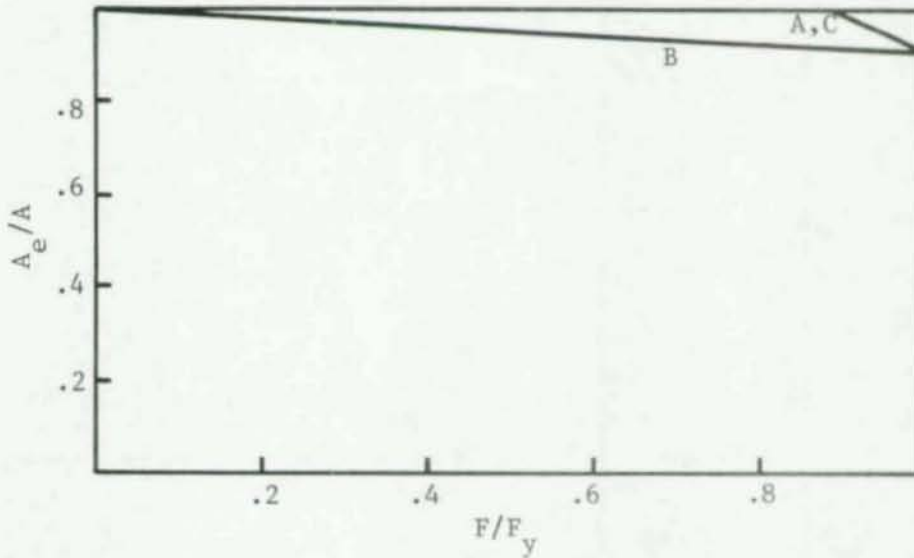of a C-Section and the width of the web is W.
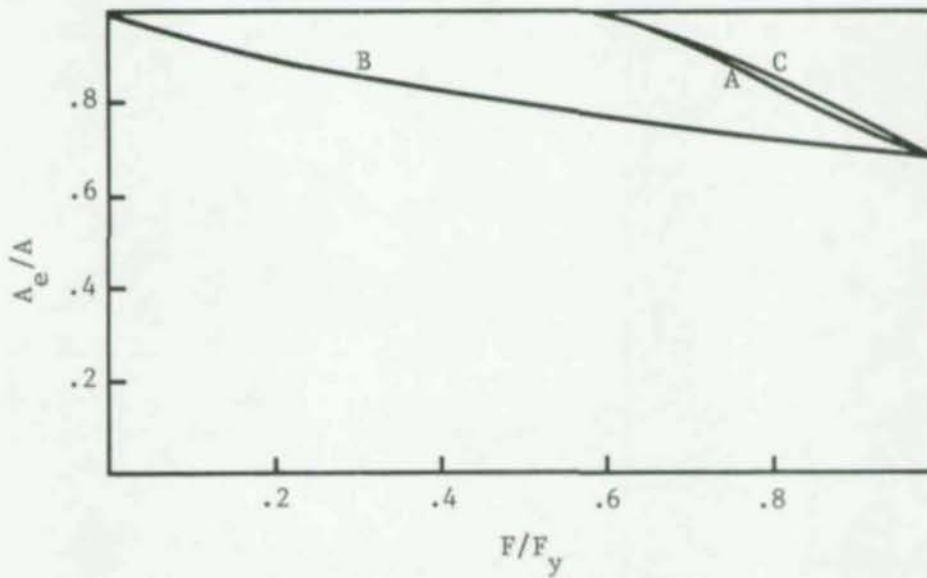
Fig. 10-27 Test no. 1 - 2 5/16 in square tube, .048 in thick
F_y = 67.6 ksi on flats
Curve A - Measured in test
Curve B - Calculated by Eqs. 10-8 and -9
Curve C - Calculated by Eqs. 10-18 and -19
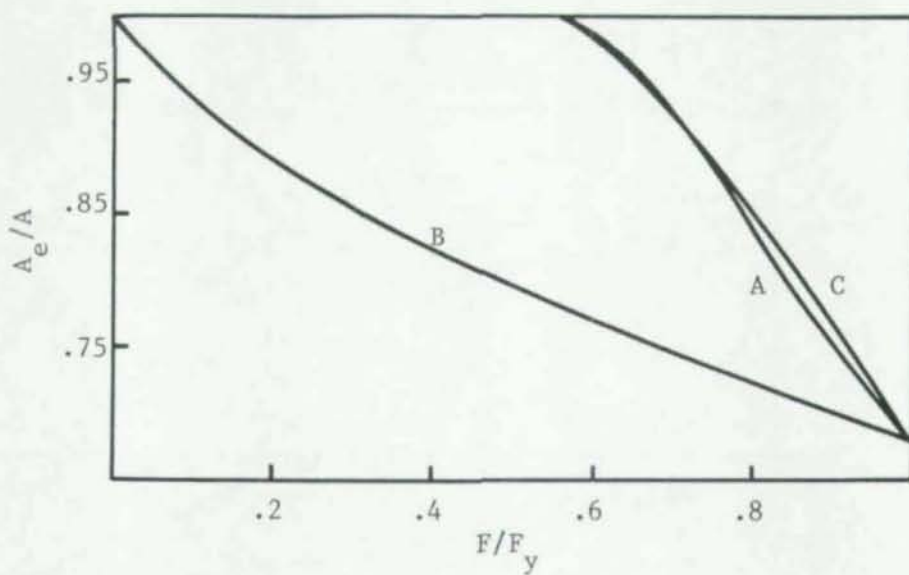
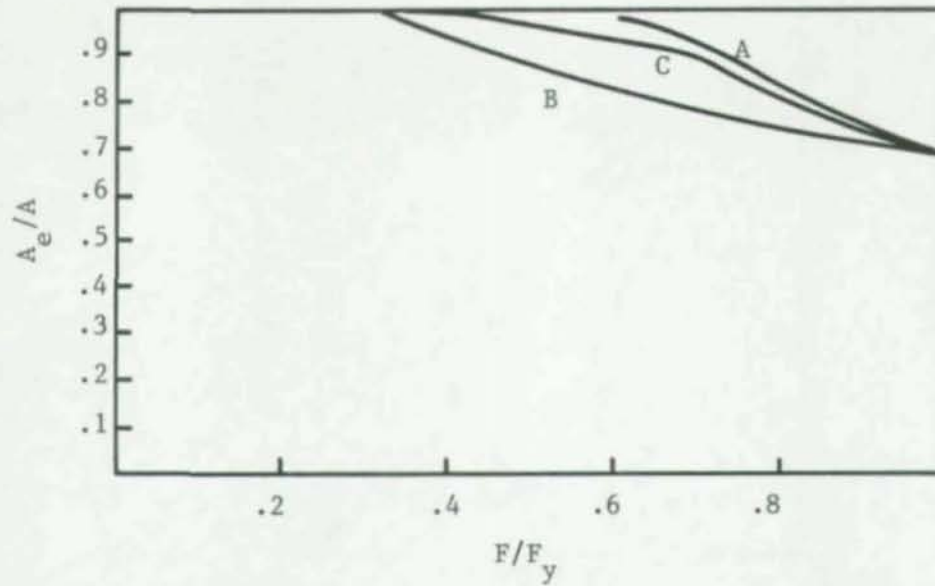Fig. 10-28 Test no. 1
        Fig. 10-27 drawn to a different scale
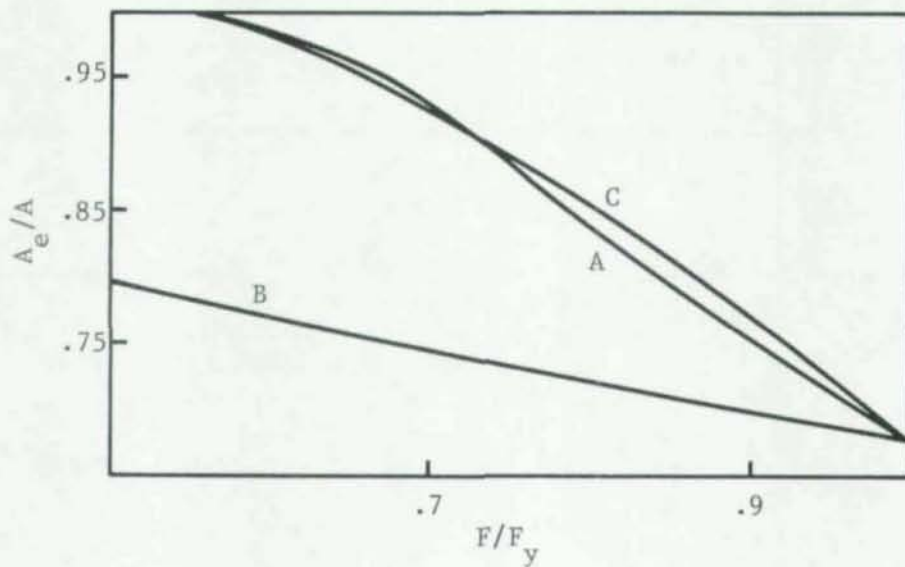
Fig. 10-29 Test no. 1
        Fig. 10-27 drawn to a different scale

Fig. 10-30 Test no. 2 - 2 5/16 in square tube, .063 in
          thick, F_y = 67.5 ksi on flats
          Curve A - Measured in test
          Curve B - Calculated by Eqs. 10-8 and -9
          Curve C - Calculated by Eqs. 10-18 and -19

Fig. 10-31 Test no. 1 - 2 5/16 in square tube, 0.48 in thick
           Observed and calculated test results
           Curve A - Measured in test
           Curve B - Calculated according to Procedure (1)
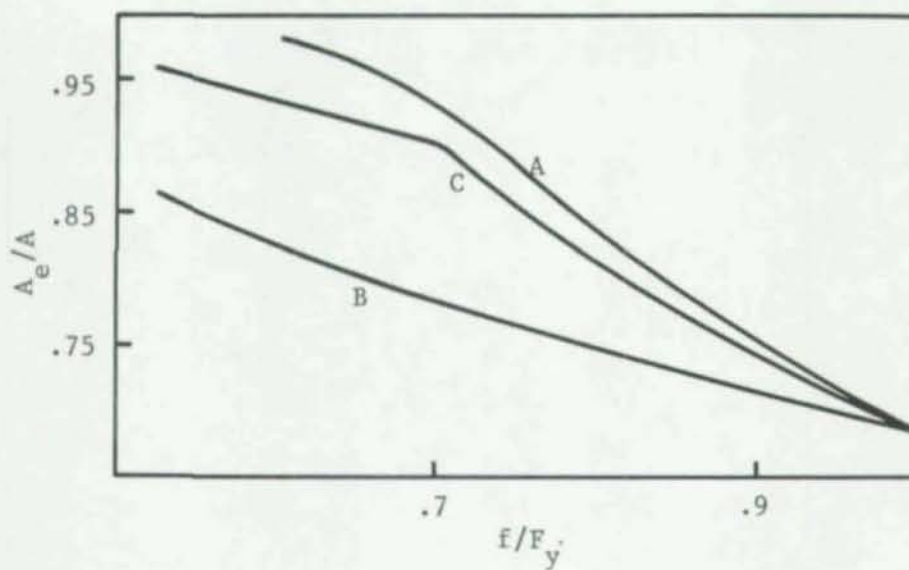   Curve C - Calculated according to Procedure (2)

Fig. 10-32 Test no. 1
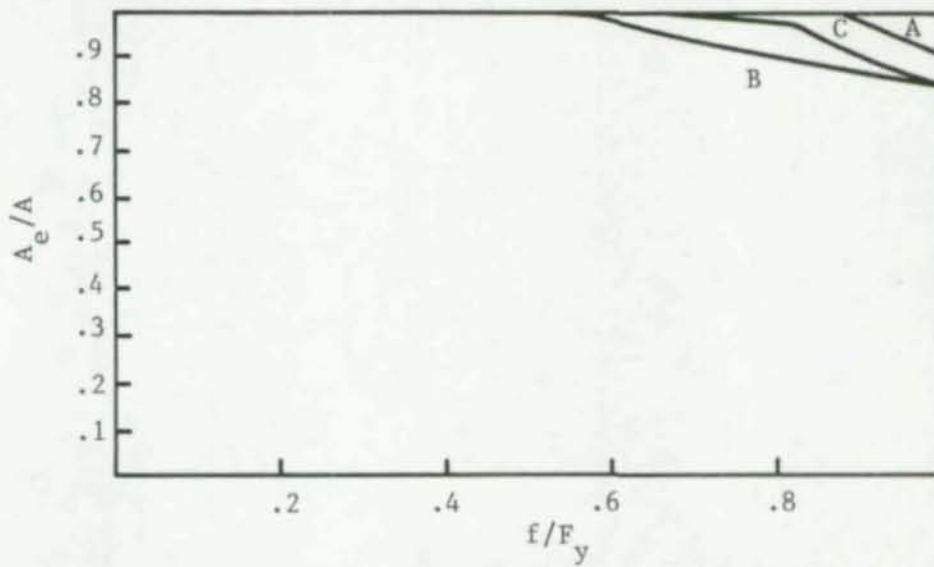   Fig. 10-31 drawn to a different scale

Fig. 10-33 Test no. 2 - 2 5/16 in square tube, .063 in thick
          Observed and calculated test results
          Curve A - Measured in test
          Curve B - Calculated according to Procedure (1)
          Curve C - Calculated according to Procedure (2)
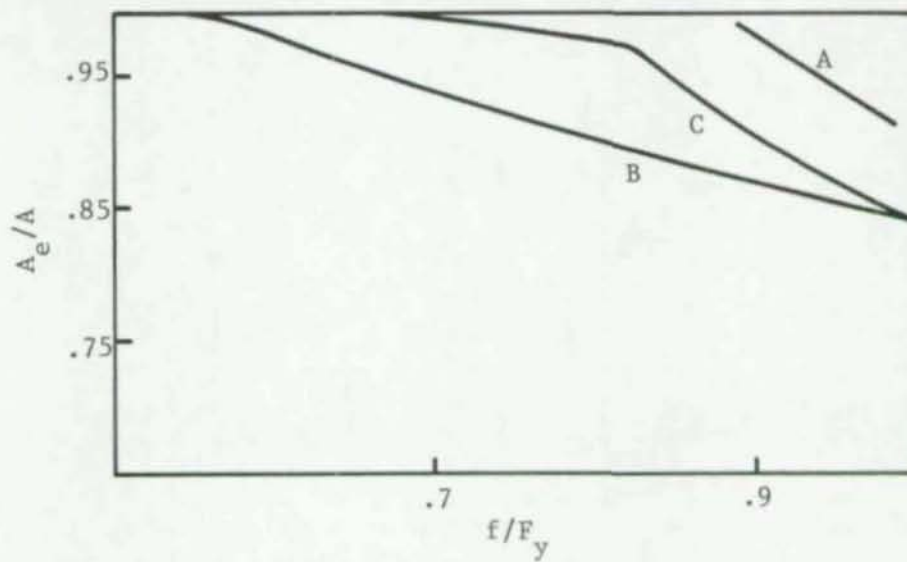

Fig. 10-34 Test no. 2
          Fig. 10-33 drawn to a different scale
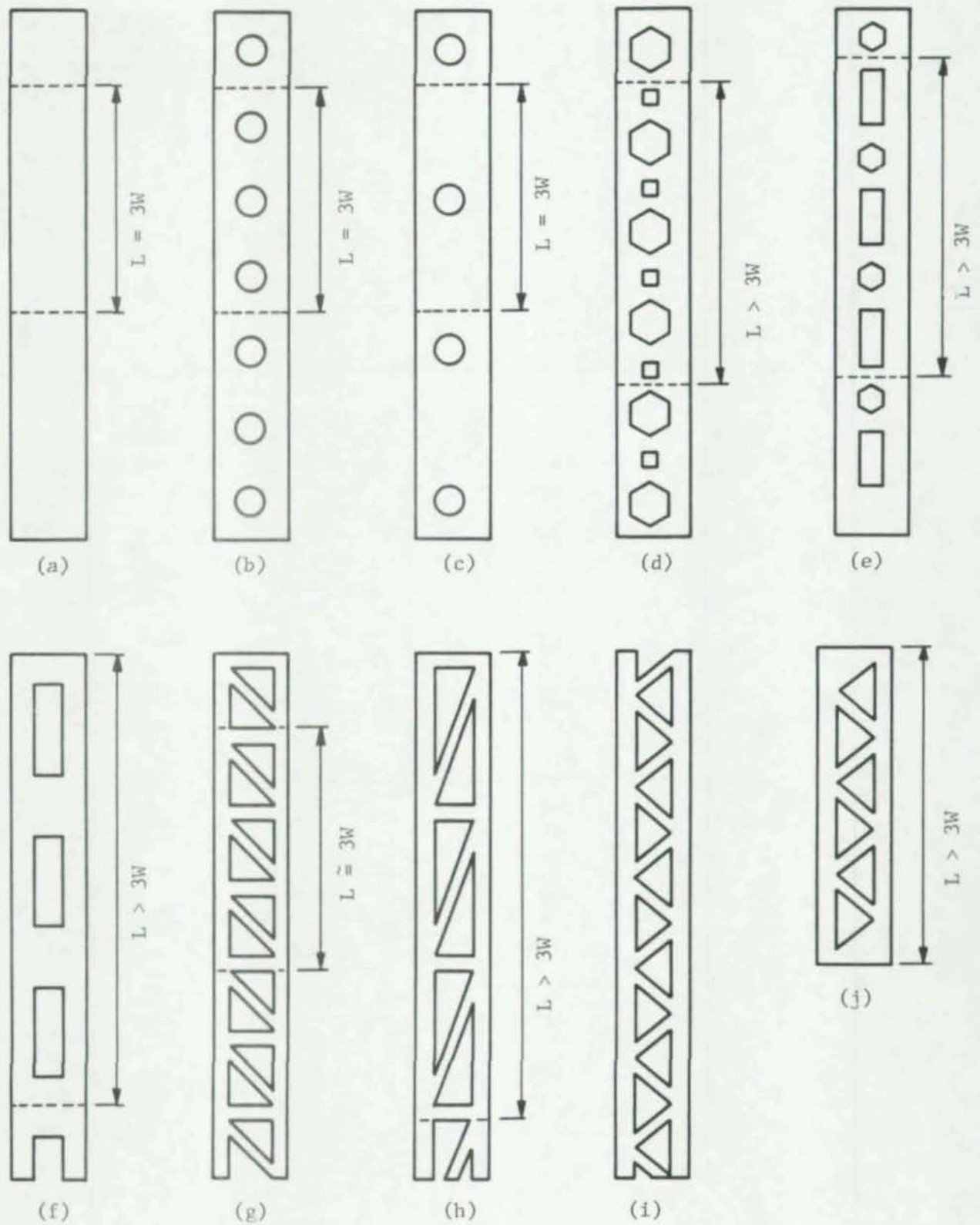
Fig. A1 Hypothetical perforation patterns and stub column length. It
         is assumed that the perforations shown are in the web of a
         C-Section and the width of the web is W.